

# INTEGRATION OF MICROFLUIDICS WITH SURFACE PLASMON RESONANCE

A Thesis

presented to

the Faculty of California Polytechnic State University,

San Luis Obispo

In Partial Fulfillment

of the Requirements for the Degree

Master of Science in Biomedical Engineering

by

Scott Bertram Fratzke

August 2010

© 2010  
Scott Fratzke  
ALL RIGHTS RESERVED

## COMMITTEE MEMBERSHIP

TITLE: Integration of Microfluidics with Surface Plasmon Resonance

AUTHOR: Scott Bertram Fratzke

DATE SUBMITTED: August 2010

COMMITTEE CHAIR: David Clague, Ph.D.  
Associate Professor, Biomedical and General Engineering  
California Polytechnic State University, San Luis Obispo

COMMITTEE MEMBER: Scott Hazelwood, Ph.D.  
Associate Professor, Biomedical and General Engineering  
California Polytechnic State University, San Luis Obispo

COMMITTEE MEMBER: Robert Crockett, Ph.D.  
Associate Professor, Biomedical and General Engineering  
California Polytechnic State University, San Luis Obispo

## ABSTRACT

### INTEGRATION OF MICROFLUIDICS WITH SURFACE PLASMON RESONANCE

Scott Bertram Fratzke

This thesis successfully integrates laminate microfluidic devices with an analytic Surface Plasmon Resonance (SPR) instrument. Integration was accomplished at low-cost using materials such as polydimethylsiloxane (PDMS), Poly(methyl methacrylate) (PMMA), Tygon tubing, and a 3-way stopcock. The main components of this thesis are the design and fabrication of the low-cost, in-house fluidics that can integrate with upstream microfluidics and the validation of the in-house fluidics using the Biosensing Instruments BI-2000 SPR instrument. The low-cost fluidics was designed and fabricated “in-house” using a novel investment casting technique that required the use of laser cutting technology to make a master cast, and candle wax to make the fluidic flow gasket.

Integration of upstream microfluidic devices is the next step towards fully integrated point-of-care (POC) diagnostics. Development of low-cost POC diagnostics will enable physicians to diagnosis patients outside of clinical settings, granting treatment access to a much wider population. Surface Plasmon Resonance is used for its detection abilities combined with its ability to perform real-time sample analysis.

Validation of the in-house fluidics was accomplished by conducting (2) experiments: (1) to compare the angular shift elicited by ethanol solutions between in-house fluidics, factory fluidics, and the literature, and (2) to compare the angular shift between in-house fluidics and factory fluidics caused by the cleaving of fibroblasts from the SPR sensor chip. Successful comparisons made in both experiments proved successful development of low-cost fluidics that could integrate upstream microfluidic devices.

Keywords: Surface Plasmon Resonance, Microfluidics, Ethanol, Fibroblasts, Point-of-Care

## ACKNOWLEDGMENTS

My most profound gratitude extends to Dr. David Clague for his tireless efforts in providing me with the technology, guidance, and support to achieve success in this thesis. Not only did he provide me with the scientific tools necessary to complete this thesis, Dr. Clague taught me invaluable project management skills that I will carry on through the rest of my life's work.

Secondly, I would like to thank Dr. Trevor Cardinal for taking the time to provide me personal assistance both with biological aspects of my thesis as well as general assistance throughout the experimentation process. Trevor also provided the fibroblasts used to validate this experiment.

I would like to thank Dr. Kristen Cardinal for providing supplies to make the fibroblasts experiments possible as well as the advice necessary to achieve success. Additionally, thanks to Dr. Scott Hazelwood for his committee membership and support throughout the process.

Finally, I would like to thank the Cal Poly Biofluidics group for all their efforts and assistance throughout the process. Specifically, I would like to thank Christopher Cummings who assisted throughout the entire design and fabrication process of the in-house fluidics. This project would have never been possible without the help of all of my colleagues and academic advisors.

# TABLE OF CONTENTS

|   | <b>Page</b> |
|---|-------------|
| List of Tables .....                      | viii        |
| List of Figures .....                     | ix          |
| <br>                                      |             |
| <b>1 Introduction .....</b>               | <b>1</b>    |
| 1.1 Hypothesis .....                      | 1           |
| 1.2 Diagnostics .....                     | 2           |
| 1.2.1 POINT-OF-CARE DIAGNOSTICS .....     | 2           |
| 1.2.2 MODULAR DESIGN OF DIAGNOSTICS ..... | 3           |
| 1.2.3 SAMPLE COLLECTION .....             | 4           |
| 1.2.4 SAMPLE PRETREATMENT .....           | 5           |
| 1.2.5 SAMPLE PREPARATION .....            | 6           |
| 1.2.6 DETECTION/POST-PROCESSING .....     | 6           |
| 1.3 SURFACE PLASMON RESONANCE .....       | 7           |
| 1.3.1 HISTORY .....                       | 8           |
| 1.3.2 PHYSICS OF SPR .....                | 9           |
| 1.4 BIOMARKERS .....                      | 13          |
| 1.5 BI-2000 SPR .....                     | 14          |
| 1.5.1 FLUIDICS .....                      | 16          |
| 1.5.2 SENSITIVITY .....                   | 17          |
| 1.6 RESTATEMENT OF GOALS .....            | 18          |
| <br>                                      |             |
| <b>2 Methods and Materials .....</b>      | <b>19</b>   |
| 2.1 SURFACE PLASMON RESONANCE .....       | 19          |
| 2.1.1 SOFTWARE .....                      | 19          |
| 2.1.2 FLOW INJECTION MODE .....           | 21          |
| 2.1.3 NOISE .....                         | 22          |
| 2.1.4 SAMPLE TIMING .....                 | 23          |
| 2.1.5 CALIBRATION .....                   | 24          |
| 2.1.6 FACTORY FLUIDICS .....              | 25          |
| 2.1.7 SYRINGE PUMP .....                  | 26          |
| 2.1.8 TUBING .....                        | 27          |
| 2.1.9 VALVES .....                        | 28          |
| 2.1.10 FLOW GASKET AND FLOW CELL .....    | 29          |
| 2.2 IN-HOUSE FLUIDICS .....               | 30          |
| 2.2.1 TUBING .....                        | 30          |
| 2.2.2 VALVES .....                        | 31          |
| 2.2.3 FLOW CELL .....                     | 33          |
| 2.2.4 FLOW GASKET .....                   | 34          |
| 2.2.5 FLOW GASKET DESIGN .....            | 35          |
| 2.2.6 GASKET MATERIAL SELECTION .....     | 36          |
| 2.3 MANUFACTURING .....                   | 36          |
| 2.3.1 AUTOCAD .....                       | 37          |
| 2.3.2 DOUBLE-SIDED TAPE DESIGN .....      | 37          |
| 2.3.3 NEGATIVE MOLD .....                 | 38          |
| 2.3.4 WAX MOLD DESIGN .....               | 39          |
| 2.3.5 LASER CUTTER .....                  | 40          |
| 2.3.6 WAX MOLD .....                      | 41          |

|   |           |
|---|-----------|
| 2.3.7 PDMS .....  | 41        |
| 2.4 ETHANOL EXPERIMENT .....                            | 42        |
| 2.5 FIBROBLAST EXPERIMENT .....                         | 43        |
| 2.6 EXPERIMENTAL DESIGN .....                           | 46        |
| 2.7 EXPERIMENTAL SET-UP .....                           | 47        |
| 2.7.1 DEGASSING SOLUTION .....                          | 47        |
| 2.7.2 WARM UP .....                                     | 47        |
| 2.7.3 CALIBRATION .....                                 | 48        |
| 2.7.3.1 EXPECTED CALIBRATION RESULTS .....              | 48        |
| 2.7.4 WATERTIGHT TESTING .....                          | 49        |
| 2.7.5 ETHANOL EXPERIMENT .....                          | 50        |
| 2.7.5.1 ETHANOL EXPERIMENT EXPECTED RESULTS .....       | 51        |
| 2.7.6 FIBROBLAST EXPERIMENT .....                       | 52        |
| 2.7.6.1 FIBROBLAST EXPERIMENT FACTORY FLUIDICS .....    | 53        |
| 2.7.6.2 FIBROBLAST EXPERIMENT IN-HOUSE FLUIDICS .....   | 54        |
| 2.7.6.3 FIBROBLAST EXPERIMENT EXPECTED RESULTS .....    | 54        |
| <b>3 RESULTS .....</b>                                  | <b>57</b> |
| 3.1 WATERTIGHT TESTING .....                            | 57        |
| 3.2 CALIBRATION VALIDATION .....                        | 59        |
| 3.3 IN-HOUSE FLUIDICS ETHANOL EXPERIMENT .....          | 61        |
| 3.4 FOLLOW-UP ETHANOL EXPERIMENT .....                  | 64        |
| 3.5 FIBROBLAST EXPERIMENT .....                         | 65        |
| 3.5.1 FACTORY FLUIDICS FIBROBLAST EXPERIMENT .....      | 66        |
| 3.5.2 IN-HOUSE FLUIDICS FIBROBLAST EXPERIMENT .....     | 68        |
| <b>4 CONCLUSIONS/DISCUSSION .....</b>                   | <b>71</b> |
| 4.1 RESTATEMENT OF GOALS .....                          | 71        |
| 4.2 CONCLUSIONS .....                                   | 72        |
| 4.3 SUMMARY .....                                       | 78        |
| 4.4 FUTURE WORK .....                                   | 79        |
| 4.4.1 FUTURE FIBROBLAST EXPERIMENTS .....               | 79        |
| 4.4.2 FUTURE EXPERIMENTAL FLUIDICS .....                | 80        |
| APPENDIX A: SURFACE PLASMON RESONANCE USER GUIDE .....  | 82        |
| APPENDIX B: COLORECTAL CANCER .....                     | 94        |
| APPENDIX C: FABRICATION USING CAL POLY FACILITIES ..... | 99        |
| APPENDIX D: BI-2000 WARM-UP AND CALIBRATION .....       | 108       |
| D.1 INSTRUMENT WARM-UP .....                            | 108       |
| D.2 INSTRUMENT CALIBRATION .....                        | 110       |
| WORKS CITED .....                                       | 114       |

## LIST OF TABLES

|   |     |
|---|-----|
| Table 1 – Characteristics of Surface Plasma Waves at Metal-Water Interface..... | 10  |
| Table 2 – Ethanol Solution Preparation Schedule for Calibration.....            | 48  |
| Table 3 – Cost of In-House Fluidics.....  | 72  |
| Table 4 – Calibration Data.....   | 112 |



## LIST OF FIGURES

|   |    |
|---|----|
| Figure 1 – Cal Poly Biofluidics Modular Flow Chart of Diagnostics.....    | 4  |
| Figure 2 – Otto Configuration Compared to Kretschmann Configuration ..... | 9  |
| Figure 3 – Graph of Dispersion Relationship .....                         | 11 |
| Figure 4 – Resonance Angle Equation .....                                 | 12 |
| Figure 5 – Fresnel Equation.....  | 12 |
| Figure 6 – Cartoon of Surface Plasmon Resonance Detection .....           | 13 |
| Figure 7 – $\alpha$ -Methylacyl-CoA Racemase Molecule .....               | 14 |
| Figure 8 – BI-2000 SPR Instrument .....                                   | 16 |
| Figure 9 – SPR Angular Shift.....   | 17 |
| Figure 10 – Biosensing Instrument Software .....                          | 20 |
| Figure 11 – Screenshot of Flow Injection Setup Screen.....                | 21 |
| Figure 12 – Screenshot of Injection Timer Screen .....                    | 23 |
| Figure 13 – Screenshot of System Calibration .....                        | 24 |
| Figure 14 – Calibration Equation .....                                    | 25 |
| Figure 15 – Dual Syringe Pump .....                                       | 27 |
| Figure 16 – Factory Fluidics Valves.....                                  | 29 |
| Figure 17 – Flow Cell and Gasket .....                                    | 30 |
| Figure 18 – Tygon Tubing with Labsmith Fittings.....                      | 31 |
| Figure 19 – Labsmith Tri-Port Valve, Three-Way Stopcock.....              | 32 |
| Figure 20 – In-House Valve Assembly.....                                  | 33 |
| Figure 21 – In-House Flow Cell .....                                      | 34 |
| Figure 22 – In-House Top View Flow Gasket.....                            | 35 |
| Figure 23 – Two Layer Flow Channel Design.....                            | 38 |
| Figure 24 – Laser Etch Flow Channel Design .....                          | 39 |
| Figure 25 – Final Wax Channel Design.....                                 | 40 |
| Figure 26 – 3T3 Fibroblast Cells .....                                    | 46 |

|  |     |
|--|-----|
| Figure 27 – Degassing Chamber.....   | 47  |
| Figure 28 – BI-2000 Expected Calibration Using Ethanol .....   | 49  |
| Figure 29 – Fibroblast Experiment Cartoon .....  | 53  |
| Figure 30 – SPR Result from Lei Experiment Cleaving Fibroblast with Trypsin .....                    | 56  |
| Figure 31 – Watertight Testing of In-House Fluidics .....  | 58  |
| Figure 32 – SPR Output: Channel 1, Channel 2, 1-2, 2-1, Calibration Check.....                       | 60  |
| Figure 33 – In-House Fluidics SPR Output: Channel 1, Channel 2, Ethanol Experiment.....              | 63  |
| Figure 34 – Factory Fluidics SPR Output: Channel 1, Channel 2, Follow-Up Calibration .....           | 64  |
| Figure 35 – Microscope Images of SPR Sensor Chips Used In Fibroblast Experiments .....               | 65  |
| Figure 36 – Factory Fluidics SPR Output: Channel 1, Fibroblast Experiment.....                       | 67  |
| Figure 37 – Factory Fluidics SPR Output: Channel 1, Channel 2, 1-2, 2-1, Fibroblast Experiment ..... | 68  |
| Figure 38 – In-House Fluidics: Rubber Stopper Used to Distribute Pressure .....                      | 69  |
| Figure 39 – In-House Fluidics SPR Output: Channel 1, Fibroblast Experiment .....                     | 70  |
| Figure 40 – Colon Polyp.....   | 95  |
| Figure 41 – Sigmoidoscopy and Colonoscopy .....  | 97  |
| Figure 42 – SPR Output: Channel 1, Channel 2, 1-2, 2-1, Drift.....                                   | 109 |
| Figure 43 – SPR Output: Channel 1, Channel 2, 1-2, 2-1, Noise .....                                  | 110 |
| Figure 44 – SPR Output: Channel 1, Channel 2, 1-2, 2-1, Calibration.....                             | 113 |

# **1 Introduction**

## **1.1 Hypothesis**

The hypothesis of this thesis is laminate microfluidics can be integrated with standard analytical instrumentation. The major goal of this project is to successfully integrate Cal Poly Biofluidics' microfluidic devices with the BI-2000 surface plasmon resonance (SPR) and demonstrate proper device function. Scientific aims for the project are as follows:

- i. Design and fabricate low-cost fluidics for the BI-2000 SPR instrument to enable integration of in-house designed microfluidic devices;
- ii. Demonstrate fluidics that are leak and bubble free;
- iii. Comparable results of in-house fluidics with factory fluidics using ethanol solutions and assess success of in-house fluidics based on direct comparison;
- iv. Perform proof of concept experiments on BI-2000 SPR instrument to compare low-cost in-house fluidics with factory fluidics using 3T3 fibroblast cells, and to use the BI software to calculate SPR signal shift due to unbinding of fibroblasts from the sensor surface.

The success criteria for the in-house fluidics include: low-cost, watertight, and able to integrate to upstream Cal Poly microfluidic devices designed in-house. If results of the in-house fluidics closely match the results of factory fluidics the experiment will be considered a successful demonstration of the in-house fluidics. By successfully integrating upstream microfluidic devices with SPR, portable biologic detection using this very sensitive technology will make great strides forward toward enabling portable diagnostics.

## **1.2 Diagnostics**

### **1.2.1 Point-of-Care Diagnostics**

The main theme of this project is real time low-cost diagnostics able to be performed at the point of initial contact, i.e., with the patient, or “point-of-care diagnostics”. An important goal in world health is low-cost point-of-care diagnostics because it allows physicians to treat patients in nontraditional clinical settings, and does not require specialized training in laboratories to perform screenings.[1] Recently, public health in the developing world has gained significant visibility due in large part to the Bill and Melinda Gates Foundation publicity and focus on improving point of care diagnostics for patient diagnosis and treatment to developing nations.[2] In keeping with the theme of low-cost diagnostics, Poly(methyl methacrylate) (PMMA) has emerged as a low-cost, durable alternative to traditional microfluidic materials, e.g. glass, polydimethylsiloxane (PDMS).[3] Integration of laminate microfluidic devices used for sample preparation with a detection device such as surface plasmon resonance is a major achievement for effective point of care diagnostic technology. A major criterion for point-of-care diagnostics is inexpensive assays. Among the issues facing world health is the overcrowded clinics in urban centers of developed nations as well as basic, in-the-field clinical support for developing nations. Low-cost integration of laminante microfluidic used for sample processing with sample detection devices will provide great progress towards enabling portable point of care diagnostics used to address local health needs.

### 1.2.2 Modular design of diagnostics

One main advantage of microfluidics diagnostics is the miniaturization of sample preparation and detection. Decreasing the size of biofluidic diagnostic tools allows greater access to populations to screen for common diseases, e.g. colorectal cancer. Through miniaturization testing becomes more affordable in terms of supplies needed to run assays, manufacturing, support equipment costs, and sample sizes needed to perform screenings. Integration of microfluidic chips to powerful diagnostic tools such as SPR presents significant advancements in real time sample analysis and quality of results. Currently miniaturization of SPR is a parallel effort supported by the United States Government.[5] Introducing simple low-cost fluidics for integration with microfluidic sample preparation devices is the other parallel effort that needs to be accomplished to realize portable, low-cost clinical diagnostics with SPR capability.

Cal Poly's Biofluidics group utilizes a modular approach to sample handling and target detection, similar to a clinical protocol. More specifically, the approach includes sample collection, sample pretreatment, sample preparation, detection, and post processing. Currently, the Cal Poly Biofluidics group has several sample preparation devices used for bioseparations. With the success of this project existing bioseparation devices can be integrated and pass purified aliquot to an SPR analytic sensor for sample detection and post processing. Shown below in Figure 1 is a block diagram that describes a modular view of the major steps in approach toward successful target detection.

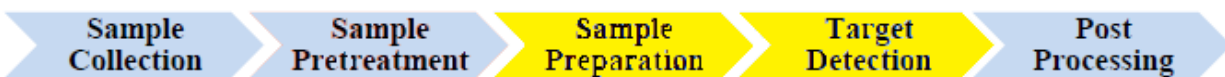


**Figure 1 – Cal Poly Biofluidics Modular Flowchart of Diagnostics**

Shown are the major components of diagnostics shown as flow chart with the integrating step being the connection of sample preparation devices with target detection. Using low-cost fabrication and materials for integration will provide a great step towards point of care diagnostics. The main theme of this project is the transition and integration of sample preparation and target detection.

### 1.2.3 Sample Collection

The initial step of the Cal Poly Biofluidics modular diagnostic paradigm is sample collection. Key to diagnostics, sample collection can be the most intricate and fragile step of the diagnostic protocol as a result of the small scale sample needed for processing.[6][7] For tools as delicate as microfluidic processing devices and SPR analysis to be effective, protocols must be in place to ensure consistent, usable samples. Another defining factor for sample collection is that it is an effective representation of the host undergoing diagnostics, meaning the sample must contain biomarker of interest as well as all other normally occurring physiologic molecules.[6] The value in effective consistent samples is for accurate comparison of a disease model to a health subject. An example is the biomarker Alpha-methylacyl-CoA racemase (AMACR) which can confidently be used to diagnose colorectal cancer.[8] If the sample is inconsistently collected, false positives or false negatives can result. Contamination, such as particulates in the atmosphere or bacterial colonization, can also negatively affect results. Contaminants, biologic or not, can negatively affect each subsequent step of the biofluidics diagnostic protocol, e.g. PCR inhibitors, oversized particulates, or sample degrading bacteria.[9][10]

In the case of this experiment, the appropriate collection and handling of the 3T3 fibroblasts is essential to the success of the experiment. Inconsistent sample collection of the fibroblasts would cause variations in SPR surface concentration, resulting in an observed experimental failure due to a poor comparison between the factory and in-house fluidics. While biologic contamination is a less significant threat to experimental success due to short exposure time, bacterial colonization of the sample may produce “noise”, or unwanted variations in measurement, on the SPR output making a comparison between factory and in-house fluidics difficult.

#### 1.2.4 Sample Pretreatment

No pretreatment is necessary for fibroblasts suspended in media. The media and fibroblasts will be provided in specified concentrations; however, for future experiments done with the in-house fluidics, sample pretreatment will be a key step in the afore mentioned diagnostics approach. Sample pretreatment is the process of conditioning the sample to achieve desired physicochemical properties including viscosity, pH, and ionic conductivity. Methods of pretreatment include utilizing buffers to attain a desired pH needed for electrophoretic manipulation, enzymatic treatment, and dilution to adjust viscosity to achieve desirable flow profiles.[7] Screening for colorectal cancer, for example, would require blood sample screening, which due to its highly viscous nature, would need pretreatment to prevent excessive flow resistance in the microchannels of the microfluidic system, including the flow channels in the SPR. Highly viscous samples such as blood serum or whole blood can significantly increase processing time, pump power requirements, clog microchannels, and interfere with flow,

ultimately rendering a device useless. Sample pretreatment may include the addition of buffers, treatment with specific enzymes, dilutions, and other adjustments of the initial sample.[7]

#### 1.2.5 Sample Preparation

Often used to “purify” a sample, sample preparation requires 60-80% of the diagnostic time with the highest associated costs.[11] Sample preparation is used to gain higher concentration of the analyte allowing for sufficient signal for detection. While SPR is extremely sensitive to the concentration changes of analyte, background noise such as electromagnetic waves emitted by the room lights can often interfere with the signal.[12] Purification of the sample includes methods such as centrifugation, salt purification, or using a bioseparations device. Bioseparation devices, such as those made by Cal Poly Biofluidics purify the sample through manipulation of analyte taking advantage of physicochemical properties. Upstream bioseparation devices, used to purify target analyte concentrations, will flow to the detection system via fluidics, and in the work discussed here; the sample will be processed through the SPR instrument using in-house laminate fluidics.

#### 1.2.6 Detection/ Post processing

The final step in the diagnostic module is detection and post processing. The focus of this project is the integration of the sample preparation step to the detection. Many methods exist for detecting analyte and the concentration at which it is present. For this work, SPR is the chosen method of detection but others include immunohistochemistry, ELISA, and various forms of spectroscopy.[13][14][15] SPR typically uses receptor-ligand technology for binding kinetic information and detection of binding.[12] Often the detection surface of SPR and other detection



methods are functionalized with antibodies specific to the analyte in question.[17] A sample is introduced, exposed to the functionalized surface analyte molecules captured, allowing other molecules in suspension to pass undetected. The captured analyte molecules cause a detectable change in mass that can be converted to concentrations. Other methods of detection use similar properties of capturing analyte by using specific antibodies, or manipulation of colloidal properties such as size, shape, or charge and converting it into a processed signal.[16]

Post-processing is interpreting the processed signal to interpret data such as presence of analyte, concentration that analyte is present, binding and unbinding kinetics or in the case of unknown solutions, composition of solution. Post-processing is most often performed by instruments using vendor software designed to interpret the data and present it in graphical form.[12] For the work presented here, the SPR instrument presents the data as a graph, depicting the angular shift per unit time of the plasmon wave. This measurement shows the addition or removal of mass from the surface of the sensing chip.

### **1.3 Surface Plasmon Resonance**

Plasmon resonance is a phenomenon created by the interaction of photons from polarized light with free electrons of a thin metal surface, e.g. gold or silver.[18] First discovered in 1902, surface plasmon resonance was not utilized as a means of analyte detection until Otto and Kretschmann both designed SPR experiments in 1968.[18] Recently, SPR has received a great deal of attention as a potential low-cost point-of-care diagnostic tool.[19] SPR is useful for several applications such as measuring molar concentration, binding kinetics, surface charge density, film thickness, and is a highly sensitive and versatile tool with the potential to serve as an effective point of care diagnostic device. [18]

### 1.3.1 History

Plasmon resonance was first realized by Wood in 1902 when he shone a laser of p-polarized light onto a mirror with a diffraction grating causing light and dark spots to appear on the surface of the mirror.[20] After Wood discovered the phenomenon Fano and Rayleigh attempted to explain surface plasmon resonance. Not until 1968, when two different teams of physicists explored SPR, was the phenomenon understood. Otto was the first physicist to utilize SPR when he positioned a thin metal film of gold very near a prism, acting as the diffraction grating, allowing sample to pass between the film and the prism and creating what is known as the Otto configuration.[21] The same year as Otto, Kretschmann and Raether developed a similar method of exciting surface plasmon resonance but instead of leaving a space between the thin, metallic film and the prism, they placed the prism against the thin film and allowed fluid to pass over the thin film which is now known as the Kretschmann configuration.[22] Almost all modern day SPR experiments utilize the Kretschmann configuration because of the experimental complexity of positioning and maintaining the small gap between the metal film and prism using the Otto configuration.[23] Use of SPR for bimolecular experiments began in 1983 in Lundstrom's pursuit of label-free, real time detection of molecular properties in which he compared different properties using ellipsometry, refractometry, and SPR. SPR was chosen as the most successful method because ellipsometry and refractometry requires light to be passed through the sample making light absorbing materials impossible to test.[24] Recently mass produced SPR instruments became available through several companies all using the Kretschmann configuration.

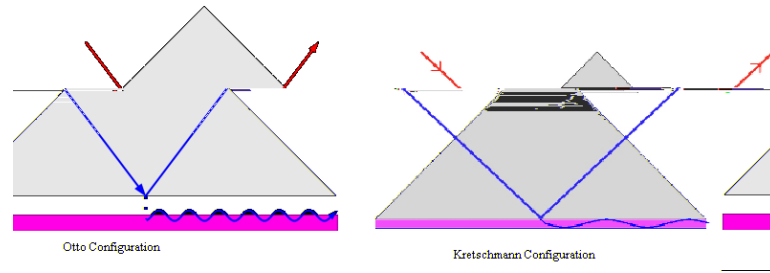


**Figure 2 – Otto Configuration compared to Kretschmann Configuration**

Developed in 1968, Otto and Kretschman created two different forms of surface plasma wave generation. Most commonly used today is the Kretschmann configuration.

### 1.3.2 Physics of SPR

Surface plasmons are oscillations of free electrons in a thin metallic film.[18] To generate a surface plasmon the essential ingredient is free electrons at the surface of the material being exposed to photons. The most common form of surface plasmon excitation is a two layer system of a metal, which acts as the source of the free electrons, and a dielectric which is an electrical insulator that can be polarized by an applied electric field. The Kretschmann configuration commonly utilizes a prism as the dielectric and a thin layer, ~50nm thick, of gold or silver as the metallic layer. Gold and silver are chosen for their surface plasma wave properties including propagation length, metal and dielectric penetration, and concentration of field in dielectric. (Table 1) Silver has slightly better characteristics than gold, but because of silver's general tendency to tarnish, gold is more frequently chosen as the metal for the metal-dielectric interface.[25]

**Table 1 – Characteristics of Surface Plasma Waves at Metal-Water Interface**

| Metal Layer supporting SPW               | Silver                     |                            | Gold                       |                            |
|--|----------------------------|----------------------------|----------------------------|----------------------------|
| Wavelength                               | $\lambda = 630 \text{ nm}$ | $\lambda = 850 \text{ nm}$ | $\lambda = 630 \text{ nm}$ | $\lambda = 850 \text{ nm}$ |
| Proagation Length ( $\mu\text{m}$ )      | 19                         | 57                         | 3                          | 24                         |
| Penetration depth into metal (nm)        | 24                         | 23                         | 29                         | 25                         |
| Penetration depth into dielectric (nm)   | 219                        | 443                        | 162                        | 400                        |
| Concentration of field in dielectric (%) | 90                         | 95                         | 85                         | 94                         |

The surface plasma wave (SPW) is an electromagnetic wave that propagates between the thin metal film and the dielectric. The SPW can be described using the dispersion relation (K) which uses the frequency of incident light ( $\omega$ ), the dielectric constants ( $\epsilon$ ) of both materials, the speed of light ( $c$ ), and the magnetic permeability ( $\mu$ ).[26]

$$K(\omega) = \frac{\omega}{c} \sqrt{\frac{\epsilon_1 \epsilon_2 \mu_1 \mu_2}{\epsilon_1 \mu_1 + \epsilon_2 \mu_2}}$$

The dielectric constant is also known as relative static permittivity and is used to describe how a material will concentrate electrostatic lines of flux.[27] The dielectric constant is a ratio of the amount of stored energy at an applied voltage relative to its permittivity in a vacuum.[28] When surface plasmons resonate with light, light will be absorbed causing a dip in the reflected frequency at which the surface plasmons resonate with the light. Essential to the SPR instrument, is the prism used to achieve a surface plasma wave of oscillating light and surface plasmons. The prism is needed because light must be slowed to match the resonant frequencies as shown in Figure 3, as light alone will never match the resonance frequency. [29]

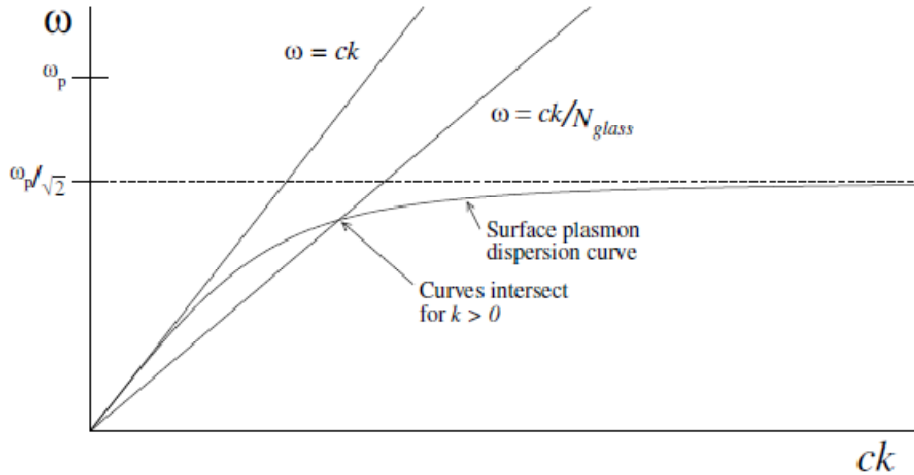


**Figure 3 – Graph of Dispersion Relationship**

When light alone ( $ck$ ) is reflected off metal the frequency ( $\omega$ ) never matches the surface plasmon dispersion curve. Using a prism ( $ck/N_{\text{glass}}$ ) allows the frequency to match the surface plasmon dispersion curve causing photons and surface plasmons to oscillate creating a surface plasmonic wave. Image provided by Stoltenberg et. al.

The surface plasmon wave then becomes extremely sensitive to any change in the index of refraction of the dielectric medium above the metallic surface. To achieve the SPW, total internal reflectance must occur causing the incident light to be totally reflected at a critical angle,  $\theta$ . Listed below is the equation for the resonance angle,  $\theta_R$ , used to describe the angle at which light will be absorbed by the metallic film to form the SPW. At wider angles,  $\theta$ , the intensity of reflected light remains high while the absorbed light at  $\theta_R$  has little reflectance causing a sharp intensity dip in the reflected beam.[18] At this critical angle an evanescent wave propagates parallel with the metal surface. Orthogonal to the surface, the electric field component penetrates into the testing medium. When the index of refraction is modified, e.g. changes in medium or surface binding/unbinding events, the reflected intensity-dip shifts. The degree of shift in the intensity-dip can be quantitatively correlated to the sample medium being tested e.g. changes in testing medium, or presence of analyte.

$$\sin(\theta_R) = \sqrt{\frac{\epsilon_1 \epsilon_m}{(\epsilon_1 + \epsilon_m) \epsilon_2}}$$

**Figure 4 – Resonance Angle Equation**

Equation used to describe the resonance angle and associated intensity dip seen in the reflected beam of an SPR instrument. In the above equation,  $\epsilon_2$  is the dielectric constant of the prism,  $\epsilon_m$  is the real part of the dielectric constant of the metal film (exposed sensor surface), and  $\epsilon_1$  is the dielectric constant of the testing medium to which the metal film is faced.

Fresnel equations, Figure 5, are used to describe the shift in resonance angle based on a function of the thickness and refractive index of the three SPR instrument layers: prism, gold, and testing medium. While the prism and gold properties remain constant, changes in the testing medium will result in a shift of the resonance angle and the corresponding intensity dip. Measurement of the shift in the reflected intensity dip indicates a change in the refractive index of the testing medium. Possibilities for changes in the refractive index include different mediums (e.g. water, air, ethanol), different concentrations of one medium, or the presence of analyte.[30]

$$\Delta\theta_R = c(n)d$$

**Figure 5 – Fresnel Equation**

In the above equation, the shift in resonance angle,  $\Delta\theta_R$ , is a function of  $c(n)$ , a function of the refractive indices of the prism, metal film, and sample medium, and their associated thicknesses,  $d$ . Using the BI-2000 changes in the refractive index of the sample medium can be measured as far out as  $d \approx 200\text{nm}$ .

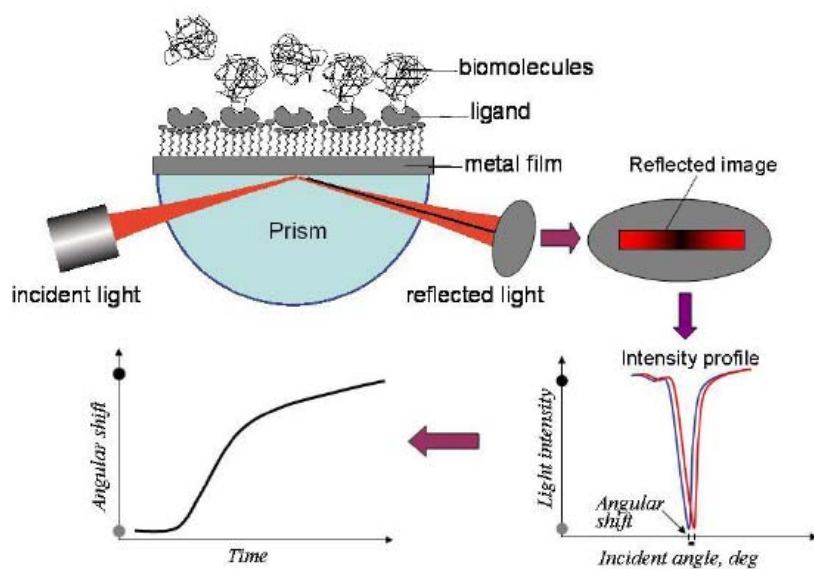


**Figure 6 – Cartoon of Surface Plasmon Resonance Detection**

As incident light passes through the prism and reflects off the metal film, photons are absorbed and resonate with surface plasmons causing a dip in the intensity profile at a specific angle  $\theta_R$ . When the refractive index in the medium above the metal film changes (biomolecules attaching to ligands bound to the metallic surface), the resonance angle,  $\theta_R$ , changes, causing a shift in the angle of the intensity dip. The difference in the dips is known as angular shift and can be monitored over time to assess the physiochemical properties of the sample. Image provided by Biosensing Instruments Inc.

## **1.4 Biomarkers**

Many of the Cal Poly Biofluidics projects were based on the goal of colorectal cancer detection. Current methods of screening, outlined in Appendix C, are intrusive and often unused by many potential colorectal cancer patients leaving them vulnerable to the disease. Current research exists providing a noninvasive approach for early detection of colorectal cancer using biomarkers. A biomarker is any molecule used to distinguish or signal a specific biologic state. Most commonly used to indicate disease state, biomarkers are any molecules, most commonly proteins, used to distinguish the pathology of a disease. Currently several biomarkers are associated with the development of colorectal cancer including high levels  $\alpha$ -Methylacyl-CoA

racemase (AMACR)[8], overexpression of cyclooxygenase-2(COX-2)[31], and adenomatous polyposis coli (APC) mutations[32]. Using microfluidic devices blood samples can be processed and purified to isolate biomarkers of interest for detection. Through proper sample processing and treatment, simple and effective tests can be utilized to screen for colorectal cancer using only a blood sample.

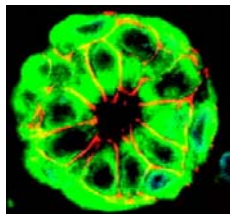


**Figure 7 –  $\alpha$ -Methylacyl-CoA Racemase Molecule**

Elevated AMACR expression strongly correlated with presence of colorectal cancer. If detected quickly, early diagnosis proven to greatly increase chances of survival. Image provided by Witkiewicz et.al.

Current methods for detecting biomarkers from processed blood samples include enzyme linked immunosorbant assay (ELISA)[13], real time polymerase chain reaction[33], and surface plasmon resonance[18]. Surface plasmon resonance is the detection method of interest offering the ability for real time sample analysis, gaining information on binding kinetics, utilizing microarray technology, and relatively simple testing procedures.[18] Detection of disease biomarkers using SPR has many advantages over traditional methods, most notably the noninvasive nature of the screening compared to a colonoscopy or sigmoidoscopy, as well as the real-time sample analysis compared to the lengthy immunoassays currently available. By creating miniaturized, low-cost detection fluidics together with a microfluidic sample processing system, disease screening could be readily available to areas lacking the means for clinical settings needed for traditional testing.



### **1.5 BI-2000 SPR**

The SPR instrument used in these experiments is the BI-2000 (Figure 8) purchased from Biosensing Instruments. The machine can be broken down into four main components: syringe pump, fluidics, sensor chip, and electronics. The syringe pumps are used to induce fluid flow through the fluidics of the system. Commonly filled with a solution conducive to the experiment the syringe pumps are first used to void the fluidics of the SPR of any air. Following a continuous flow from the syringe pumps the inject port of the fluidics are used to introduce sample to one line of the fluidics. The other line of the fluidic system remains free from analyte to provide a comparison and using computer algorithms cancel any environmental noise. The fluidics move test samples to the gasket covering the sensor chip which is divided into two channels, one channel used as a control for the experiment and the other channel used to conduct the SPR experiment. The sensor chip is composed of a thin gold layer, chosen for its electromagnetic wave properties, and BK-7 optical glass. The surface chip is often functionalized with molecules intended to interact with the analyte. Underneath the sensor chip lays a prism of BK-7 glass through which an incident infrared beam of p-polarized light is passed and reflected back to an optical sensor. Once the analyte has reached the sensor chip and interaction has begun a shift in the reflected beam should be detected and the resulting magnitude of the shift plotted onto the accompanying software. The angle and length of the reflected beam shift can be used to calculate specific properties of the experiment including kinetics, concentration, charge, and other physicochemical properties. The sample is then washed through the outlet valve to a waste beaker.

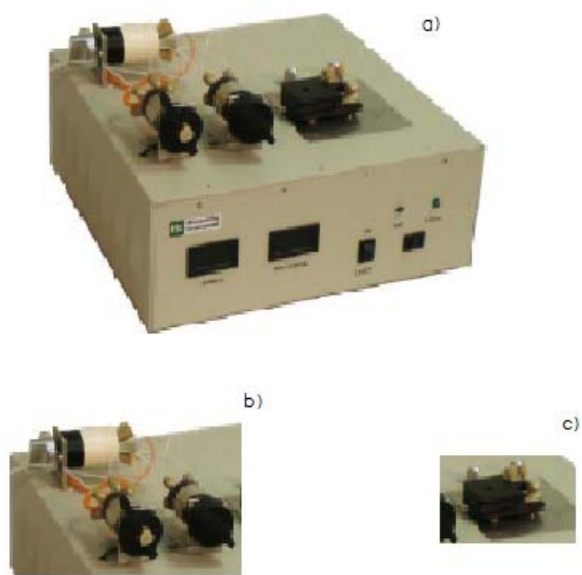


**Figure 8 – BI-2000 SPR Device**

a) Full view of the BI-2000 b) View of factory fluidics including injection port pictured in bottom left of image c) View of factory flow gasket with two inlets for two channel flow and outlet for waste.

### 1.5.1 Fluidics

Fluidics is used to describe the conduit system used to transfer fluid and samples from microfluidic devices or sample injection valves to the sensing chip. Current fluidics allows for sample injection through the injection port (Figure 8 b) but does not allow for a direct connection to any other biofluidic device. Replacement parts for factory fluidics are also very expensive making the factory fluidics impractical for inexpensive point of care diagnostics used in world health. Fluidics are made up of 1/16" OD fluorinated ethylene propylene tubing flowing into channel selection valves leading to a flow injection valve. The flow injection valve leads to flow gasket allowing sample to pass over sensor chip and bind analyte. Channel selector valves and the flow injector valve make miniaturization impractical due to size and cost, raising need for low-cost effective valves for introduction of sample. Valves should also include universal fitting to allow direct connection to any future Cal Poly Biofluidics' microfluidic device.

### 1.5.2 Sensitivity

Instrument sensitivity is often a determining factor in detection device selection. Assessing sensitivity on the BI-2000 can be difficult to describe as with any SPR instrument. There are several metrics in describing the sensitivity of SPR and because the BI-2000 utilizes the Kretschmann configuration, angular sensitivity is often used to describe detection ability. Angular sensitivity refers to the machines ability to detect a shift in the reflected dip resulting from a change in the refractive index of the sample medium. Detection of the angular shift depends on several factors that contribute to the angular sensitivity of the machine. Prism material plays a huge role because the dielectric constant is a governing factor in the generation and propagation of the SPW. The wavelength of light used in the incident beam factors in detection of angular shift as a result of the penetration depth of different wavelengths in different metals (see Table 1). Choice of metal for the sensor surface has significant impact on the levels of refracted light and the amount of absorbed light to create the detectable dip in intensity.[35]

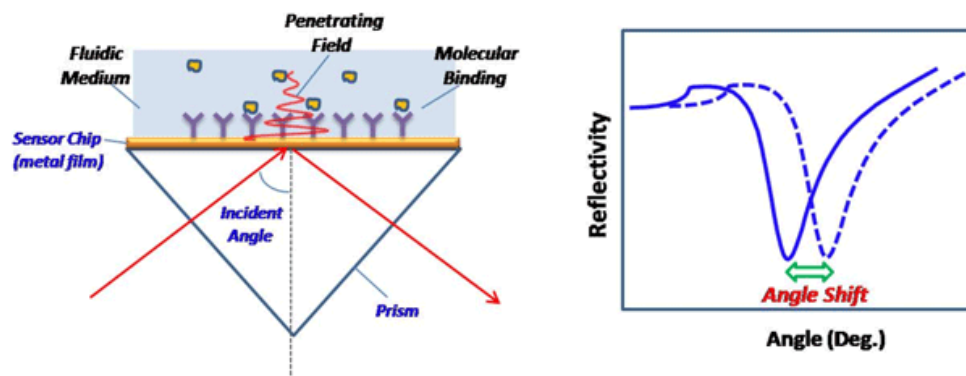


**Figure 9 – SPR Angular Shift**

Mass added to the surface of the sensor causes the resonant frequency to change resulting in a change of the absorbed frequency causing an angular shift. The angular shift is used to assess the presence of analyte and can be used to determine the concentration that the analyte is present.

Another metric used to assess SPR sensitivity is the change in the refractive index resulting from the medium being passed over the sensor chip. Changes in the refractive index are measured by refractive index units (RIUs). Changes in RIU can be used to assess changes in concentration, but does not effectively assess molecular binding to the surface of the chip. Measuring molecular binding is paramount in the proof of concept in this thesis. Molecular binding is often measured by surface mass measured in picograms per millimeter squared ( $\text{pg/mm}^2$ ). A term coined by the SPR community, resonant unit (RU), is equal to  $1 \text{ pg/mm}^2$  and an excellent metric for molecular binding.[34]

## **1.6 Restatement of Goals**

The goal of this project is the successful integration of upstream microfluidic devices with the BI-2000 SPR instrument, a feature the factory fluidics does not offer. Integrating the microfluidic bioseparation devices with a highly sensitive detection device is a major step towards low-cost point of care diagnostic systems needed throughout the world. In maintaining the theme of world health point of care diagnostics, the integration of the microfluidic devices should be low-cost and easily reproducible. To validate the in-house fluidic system a direct comparison between the factory fluidics and the in-house fluidics will be made using similar ethanol solutions. An additional proof-of-concept test will include binding 3T3 fibroblasts to the sensor surface and detecting the cleavage of cells using trypsin. A successful demonstration of the in-house fluidic system will have no leaks, form no air bubbles, and produce comparable results to factory fluidics. The in-house fluidic system will be able to establish independent flow in each channel of the detection surface. Another project goal is that the fluidics will be made only from mass produced, inexpensive equipment.

## **2 Methods and Materials**

### **2.1 Surface Plasmon Resonance**

Experiments conducted in this project were the first done on Cal Poly Biofluidics' BI-2000 surface plasmon resonance instrument. Before experiments could be conducted the instrument needed to be set up and calibrated. As partial fulfillment of this thesis and Robert Natividad's senior project a protocol for setting up and calibrating the surface plasmon resonance was developed and tested. Calibration is paramount to assuring detection ability and reducing instrument variation for further experiments. To assure accuracy calibration must be done from time to time to monitor instrument performance. Initial calibration was performed per Robert Natividad's protocol (Appendix A).

#### **2.1.1 Software**

Provided with the instrument, the Biosensing Instruments software is used to analyze and interpret results from the SPR optical sensor and display them as a graph of angular shift over time for each channel and as the difference in angular shift between the two channels.

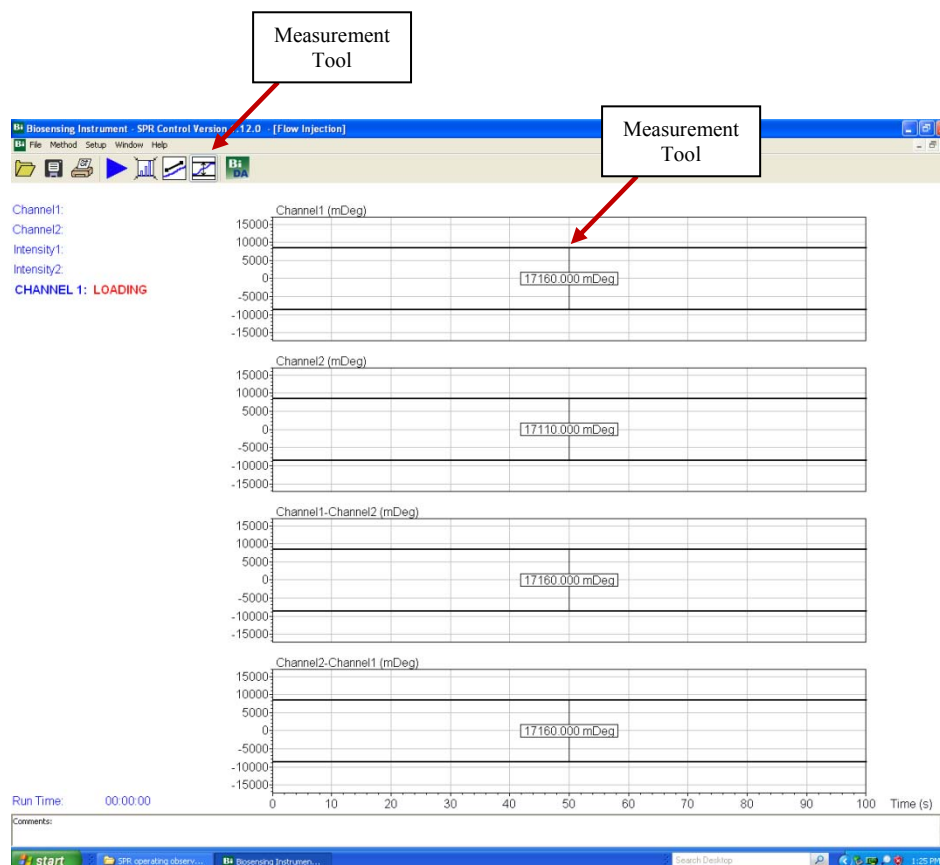


**Figure 10 – Screenshot of Biosensing Instrument Software**

Screenshot of the main user interface for monitoring the angular shift on the BI-2000 SPR instrument. The three charts are used to monitor each individual channel and the difference between the channels during experimentation. Highlighted is the measurement tool built into the software to measure SPR angular shift.

The common mode of operation for the SPR software is flow injection mode which will detect the difference in angular shift based on the change in resonant frequency at the sensor chip surface and plot it as a function of time. Also available is the electrochemistry mode which will plot the angular shift as a function of potential.

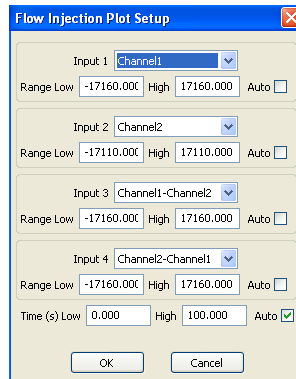


**Figure 11 – Screenshot of Flow Injection Setup Screen**

Screenshot of the Flow Injection Menu used to allow the user to control the parameters of the detection plot. Used to control which channels are monitored and the range of angular shift that needs to be incorporated in the plot.

### 2.1.2 Flow Injection Mode

In flow injection mode the results from angular shift over time can be plotted per channel or as a difference between the channels over time. The software can be used to control the amplification at which the optical sensors detect angular shift. Amplification can range from 1X to 1000X, however, using higher gains, such as 100X or 1000X, limits angular shift detection limits and should only be used to detect extremely small changes in shift. For calibration the gain will be set to 10X and is able to detect shifts of  $\pm 2.5$  degrees. Sampling rate is another degree of freedom offered by the BI software usually kept between 1-10 Samples per second (S/s). Once calibration is complete the results from the calibration can be input in the calibration menu to control the sensitivity of the instrument and assure that the factory standard sensitivity is achieved.

### 2.1.3 Noise

Noise is the presence of artificial angular shift caused by outside influence other than the analyte such as lights, heat fluctuation, or flow variation. During experimentation the sensor chips detect angular shifts across both channels and plot the results in real time for each channel. Two-channel detection is a very useful tool in maintaining a control to compare resonant frequency shifts between solution with analyte and solution without analyte. During calibration each channel was separately injected with incremental dilutions of ethanol and compared to a factory standard to accurately calibrate each channel. The software also includes a real time plot of the difference between angular shifts in the channels to effectively eliminate room noise leaving only the shift resulting from the presence of analyte. Thermal noise equally affects both channels making it hard to control using the difference algorithm programmed into the software resulting in slightly skewed results unless room temperature can effectively be controlled. Limitations in noise reduction exist because when the fluidics is set in serial mode flow is stopped in the control channel allowing thermal drift to more dramatically affect one channel and not the other. Truly parallel fluidics that offered continuous flow throughout the experiment would be the best solution to effectively using the difference algorithm and reducing thermal noise.



#### 2.1.4 Sample Timing

Timing is critical for experimental control when injecting sample over the SPR detection chips. A sample timing calculator is also built into the BI software taking user input of sample size and flow rate to calculate the time it takes the sample to travel the 100  $\mu\text{L}$  loop leading to the SPR sensing chip. Initially analyte is injected into the injection valve which is set to inject. The injection valve is then turned to load to allow the analyte to enter the fluidics. Changing the injection port from inject to load starts the timer on the software main screen. In-house fluidics will not be able to tie into the factory fluidics timer system making it necessary to use clear tubing and solution dye to test unknown solutions. Experiments must be done to assess the shift in SPW caused by inert dyes.

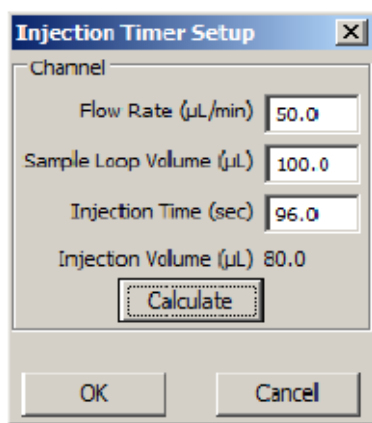


**Figure 12 – Screenshot of Injection Timer Screen**

Screenshot of the injection timer menu used to calculate the time sample needs to reach the flow cell. Once loaded with all experimental parameters the injection time will load into the main screen letting the user know when the injected solution has reached the surface of the chip.

### 2.1.5 Calibration

Calibration was conducted per Robert Natividad's protocol (Appendix A) using prescribed dilutions of 200 proof ethanol. Dilutions of 1, 0.5, 0.25, 0.0125, 0.00625 percent ethanol diluted in deionized water were used to determine the sensitivity of each channel. Ethanol was chosen for calibration because of the predetermined expected angular shift defined by Biosensing USA. Each channel was individually calibrated with two goals, first to assign a new calibration value and second to assure that the change in angular shift directly correlates with the strength of ethanol solution.

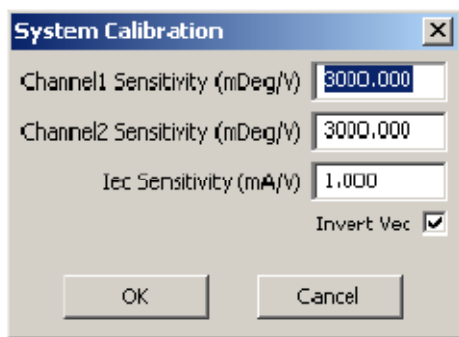


**Figure 13 – Screenshot of System Calibration**

Screenshot of the System Calibration menu where each channel is default set to 3000 mDeg/V on both channels. Once calibration is performed a unique value based on the equation listed in Figure 14 will be assigned for both channels.

From the factory the SPR is assigned a calibration value of 3000 mDeg/V, however, because of the sensitivity of the SPR instrument and the inherent differences from instrument to instrument, a new calibration value was assigned unique to the Cal Poly BI-2000 SPR instrument. The factory specification for angular shift of 1% ethanol injected into a deionized water system is 1.0 mDeg. Using the new-calibration-value equation defined by Biosensing USA (figure 14) the unique calibration value is determined by comparing the measured angular shift from a 1% ethanol solution injected into to pure deionized water system.

$$\text{New Calibration Value} = \text{Old Calibration Value} \times \frac{\text{Expected}}{\text{Measured}}$$

**Figure 14 – Calibration Equation**

Used to assign unique calibration value to each channel based on calibration experimental results.

Aside from the new calibration value, the calibration was also done to assure that a linear relationship exists between the percentage of ethanol and the change in angular shift. Calibration should show that if a 1% solution of ethanol causes a 1.0 mDeg shift than a 0.5% solution of ethanol should result in a 0.5 mDeg shift. Each dilution in the calibration procedure was a half step below the previous starting at 1% ethanol and ending at 0.00625%. After injection of each sample a comparison was made to assure that the angular shift resulting from each dilution was approximately half of the angular shift of the sample before it. This process is done on both channels for calibration.

#### 2.1.6 Factory Fluidics

Packaged on the BI-2000 SPR instrument is fluidics used to introduce and transfer solution and analyte. Fluidics is the term used to describe the system of valves, tubing, and pumps used in fluid movement during SPR experimentation. Central to this thesis is the premise that sample detection must be low cost and easily integrated. Developing new fluidics required a full understanding of the equipment involved in the factory fluidics. The factory fluidics is made up of a syringe pump, micro diameter tubing, switch valves, and a flow cell with gasket. These parts in concert create fully developed flow over the SPR sensor chip allowing nearly seamless

introduction of analyte for experimentation. The short comings of the current system are the lack of a junction point to tie in outside microfluidic devices used in sample pretreatment and the lack of independent flow in each channel.

#### 2.1.7 Syringe Pump

Experimentation on the SPR instrument began with the experimental buffer solution used to establish flow and a signal baseline. Maintaining constant flow throughout the experiment requires the use of syringe pumps containing experimental buffer solution. Provided with the BI-2000 is a dual-syringe pump used to establish steady flow across both lines. Precision crafted drive screws slowly advance a carriage against two syringe plungers to introduce experimental buffer solution into the system. Flow rate can be controlled on the syringe pump from 10 nL/min to 10 mL/min and can carry syringes varying in size from 10  $\mu$ L to 60 mL. Varied flow rates can drastically affect the angular shift of the SPR instrument, making precision controlled flow essential to experimental success. The need for precision controlled flow makes the syringe pump an essential part of both the factory fluidics and the in-house fluidics.



### **Figure 15 – Dual Syringe Pump**

Pictured is the dual syringe pump is used to control flow to both lines of fluidics. Controls on the front allow manipulation of pump speed based on syringe size inputs.

#### 2.1.8 Tubing

Tubing provided by the manufacture for the fluidic system has several limitations with regards to bridging sample pretreatment devices to the sample detection system. Fluorinated ethylene propylene (FEP) was the tubing of choice for the BI-2000 fluidics. While the tubing effectively serves as a conduit for sample passage from the syringe pumps through the channel selection valves to the flow cell, FEP's ability to form simple junctions is limited by its rigidity. Connections between the FEP tubing and valves, pumps, and the flow cell on the BI-2000 are created with the help of specially made lure fittings on each end of every tube. Receiving the special made lure at the end of each tube also requires special fittings for each component of the fluidic system. High costs associated with the tubing and fittings needed to effectively connect the tubing to the different components makes it prohibitive as a low cost solution in bridging the gap between sample pretreatment and sample detection.

#### 2.1.9 Valves

Physical manipulation of the fluidics was done using three valves, a six-port through-the-handle injection valve, a four-port channel selection valve, and a six-port mode select valve. The channel selection valve was used to control the line flow to each channel. The mode select valve was used to manipulate the style of flow through the channels with the choice of either single or

series. Single flow refers to line independent flow while series runs both lines together. The injection valve was used to introduce sample solution for detection. The injection valve provided with the BI-2000 is a very sophisticated valve able to effectively eliminate air bubbles and connect to the manufacturer's software to accurately time the movement of analyte. Because of their sophistication, injection and channel selection valves used in the BI-2000 fluidics are the most problematic portion of the low cost connection between sample pretreatment and sample detection. The injection valve ties in both lines from the syringe pump and using the channel selection valve analyte can be introduced to either or both channels. Before experimental solutions reach the SPR sensor chip it passes through three valves shown below (Figure 16) starting with the mode valve that allows use the use of one or both channels, if both channels are used the channel that the analyte is introduced to can be selected using the channel selection valve, and finally the injection valve used to introduce analyte. While the system is very sophisticated and allows a high degree of variability in experimentation, it also presents several limitations. Use of the injection valve requires a precision made syringe with a specific gauged needle for sample injection. The valves individually are also very cost prohibitive at approximately \$800.00 per valve.

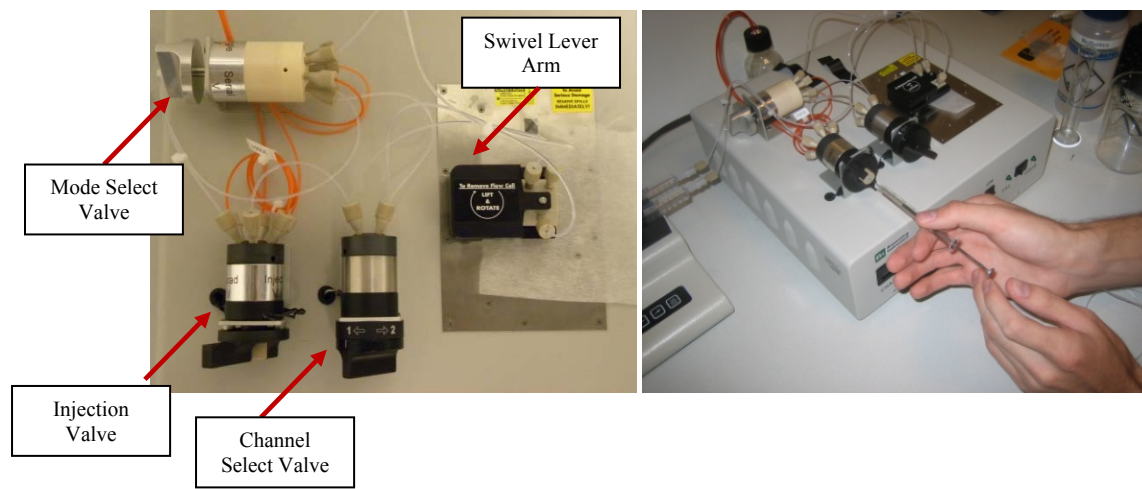


### Figure 16 – Factory Fluidics Valves

Left: Actual image of the three valves used to manipulate the movement of the fluidics as they travel to the flow cell. Right: Sample introduction through the handle injection port.

#### 2.1.10 Flow Cell and Flow Gasket

The final component of the fluidics system factory installed on the BI-2000 SPR instrument is the Polyether ether ketone (PEEK) flow cell and PDMS gasket. Used to develop laminar flow at the site of the SPW, the flow cell and flow gasket offered the greatest challenge in creating the low cost connection between microfluidic pretreatment devices and the SPR sensor chip. Comprised of two inlet ports tied into the fluidics system with special fittings designed to hold the FEP tubing and one outlet going to a waste beaker, the flow cell and gasket maintains a watertight seal over the SPR sensor chip using only force provided by a swivel arm component of the instrument. The swivel arm component of the instrument is designed specifically to fit the dimensions of the flow cell. Complex design and specialized fittings make the factory flow cell and flow gasket incompatible with the idea of low cost integrable diagnostic fluidics.

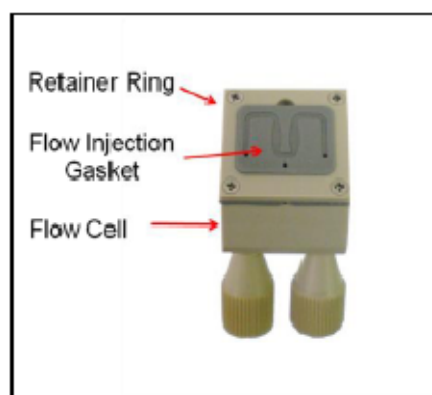


### **Figure 17 – Flow Cell and Gasket**

Pictured is the factory flow cell made of PEEK and includes specialized fittings (bottom) to accept tubing. Flow gasket made of PDMS with W design creating fully developed laminar flow as the fluid passes over the SPW which forms on the inner two tracks towards the center of the gasket.

## **2.2 In-House Fluidics**

### **2.2.1 Tubing**

Factory fluidics for the BI-2000 SPR use FEP tubing which is a fairly expensive, rigid plastic polymer. Due to the rigidity of the FEP tubing creating junctions between switch valves, inlets, and outlets made it difficult to manipulate using limited resources. While FEP tubing is stronger, the less expensive tygon tubing will be used because of its elasticity and ease of junction between inexpensive valve switches, other tygon tubing, syringes, and the experimental flow cell. Tygon tubing with similar inner diameter as the factory fluidics, 0.02", is readily available at approximately \$0.36 per foot compared to the FEP at \$1.00 per foot. Tygon tubing was joined using a sheared 24 gauge syringe tip which can press fit inside the tubing to join two ends of tubing or serve as a brace to hold the small parts fittings while bonding using epoxy.





### **Figure 18 – Tygon tubing with Labsmith Fittings**

Pictured is the fittings provided with the Labsmith 3 port valves. 360  $\mu$ M fittings used to interchangeably tie into the valve. Using a syringe tip for support, the tygon tubing was bonded to the fitting using epoxy.

#### 2.2.2 Valves

LabSmith 3 port manual channel selecting valves (Figure 19) were used to allow analyte introduction in the in-house fluidics. Labsmith also provides 360  $\mu$ m fittings that can be bonded to the Tygon tubing using epoxy as shown below (Figure 18) allowing interchangeability between which lines are controlled by each port. The valves were selected because of their low cost microfluidic nature and relative ease of analyte introduction to the fluidic system. At each site of fluid introduction to the in-house fluidics a 24 gauge syringe tip was inserted intended to be used multiple times but easily replaced if contamination occurs. The syringe tips fit a universal syringe head allowing multiple volume syringes to be attached to the fluidic system for analyte introduction or solution flow. Shown in Figure 20, the main flow will run through valve 1 into 2. Valve 1 will lead to the syringe pump while Valve 2 for each line will lead to the inlets of the flow cell. At the time of sample injection the valve will be switch to ports 2 and 3 allowing sample injection through port 3. Once the entire sample has been injected through port 3 into the main line leading to the SPR sensor chip the valve will be switched back to port 1 and 2 resuming flow and allowing the analyte to pass over the SPR chip.

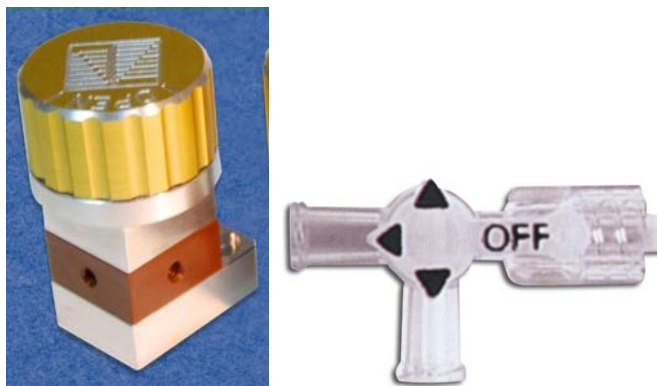


**Figure 19 – Labsmith Tri-Port Valve, Three-Way Stopcock**

Left: Pictured is the Labsmith 3-port valve used in the in-house fluidic system. The Valve consists of three inlets with a two channel selector knob on top using one port for flow from the syringe pump, one port for flow to the flow cell, and the last port for sample introduction. Right: 3-way stopcock used to replace the Labsmith 3-port valve for the ethanol experiments.

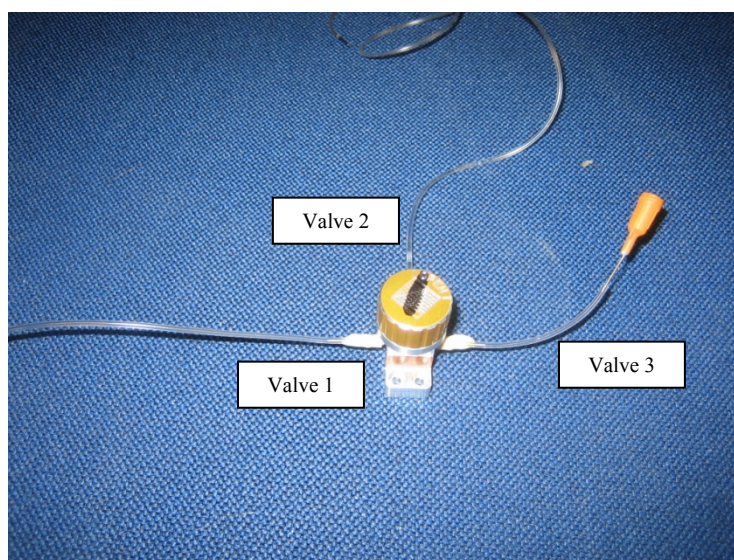


**Figure 20 – In-House Valve Assembly**

Pictured is the in-house fluidic system including the Labsmith 3-port valve and the three lines the valve controls. Valve 1 leads from the syringe pump and is used to maintain system flow of experimental buffer solution. Valve 2 leads to flow cell inlet. Valve 3 is used for sample injection.

### 2.2.3 Flow Cell

The inlets and the outlets were formed by placing a thin PMMA plate over the PDMS gasket with three separate 1/16" holes drilled through allowing access to each channel. The Tygon tubing was loaded slightly farther than the entire width of the PMMA plate allowing penetration into the gasket and a seal was formed between the PMMA plate and the three tubes using epoxy. The use of epoxy means that periodically new tubing and a new plate may need to be used as they are not interchangeable due to the permanent nature of the epoxy bond. The seal between the PMMA plate was formed by applying slight even pressure to the PMMA plate against the PDMS gasket and the SPR sensor chip. To maintain the tubing that is bound to the Labsmith 3 port channel selection valve, a sheared syringe tip is used to bind the main line feeding into each inlet to a small segment of tubing extending from each inlet and the outlet of the PMMA plate.

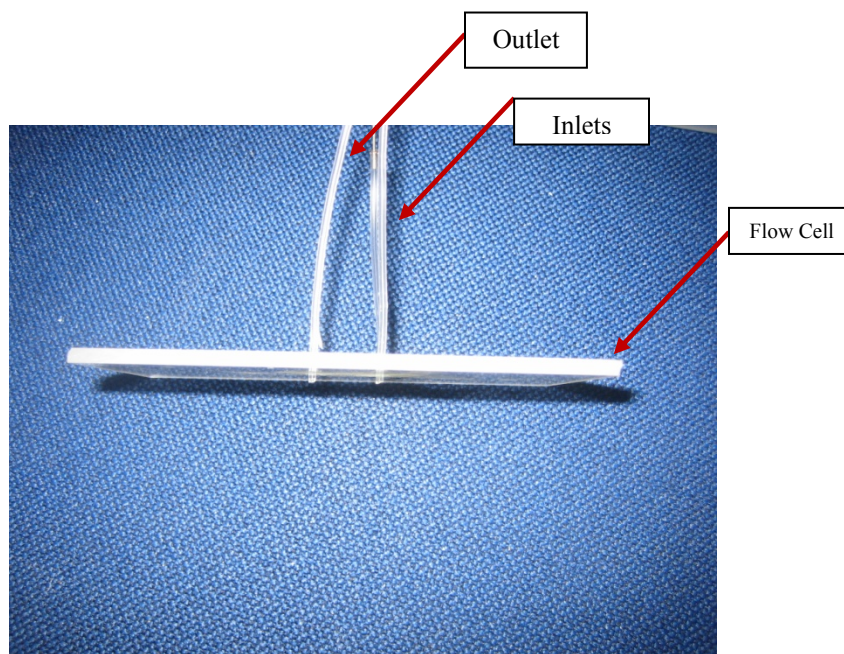


**Figure 21 – In-House Flow Cell**

Pictured is the flow cell with the inlet and outlet lines that have been held in place with epoxy. The flow cell is a 1/4" plate of PMMA used to sandwich the flow gasket against the SPR sensor chip.

#### 2.2.4 Flow Gasket

The most intricate and integral part of the fluidic system is the two channel flow gasket that allows independent flow over the SPR sensor chip. The gasket required several iterations to achieve a watertight flow that allowed unrestricted access of the sample solutions to the SPR sensor chip. The flow gasket also needed to be able to form the watertight seal using only pressure and no permanent binding allowing the SPR sensor chips to be reused. Generation of a plasmonic wave requires the SPR sensor chip to have smooth, even seating over the prism with direct contact on the thin layer of index matching oil. Any mass that accumulate on the bottom of the chip will cause the chip to no longer be parallel causing the SPW to diminish, thus making it impossible to incorporate the chip in anyway to the flow gasket. Each of these requirements teamed with the theme of low cost fluidics were considered in the design of the flow gasket.

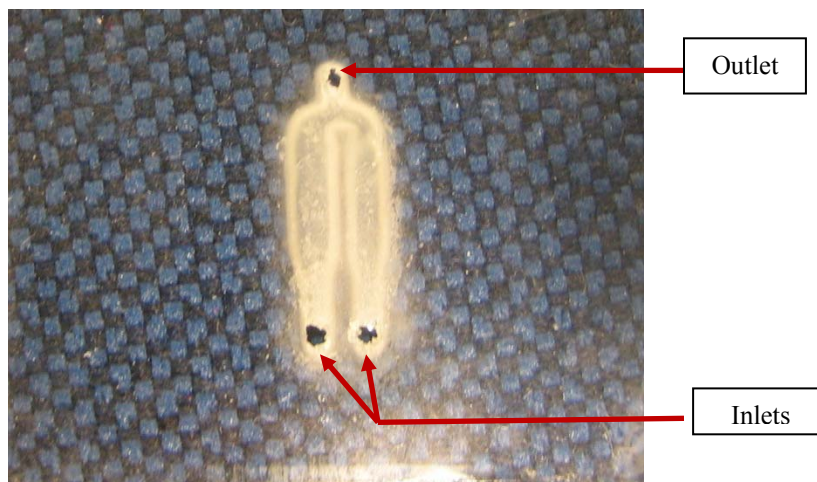


**Figure 22 – Top View In-House Flow Gasket**

Pictured is the in-house SPR flow cell. When placed on a SPR sensor chip and the flow cell is pressed on top of the flow gasket a water-tight seal is formed and flow will travel from the two channels to the outlet.

#### 2.2.5 Flow Gasket Design

The two channel design of the experimental flow gasket was a simple derivation from the factory gasket. Production SPR instruments like the BI-2000 have an encased laser and sensor assembly which limits the possibilities in the size or arrangement of flow channels. Through contact with Biosensing USA, detailed drawings of the factory flow gasket were provided to help in the design of the experimental flow gasket. Both gaskets contain three main parts, starting with the two inlets which widen into the two detection channels and converge to one main outlet. The experimental gasket's detection channels and outlet have the exact same dimensions as the factory fluidics to maintain similarity in SPR signal. The inlet channels deviate from the original design for simplicity and to allow access using the low cost tygon tubing. The original design incorporates a "W" channel design to establish laminar flow. For the in-house fluidics the inlet channels were widened and all bends were removed creating a straight path that tapers directly into the detection channels. Using AutoCAD as an electronic drafting tool, the design was created and imported into an FEM modeling software, COMSOL, to assure laminar flow would be achieved. Once design were created and verified the next step was to create the actual gasket. Several manufacturing techniques were used to develop an effective prototype.

#### 2.2.6 Gasket Material Selection

Initial attempts at developing a flow gasket incorporated the use of store bought scrapbooking double sided tape. Cutting channels into the tape and sandwiching the tape between the SPR sensor chip and a thin PMMA plate would allow for simple, low cost, reusable microfluidics. Tape was placed firmly against a 2"x3"x1/4" PMMA plate and using the laser cutter, channels were cut out of the tape, then holes were cut through both the tape and the PMMA at the inlets and the outlet. Using tape, however, consistently failed the watertight test

allowing flow between outside of the channels. The next iteration involved developing a negative mold by laser etching into the PMMA. Several materials were poured into the mold to create a watertight cast including, PDMS, store bought silicone adhesive, and Gelest OE43. While PDMS showed the most promise as a low cost watertight solution, ridges carved into the PMMA mold during the laser etching process created pathways for fluid to escape the channels. The final iteration involved a novel approach to developing micro-mold systems using store bought candle wax.

## **2.3 Manufacturing**

Inherent to world health diagnostics is low cost supplies made from easily accessible materials such as plastics. Precision manipulation of plastics and polymers requires moderately sophisticated tooling creating the need for a master mold which could easily be replicated. Available at California State Polytechnic in San Luis Obispo, California is a 100 watt laser cutter capable of precision carving  $\frac{1}{4}$ " thick PMMA. The laser cutter offers a high degree of precision and variability in cutting depths. Able to penetrate as deep as  $\frac{1}{2}$ " PMMA or simply etch a microchannel pattern in 40 micron tape leaving the underlying PMMA unmarked, the laser cutter proved to be the perfect tool for developing low cost diagnostic tools. Using procedures outlined in Appendix C, an AutoCAD model of the experimental flow gasket was designed to create a master mold.

### **2.3.1 AutoCAD**

Use of the laser cutter requires a moderately advanced level of understanding of the AutoCAD system. Built into AutoCAD are drivers that correlate line types used in the design to

the specifications with which the laser cuts. Other software such as Adobe Illustrator may also be used to import designs to the laser cutter, however, because of prior knowledge and use AutoCAD was the preferred software. AutoCAD also offers a highly advantageous design platform for designing intricate features on the micro-scale. The highly developed design platform also poses as a disadvantage to many designers as the multitude of commands, tools, and features requires a degree of training to be able to create a useable design. Once trained, the software offers several possibilities for microchip manufacturing.

### 2.3.2 Double Sided Tape Design

Several designs were considered for the flow cell and gasket resulting in several AutoCAD designs, all with different features and line styles. The original design utilized double sided scrapbooking tape requiring a two layer system on AutoCAD. Shown below (Figure 23) the red layer used a vector cut at speed of 4, power at 100 percent, and pulses per inch maxed out at 1000. Using these settings the red layer was programmed to pass through a 1/4" piece of PMMA and a piece of double sided tape. The purpose of the 3 red through holes was to provide inlets and an outlet for the flow cell. The blue layer was used to create the channels of the flow gasket by cutting only through the 40 micron tape leaving the PMMA unchanged. The specifications of the blue layer are speed set to 2, power set to 1%, and the pulses per inch dialed down to 970. The blue layer cut was able to successfully cut the tape while preserving the PMMA. The tape inside the channels was then carefully removed using #7 surgical tweezers under a stereo microscope to preserve the channel quality and assure no debris was left inside. As stated above the double sided tape proved to be too weak of a bond to maintain a watertight seal.



**Figure 23 – 2 Layer Flow Channel Design**

Above is a screenshot of the AutoCAD design used for the double sided tape flow cell. The design is broken into two layers, blue is used to etch through the tape and red is used for a through cut that will pass through both the tape and the PMMA.

### 2.3.3 Negative Mold

After abandoning the initial double sided tape design a new design using a negative master mold which could then be used to make multiple casts of the flow gasket was adopted. Designing a negative mold requires that the area surrounding the flow gasket be carefully etched away leaving the channels raised on the mold. Once a compound such as PDMS is poured on the mold it will fill in the etched area creating microchannels for fluid to pass through. Creating an etch pattern around the desired microchannels was done using the design below (Figure 24). Laser etching requires the use of a hatch pattern shown in green. When imported from AutoCAD to the laser, the hatch will translate to a tight raster pattern for the laser. Creating the hatch required making a small ring around the original design and filling it using the “hatch” command. The green layer will be etched into the PMMA by maxing speed at 100, maxing power at 100%, and maxing pulses per inch at 1000. Because the solid hatch pattern translates to a raster cut, the laser will only cut approximately 500 microns deep.



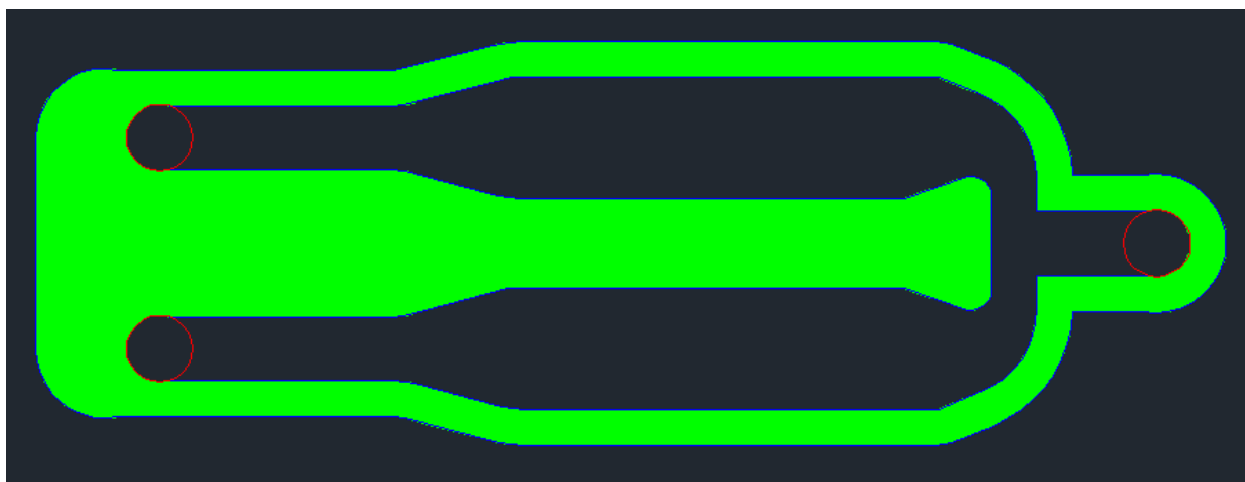


**Figure 24 – Laser Etch Flow Channel Design**

Screenshot of the AutoCAD model used to create the negative mold. The green layer will etch into the PMMA creating a negative mold for the PDMS to be poured into. The red layer is used for a through cut in the PMMA.

#### 2.3.4 Wax Mold Design

The final design is a simple form of the original design where the only cut will be a through cut to completely remove the channels from the PMMA plate. The through holes of the first design were removed and instead of the blue etch layer the whole part will be turned to a red through cut layer. Settings for the red layer remained the same for the laser cutter and the pattern was cut from the PMMA plate to create a form for the candle wax mold. Removing the raster etch from the master mold design eliminated the ridges formed by the laser rastering the PMMA. While the laser etch serves to be a useful tools in many biofluidics applications, the resulting ridges created by negative etch will make it difficult to create a watertight seal when used s a mold for a PDMS cast.



**Figure 25 – Final Wax Channel Design**

Screenshot of the AutoCAD model used to create the wax mold for the flow gasket. The red layer is used to make a cut through the PMMA creating a void for the wax to pour into.

### 2.3.5 Laser Cutter

The Cal Poly laser cutter found in the Mustang '60 lab in the Bonderson building offers the ability to serve many low cost biofluidics needs. After training and certification listed in Appendix C, any student can gain access to the laser cutter. Most commonly used to cut PMMA materials, the laser cutter is a powerful tool in making precision cuts based on a preloaded design. Limitations on size exist for the laser cutter as the size of the part begins to fall below 100 microns because the laser has a tendency to melt the PMMA causing it to pool in the channels or microfeatures refilling what it initially cut.

### 2.3.6 Wax Mold

The final two stages in developing the flow gasket required careful preparation creating first a wax mold and then a PDMS mold from the wax. Preparation of the wax mold was done in

the Cal Poly ATL, having no real cleanliness requirements; a wax candle was placed in an aluminum foil boat on a hot plate at 80° C for 10 minutes to allow the wax to melt. Once melted, the wax was carefully poured into the void created by the through cut of the laser and excess wax was scraped off using the edge of a glass slide. After smoothing the top and bottom of the still viscous wax with the edge of a glass slide, the PMMA plate containing the wax mold was placed in a refrigerator for 5 minutes to allow the wax to fully harden. The hardened wax then simply pressed out of the mold due to slight shrinkage from cooling and a perfect cast of the channels was made from wax. Following the creation of the wax mold PDMS must be prepared to create the final flow gasket.

#### 2.3.7 PDMS

PDMS is a silicone based polymer used in many biomedical applications. Useful because of its ability to be mixed as a liquid and set as an elastic solid, PDMS is the gasket of choice for the experimental SPR flow cell. Many biofluidics projects that utilize a PDMS mold require a clean room setting to reduce contamination, however, because of the simplicity and size of the channels used in the flow gasket, use of a clean room was not necessary. PDMS comes in a two part mixture that when separate remain in a liquid form but when combined will form a rubbery solid after a setting period. Using the vacuum chamber located in the SPR lab of Cal Poly, the PDMS was degassed at approximately 1 atm, gauge pressure, until all visible bubbles fell out of solution. Degassing the PDMS removes all the air bubbles and allows the liquid PDMS to conform to every contour of the mold. Normally PDMS could be placed in a lab oven at 150° C for 15 minutes to set, as was done for the second flow gasket design, but because the PDMS must conform to the wax mold it must stay at room temperature for 24 hours to set. After 24

hours the PDMS will harden around the wax mold. Removing the wax required the use of a lab oven set to 80° C causing the wax to liquefy and pour out leaving smooth watertight flow channels.

## **2.4 Ethanol Experiments**

Validation of the in-house fluidics will be achieved through experiments measuring the angular shift caused by ethanol solutions. Using the literature provided by the manufacture, known angular shifts will be elicited by using specific dilutions of ethanol. These dilutions of ethanol will be injection into both the factory fluidics and the in-house fluidics for direct comparison. The ethanol experiment will follow all the same protocols as Robert Natividad's calibration protocol (Appendix A) using the same materials only using the in-house fluidic system in lieu of the factory fluidics and using one concentration of ethanol.

A 1% and 0.5% ethanol injection will be done on the in-house fluidics for comparison to the factory fluidics. The choice for 1% and 0.5% ethanol is based on the calibration of the SPR instrument and the background knowledge of the effects of ethanol on the Cal Poly BI-2000 SPR instrument. The 1% and 0.5% dilutions of ethanol will be from the same batch as those used in calibration and following the in-house fluidics experiment a follow up calibration will be done on the factory fluidics to validate the results.

## **2.5 Fibroblast Experiment**

A more complex experiment to gauge the ability of the experimental fluidic system, involves the detection of the removal of fibroblasts from the SPR sensor chip's surface using 1X trypsin. Fibroblasts are stem cells critical in wound healing and are found in the extracellular

matrix in mammals. Best known for their resilience, fibroblasts are also relatively inexpensive, easy to culture, and readily available in the Cal Poly Biomedical Engineering department.

Through the assistance of Tommy Harper and Dr. Trevor Cardinal, 3T3 fibroblasts were cultured onto 6 SPR sensor chips over a two day period. 3T3 fibroblasts are a mouse strain of fibroblast and the most common used in fibroblast stem cell research. During the two day culture the cells were kept in a carbon dioxide incubator used to control temperature, humidity, carbon dioxide content, and oxygen content promoting cell replication and growth. The cells are initially suspended in a media that provides nutrients to the cells allowing metabolic functions to proceed as cell replication occurs. Throughout the two day period the cells will begin to adhere to the surface of the chip due to extracellular matrix protein secretion. The target confluence, or cell coverage on the surface of the chip, is achieved at 100% assuring an even distribution of cells on the chips surface.

At the time of experiment, the SPR sensor chips with the cells adhered to the gold surface were removed from the incubator and imaged using a stereo microscope. Before experimentation the SPR laser was warmed for an hour up using a “dummy” chip and flowing phosphate buffered saline (PBS) solution to establish a steady baseline of intensity dip. Once a baseline was established and the chips were initially imaged using the stereo microscope, an SPR chip with a confluent layer of 3T3 fibroblasts was washed using PBS solution and placed on the SPR prism and the factory flow cell was lowered over the channel to begin experimentation. The chip is washed with PBS solution prior to experimentation to clear the chip of any media because the media would act to deactivate the trypsin. Once the SPR chip loaded with fibroblasts is placed on the prism and the incident beam was turned on the plasmonic wave began to form and an intensity dip baseline was created.

PBS was flowing over the top of the fibroblast loaded cell at 0.150 ml/min. Once a baseline was established for an SPR sensor chip loaded with 3T3 fibroblasts with PBS solution passing over, a 50 $\mu$ L sample of 1X trypsin was introduced into the fluidics. Using the Biosensing software sample calculator the time it takes for the trypsin to reach and pass over the SPR sensing chip based on injection size, and flow rate was calculated. Once the trypsin passed over the top of the SPR sensor chip the flow was stopped to allow the trypsin to cleave the cells from the surface using hydrolytic actions. The trypsin was given one minute to react with the cells based on recommendations from Dr. Kristen Cardinal. After one minute, flow was resumed at 0.150 ml/min allowing PBS solution to wash away any cleaved cells. After allowing a baseline to reestablish, post trypsin injection, the surface of the chip was cleaned with a lens wipe to mechanically remove any cells on the surface and the new baseline was monitored.

A second SPR chip loaded with fibroblasts was run on the factory fluidic system under the same initial conditions. The second run of the factory fluidics on the fibroblast loaded SPR chip will vary from the first run after the trypsin has passed by placing the sensor chip back into the media well without wiping the surface clean. The purpose of the variation is to image the second cell and visualize the removed cells from the trypsin filled channels. During each experiment, real-time angular shift will be plotted using the Biosensing software and saved for comparison to the in-house fluidics under the same conditions.

The in-house fluidics was then set up next to the factory fluidics utilizing the same syringe pump setup to flow PBS at 0.150 ml/min. The initial use of the factory fluidics attempted to use the lever arm that secures the factory fluidics to the top of the SPR sensing chip. The lever arm caused the experimental flow cell to bow proving to be ineffective at maintaining a

watertight seal in the channels. Hand force was applied to the in-house fluidics to maintain watertight flow. Two runs were done on the in-house fluidics similar to the factory fluidics.

The first run established a baseline with PBS solution passing over the fibroblast loaded sensor chip, followed by introduction of 50  $\mu$ L of 1X trypsin. To gauge when the trypsin is over the sensor chip the pink trypsin was monitored through the clear tygon tubing. Once over the sensor chip, flow was stopped allowing the trypsin to hydrolyze the bonds holding the fibroblasts to the surface, releasing them into solution. After one minute, PBS flow was resumed. Once intensity dip baseline was reestablished, the surface of the SPR sensor chip was wiped clean to mechanically remove all cells on the surface.

The second run of the in-house fluidics did not include wiping the surface of the chip at the end of the experiment but the chip was placed back into media to be examined under the stereo microscope. After the experiments the whole system was cleaned with ethanol and all supplies were disposed of as biohazard waste.



### **Figure 26 – 3T3 Fibroblast Cells**

Pictured is mouse fibroblast stem cells used in initial experiment. Cells have secreted extra cellular matrix protein allowing them to bind to surface.

## **2.6 Experimental Design**

Experiments conducted during this thesis were designed to achieve the goals stated in Section 1.1 and answer the following questions:

- Can the factory BI-2000 SPR instrument be calibrated per Robert Natividad's protocol (Appendix A)?
- Can a fluidic system be developed that allows leak-free flow from in-house biofluidic devices to the SPR instrument for low cost?
- Can a detection comparison be made between the factory fluidics and the experimental fluidics using trypsin to cleave 3T3 fibroblast cells from the surface of an SPR chip?
- Can a detection comparison be made between the factory fluidics and the experimental fluidics using dilutions of ethanol?

To answer these questions several experiments will be set up and conducted as described in Section 2.7.

## **2.7 Experimental Set-Up**

### **2.7.1 Degassing Solution**

The purpose of degassing solutions was to avoid experimental error caused by bubbles falling out of solution in the fluidic system. All experimental solutions must be degassed before use in the SPR instrument. To degas solutions, the solutions were placed in open containers inside the vacuum chamber (Figure 27) and a vacuum of approximately 20 psi was drawn for 10-15 minutes. During degassing the containers were agitated to remove any air bubbles.





**Figure 27 – Degassing Chamber**

Degassing chamber located in the Cal Poly SPR lab, used to degas all solutions used in the SPR instrument.

### 2.7.2 Warm Up

The purpose of the warm up is to achieve consistent results when experimenting with the BI-2000 SPR instrument. Before any experimentation was conducted on the SPR instrument, the machine was warmed up. Warm up was conducted by flowing degassed deionized water through the factory fluidics, over the calibration SPR sensor chip. Syringe pumps flowed deionized water at a rate of 0.150mL/min and the factory data acquisition software was set to record. During warm up the SPR signal will drift significantly, approximately 150-250 millidegrees(mDeg), over the course of 60-90 minutes. Warm up was completed once the signal evened out and experimentation could begin.

### 2.7.3 Calibration

The purpose of the calibration is to create accurate, repeatable experiments in the future when using the Cal Poly BI-2000 SPR instrument. Calibration was performed per Robert Natividad's protocol (Appendix A), using all prescribed equipment. Initially a 10% ethanol solution was created by using Thermo Scientific micropipettes to aliquot Acros 200 Proof ethanol into 9 mL of deionized water. The 10 mL of the 10% solution will be used in all dilutions for experimental consistency. The smaller dilutions will be prepared as follows (Table 2) using

either the Thermo Scientific 100-1000  $\mu\text{L}$  micropipette or the 20-200  $\mu\text{L}$  micropipette, as appropriate:

**Table 2: Ethanol Solution Preparation Schedule for Calibration**

| <b>10% Ethanol (mL)</b> | <b>Deionized Water (mL)</b> | <b>% Ethanol</b> |
|-------------------------|-----------------------------|------------------|
| 1                       | 9                           | 1.0000           |
| 0.5                     | 9.5                         | 0.5000           |
| 0.25                    | 9.75                        | 0.2500           |
| 0.125                   | 9.875                       | 0.1250           |
| 0.0625                  | 9.9375                      | 0.0625           |

Calibration was conducted at approximately 70° F along with all other experiments for experimental control. Before experimentation the machine was allowed a warm up as described in Section 2.7.2, all solutions were degassed per Section 2.7.1.

#### 2.7.3.1 Expected Calibration Results

Provided in the BI-2000 User's Manual, are the expected results of a calibration of the instrument. Shown below, Figure 28, is the expected shift profile observed with each dilution of ethanol. As seen in Figure 28, the 1% ethanol solution is supposed to elicit a 60 mDeg shift upward, followed by a plateau period while the solution remains inside the channels, and a sharp decline back to baseline. Each subsequent dilution of ethanol listed in Table 2 should elicit half the angular shift as the dilution before it.

B

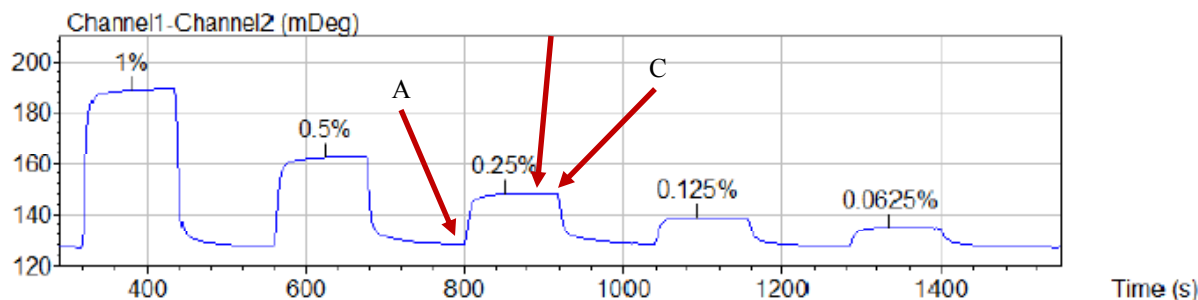


**Figure 28 – BI-2000 Expected Calibration Using Ethanol**

Pictured above are the ideal calibration results using the BI-2000 SPR instrument and the dilutions of ethanol prescribed in Table 2. A) Spike seen after ethanol injection. B) Plateau experience while ethanol is inside the flow channels. C) Sharp decline back to baseline upon resumed flow of deionized water.

Any shift different than the 60 mDeg expected shift caused by the 1% solution required the use of the New-Calibration-Value equation, Figure 14. Once a new calibration value was calculated it was entered into the System Calibration, Figure 13.

#### 2.7.4 Watertight Testing

The purpose of the watertight testing is to assure no leaks form in the in-house fluidic system during use. A visual test is done using Fast Green FCF, also known as Green Dye #3, over white paper to highlight any potential leaks. The syringe pumps shown in Figure 15, used to control the flow through all fluidic systems, were set to a max flow rate of 0.150 mL/min, the maximum flow rate seen in experimentation. Watertight testing must be done on all fluidic parts to assure no leaks exist at any junctions. Junctions include: syringe tip junctions in tubing, tubing junctions at the flow cell, the flow cell/flow gasket/SPR sensor chip junction, and the junctions at the Labsmith 3-port valves. In place of the SPR chip during watertight testing, a glass microscope slide was used for watertight testing. It is expected that no leaks exist before beginning experimentation.

### 2.7.5 Ethanol Experiment

The purpose of the ethanol experiment is to provide a comparison between the results generated using the factory fluidics to the results generated using the in-house fluidics. Similar in purpose to the Fibroblast Experiment, Section 2.7.6, a better comparison between the factory fluidics and in-house fluidics can be made because the response produced by the ethanol is well known. The fluidic system went through a modification, for ease of experiment purposes, exchanging the Labsmith 3-port valve with a generic three-way stopcock with luer-lok fittings. The experiment followed the same protocol as the calibration, only using two dilutions of ethanol, 1.0% and 0.5%. Two BD 10 mL syringes were filled with degassed deionized water to serve as the carrier buffer solution. The two dilutions of ethanol, 1.0% and 0.5%, were taken from the sample prepared for calibration, Section 2.7.3. Two BD 1 mL syringes with luer-lok tips were filled with 1 mL of degassed 1% ethanol and were tied directly to the three-way stopcock. The experiment began with the stopcock valve leading to the ethanol syringes turned off and allowing flow from the syringe pumps to pass through at 0.050 mL/min. Once a baseline was established the stopcock valve was turned to stop flow from the syringe pump and allow flow from the syringes. The entirety of both syringes was injected at the same time allowing ethanol to enter both channels independently. Once the full injection of ethanol had been given, the stopcock valve was adjusted to stop flow from the syringes and open flow to the syringe pump which was flowing at 0.050 mL/min. While the 1% ethanol solution passed through the SPR fluidics, two BD 1 mL syringes were filled with 0.5% ethanol and tied injection port of the three-way stopcock. Once baseline was reestablished from the 1% ethanol injection, the 0.5% ethanol injection can be performed. Similar to the 1% injection, for the 0.5% injection the

stopcock valve was turned so flow from the syringe pump was blocked and the entirety of both syringes could be loaded into the in-house fluidics. After injecting the ethanol, the stopcock valve was turned to allow flow from the syringe pump and reestablish baseline. The results were then compared to a post experiment calibration.

#### 2.7.5.1 Expected Ethanol Experiment Results

The results from the ethanol experiment conducted on the in-house fluidics should produce similar angular shift profiles to those seen in the calibration. For the 1% ethanol solution, a 60 mDeg upward shift should occur followed by a decline back to the baseline. The 0.5% ethanol solution should produce approximately half the shift seen in the 1% injection at 30 mDeg. The standard upward spike followed by the plateau and quick drop back to baseline seen in Figure 28 may not be seen in the in-house fluidics because of the variable timing of the ethanol injection. The ethanol injection for the in-house fluidics will be done by hand, while the factory fluidics controlled the injection from the injection valve, Figure 16, maintaining consistent flow throughout the experiment. The varied flow from the manual injection into the in-house fluidics will likely produce a more rounded peak of angular shift, opposed to the square profile seen using the factory fluidics.

#### 2.7.6 Fibroblast Experiment

The purpose of the fibroblast experiment is to provide a comparison between the results generated using the factory fluidics to the results generated using the in-house fluidics. 3T3 fibroblast cells cultured in Cal Poly's tissue engineering lab were prepared in media containing

Dulbecco's Modified Eagle Medium (DMEM) High Glucose, Fetal Bovine Serum, penicillin streptomycin (P/S), and Fungizone. The purpose of the media is to provide the cells with nutrients and prevent bacterial growth during culture. For culturing, the cells were kept in a Corning 6 chamber cell culture dish and cultured in a SL Labs CO<sub>2</sub> incubator at 37°C and 5.0% CO<sub>2</sub> for 72 hours to allow 100% confluence. After incubation, the cells were taken directly from the incubator and imaged using an Olympus BX41 microscope at 10X. After imaging the cells were taken directly to the SPR lab. At the time of experiment the room was 70° F and all supplies, besides the SPR sensor chips containing the fibroblast cells and the 1X trypsin, were kept at room temperature. The sensor chips were slightly warmer than room temperature due to incubation in the SL Labs incubator and the trypsin was cooler than room temperature at 38°F, due to necessary refrigeration during storage. The trypsin used was graciously provided by Kristen Cardinal, however, because of preparation time and cost involved with the trypsin, only 1 mL of trypsin was provided, limiting experimentation to four trials. One-hundred mL of Phosphate Buffer Solution (PBS) was prepared and provided by Trevor Cardinal, and served as the carrier buffer solution. Both the PBS and trypsin were degassed for 15 minutes prior to experimentation per section 2.7.1. The SPR sensor chips were all grabbed using the 2ASA Technik forceps from the upper right corner to avoid damaging cells in the center of the chip.

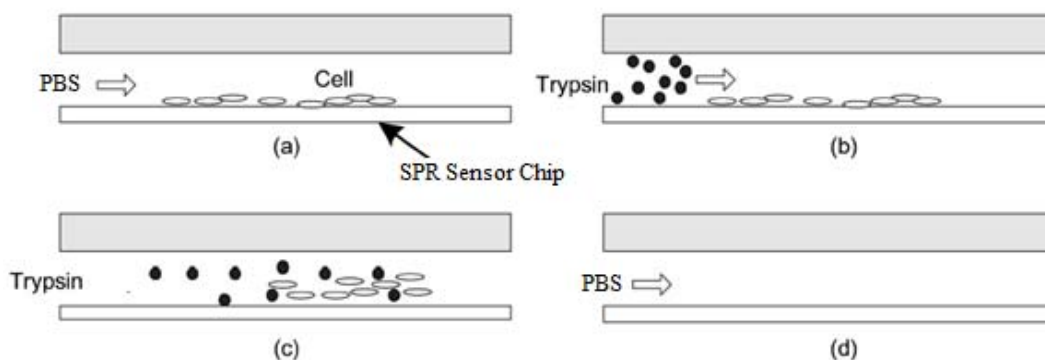


**Figure 29 – Fibroblast Experiment Cartoon**

Cartoon of fibroblast experiment conducted on both factory and in-house fluidics. A) Establish baseline by flowing PBS over 3T3 Fibroblast Cells B) Introduce trypsin to the flow cell C) Stop flow allowing trypsin to cleave cells D) Resume PBS flow to clear flow cell. Image replicated from Lei et al. [16]

#### 2.7.6.1 Fibroblast Experiment with Factory Fluidics

The chip was placed in a manner similar to the calibration experiment to avoid bubble formation underneath the chip in the index matching fluid provided by Biosensing Instruments. Following degassing, the factory syringes were each filled with 10 mL of PBS to serve as the carrier buffer solution. Once the SPR chip was in place, using the factory fluidics, the mode valve was set to “serial” and the syringe pumps were started at a rate of 0.150 mL/min (Figure 29-A) After establishing a baseline with the PBS, 250  $\mu$ L of 1X trypsin was loaded into the Hamilton 250  $\mu$ L syringe and injected into the injection valve (Figure 29-B). Using the injection timer, flow was stopped by turning off the syringe pump once the trypsin reached the SPR sensor chip and allowed to sit for 1 minute per Kristen Cardinal’s advice (Figure 29-C). After 1 minute, PBS flow resumed (Figure 29-D). For trial 2 the chip surface was wiped clean using a Kimwipe tissue, and placed back on the SPR to reestablish baseline with PBS. Trial 1 was not wiped clean, instead the SPR sensor chip was immediately imaged under the microscope.

#### 2.7.6.2 Fibroblast Experiment with In-House Fluidics

The in-house fluidic experiment required the factory flow cell to be removed from the swivel lever arm, Figure 16, allowing pressure to sandwich the flow gasket between the flow cell and SPR sensor chip. Once the flow cell assembly was firmly in place the experiment could begin. First, two BD 10 mL syringes, with Luer-Lok Tips loaded with 24 gauge blunt syringe tips, were each filled with 10 mL of PBS and placed in the syringe pump. Similar to the factory fluidics, the syringe pump was set to flow PBS at 0.150 mL/min to establish a baseline. Once baseline was established a BD 1 mL syringe  $\frac{1}{4}$  full of trypsin was tied onto the injection line. The Labsmith 3-port valve was switched over to the injection line to allow the trypsin to be injected. Once all the trypsin was injected the syringe pumps were turned on to move the pink trypsin down the line into the flow cell. After the trypsin reached the flow cell, flow was stopped for 1 minute to allow the trypsin time to cleave the cells. After 1 minute, PBS flow resumed. Trial 3 required that the SPR sensor chip be saved for imaging immediately following the experiment. Trial 4 required that the SPR sensor chip be wiped clean and a baseline be allowed to reestablish.

#### 2.7.6.3 Fibroblast Experiment Expected Results

All previous work performed on the Cal Poly SPR instrument only involved the use of ethanol, making the experiment involving fibroblast cells and trypsin the first of its kind at Cal Poly. Precedence does exist using a SPR instrument to detect the cleavage of cells using trypsin in the Lei et al. article, *A vortex pump-based optically-transparent microfluidic platform for biotech and medical applications*.<sup>[16]</sup> In the article, a proof-of-concept experiment was conducted, cleaving mouse L929 fibroblast cells from a gold sensor using trypsin. The L929



cells in the article were cultured in RPMI Medium 1640, a medium similar to the DMEM used in this experiment. Two main differences between the Lei experiment and the experiment done in this thesis is that the Lei experiment uses the RPMI medium as the carrier buffer solution, and then introduces a continual flow of trypsin to cleave the cells followed by a return flow of the RPMI. The work done for this thesis, in an effort to conserve, stops the flow of trypsin over the cells allowing it to cleave and uses PBS as the carrier buffer solution. The reason for using PBS as opposed to the DMEM is that trypsin can easily be deactivated by media. In an effort to maintain effective cleaving action using the small amount of trypsin in the thesis experiment, PBS was used instead of media. While the carrier buffer solution is different, and different volumes of trypsin were used, the angular shift profile seen in the Lei experiment (Figure 30) is roughly the profile expected during this experiment. The expectation is that after a baseline is established (Figure 30-A) the trypsin should induce an exponential curve downward (Figure 30-B) caused by the cleaving cells followed by a leveled out baseline lower than the original baseline (Figure 30-C).

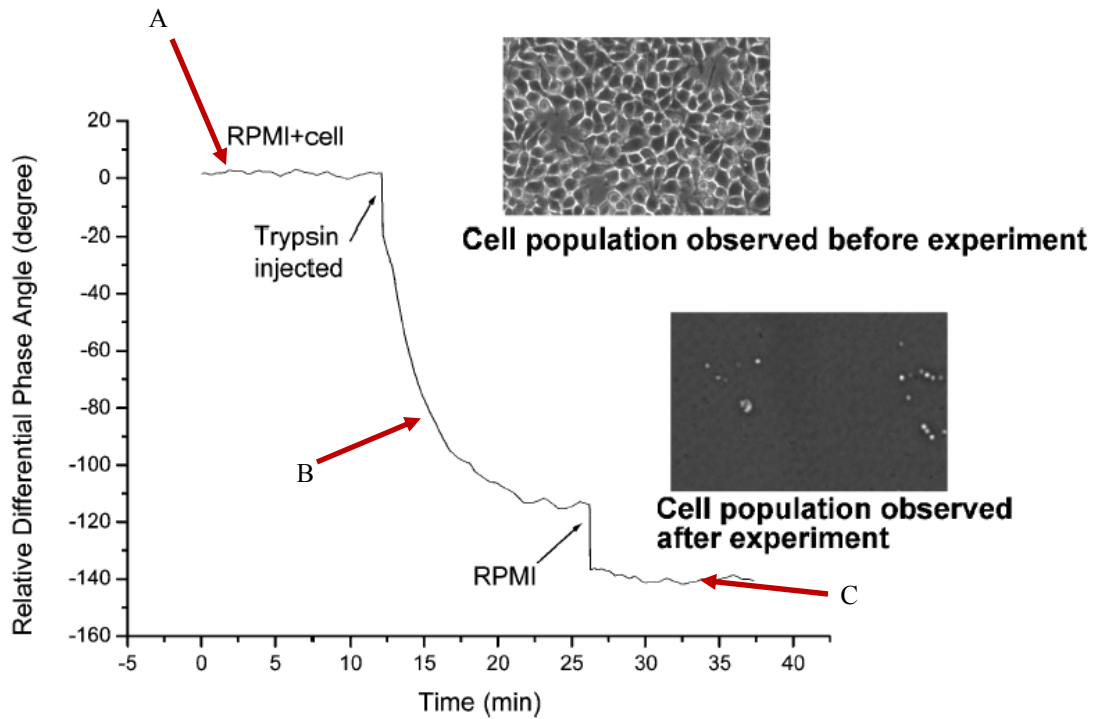


**Figure 30 – SPR Results from Lei. Experiment Cleaving Fibroblasts with Trypsin**  
 Shown above is the resulting SPR angular shift caused by cleaving L929 fibroblast cells with trypsin. A) Baseline created by RPMI media flowing over SPR sensor chip loaded with fibroblast cells B) Exponential curve caused by flowing trypsin over cells to cleave them from the surface of the chip C) New baseline created by RPMI media flowing over a blank SPR sensor chip. Image provided by Lei et al. [16]

## **3 Results**

### **3.1 Watertight Testing**

Before beginning experimentation, the fluidics were subjected to watertight testing. Green dye was used to evaluate the fluidic system by flowing through Tygon tubing bonded to the Labsmith 360  $\mu$ M fittings using epoxy (Figure 18). The test showed that the tubing could successfully act as a conduit for the fluid without leaks. Testing was performed on both lines leading to the two separate SPR detection channels. The green dye allowed the flow to be visualized through the transparent tubing for monitoring flow, air bubble formation, and any leaks. Line 1 proved to be problematic showing significant resistant flow and no flow through the 3-port valve. It was determined that the valve itself was impeding flow. Once a new 3-port valve was exchanged for the problematic valve, flow occurred as expected. Flow was established through line 2 and maintained when switching the Labsmith 3-port valve to the injection port (Figure 20). In both fluidic assemblies, initial runs of the green dye proved difficult as a result of the length of the line. Fluidic resistance due to the small diameter tubing in long lengths caused significant resistance such that the syringe pumps were unable to move fluid through. As a result of the high resistance caused by the long length of microbore tubing, the tubing was cut, from 5' to 1', the shortest length possible to carry out experimentation on the BI-2000 SPR. Calculations using the Hagan-Poiseuille equation show an order of magnitude reduction in the pressure needed to move fluid through the 1' line.

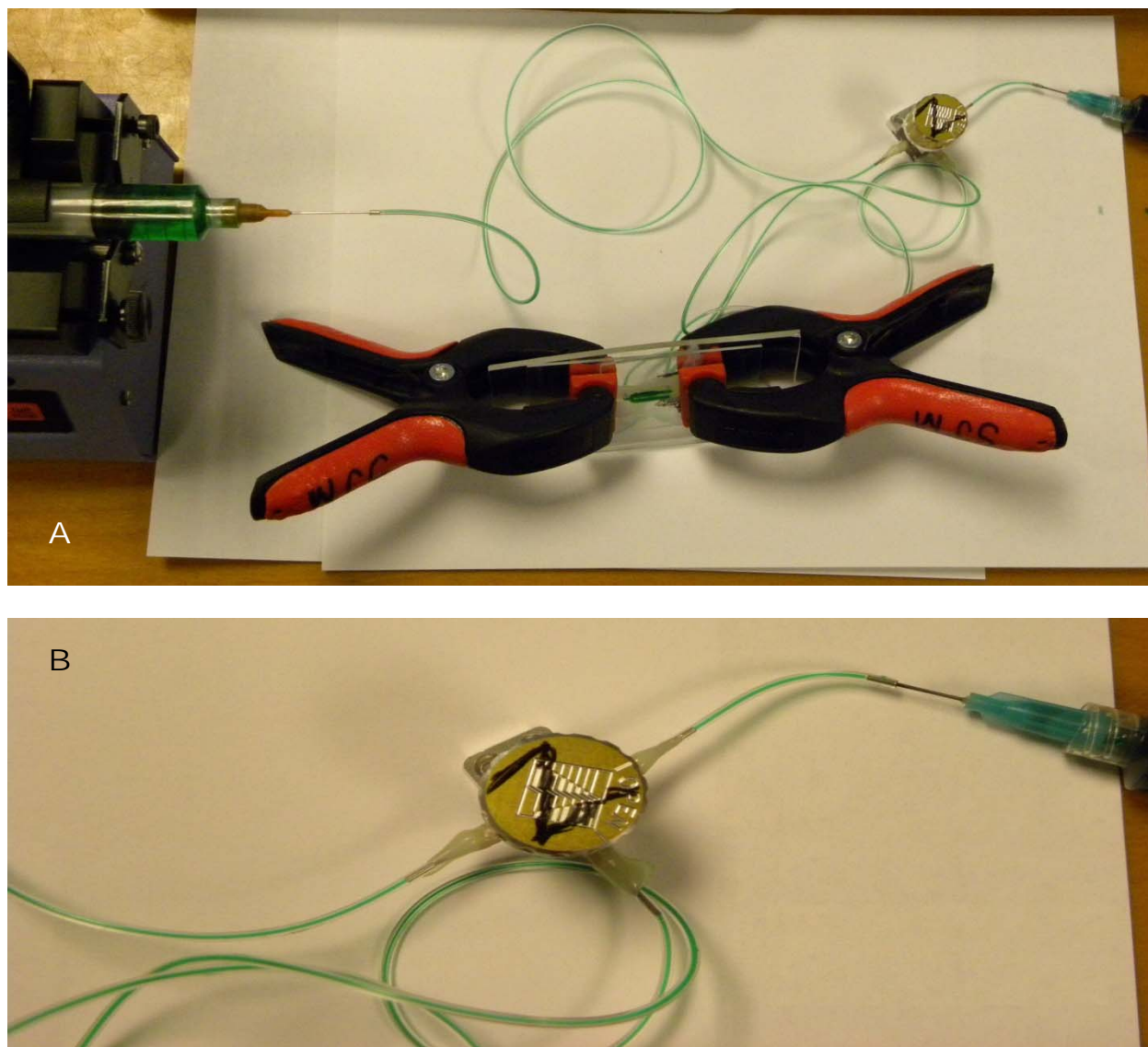


**Figure 31 – Watertight Testing of In-House Fluidics**

A) Green food dye was run through the lines at a rate of 0.150 ml/min, equivalent to the highest flow experience during experimentation, for the purpose of testing for leaks. The flow gasket was pinched between the flow cell and a glass slide using rubber clamps and flow was successfully established without leaks.

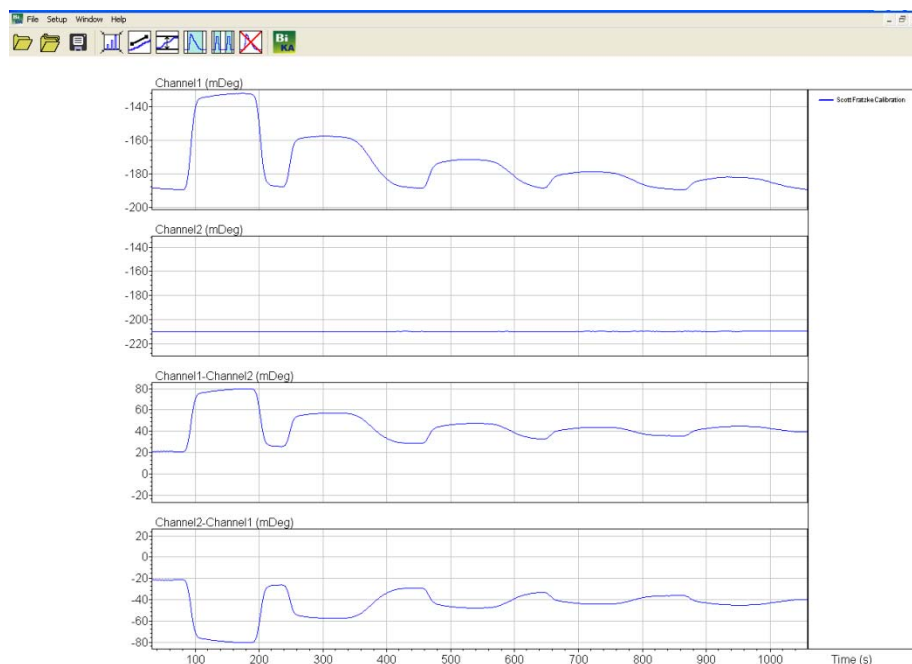
B) Using the 3-port valve, green dye was run through the injection line by slowly injecting to assure steady flow could be established. The valve successfully allowed a second sample line to tie into the main flow line coming from the syringe pump going to the flow cell.

While correcting flow problems due to the resistance of long microbore tubing and replacement of the non-working 3-port valve were relatively easy to correct, the greatest challenge in creating successful fluidics was developing watertight flow through the flow cell and flow gasket. The flow gasket, developed from PDMS, required access ports to the detection region. The flow gasket created two separate channels (Figure 22) through which sample solution could independently pass. The tubing was connected to the flow cell through the use of epoxy which created a strong watertight bond. The system proved to be watertight in an experiment that used green dye pumped through the system at 0.150 mL/min by the syringe pump, the max flow rate used in experimentation. To assure no leaks formed in any of the tubing junctions or the flow cell and gasket, green dye was successfully run through the tubing over white paper. To cross check and finalize the watertight testing green dye was injected manually by a syringe through each injection line and evaluated for any sign of leaks.

### **3.2 Calibration Validation**

Calibration was conducted on the Cal Poly BI-2000 (Appendix D) to validate the instrument. Validation was done by comparing the SPR signal shifts caused by injection different dilutions of ethanol solution listed in Table 2 against a deionized water baseline. Shown below is the angular shift response, in both channels, of the 5 ethanol injection listed in Table 2 on the Cal Poly BI-2000. (Figure 32)

A



B

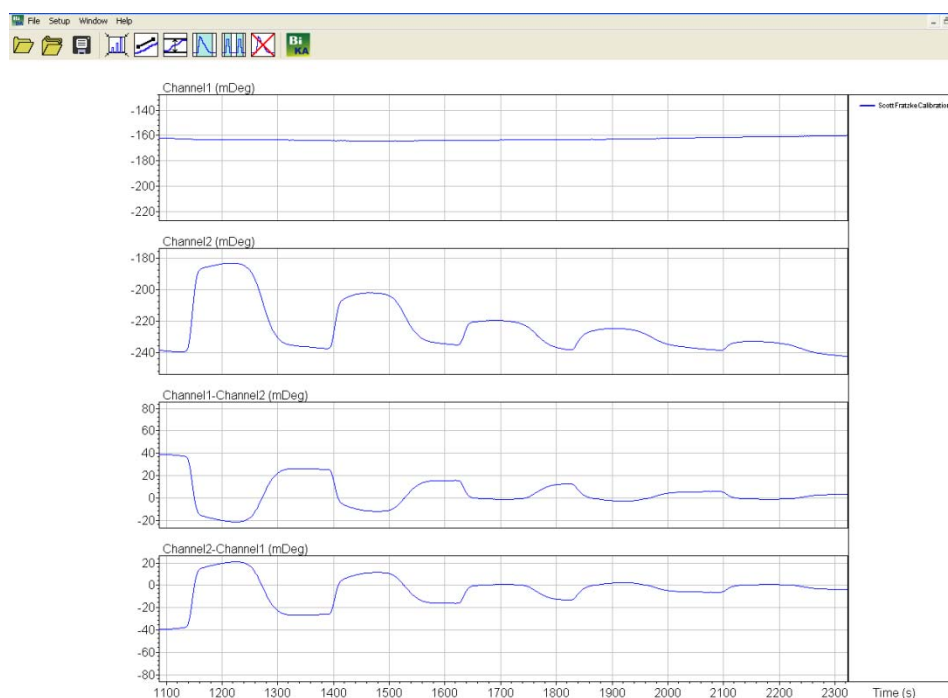


**Figure 32 – SPR Output: Channel 1, Channel 2, 1-2 and 2-1, Calibration Check**  
 Results of the calibration validation on both channels, showing the half step pattern that directly correlates to the half step dilution injection. Each dilution was injected three times and labeled as follows: 1-1.0000%, 2-0.5000%, 3-0.2500%, 4-0.1250%, 5-0.0625%. The half step pattern is the expected profile for calibration.

Shown in Figure 32, both channels of the Cal Poly BI-2000 SPR machine produced angular shifts that matched the expected angular shifts listed in the literature provided by the manufacture. The two conditions of successful validation are that a 1.0% ethanol solution elicits a 60 mDeg response against a deionized water baseline and that a linear correlation exists between the angular shift elicited and the dilution of ethanol. Figure 34 shows that, in both channels, a 60 mDeg response is observed upon injection of 1% ethanol and each successive injection, which was half the dilution as the one before it, elicited half the response. Successful conduction of the calibration validates the instrument for testing on the in-house fluidics.

### **3.3 In-House Fluidics Ethanol Experiment**

Key to the criteria of success of the experimental fluidic system was comparable results to the factory fluidics using a well developed experimental model. The proof of concept experiment used to measure the success of the experimental fluidics used the first two dilutions of ethanol similar to the calibration, 1.0% and 0.5%. The purpose of using the 1.0% dilution of ethanol in the in-house fluidics was to compare the angular shift seen using the in-house fluidics to the factory standard designated for calibration by Biosensing Instruments. The purpose for using the 0.5% dilution was to assure that a half step relationship exists between the dilution of ethanol used in the experiment and the resulting angular shift.

Using the lever arm, the in-house flow cell and flow gasket were firmly placed over the SPR sensor chip, all held firmly with the carved rubber stopper developed during the fibroblast experiment. Once in place, the syringe pumps began the flow of deionized water over the SPR sensor chip at 0.050 mL/min to develop a baseline and to check for air bubbles or leaks. The absence of air bubbles was confirmed using the machines built in viewing window that showed

two dark squares signifying the two flow channels were full and void of bubbles. After 5 minutes of steady deionized water flow, no visible leaks were detected and no air bubbles had formed allowing the signal baseline to form at 610 mDeg for channel 1 and 1040 mDeg for channel 2. Once a baseline was established on both channels, the three-way stopcock, used in place of the Labsmith 3-port valve, was switched from the carrier solution line to the injection syringe, and 1 mL of 1.00% ethanol was injected into each line. The injected ethanol was pushed forward through the fluidics by switching the stopcock back to the carrier solution line where the syringe pump began injecting deionized water behind the ethanol bolus. As the ethanol reached the SPR sensor chip, a 60 mDeg shift in SPR signal was observed for channel 1 and channel 2 (Figure 33). As the ethanol was being inject small tremors are noticed in the signal due to the uneven nature of the manual load, however, after the injection a smooth rounded angular shift is noticed for both injections. The rounded profiles observed in the results of the in-house fluidics are due to the evacuation time required for the larger channels. The same method for introducing the 1.0% ethanol was used for the 0.5% ethanol. The 0.5% ethanol produced an angular shift of 30 mDeg for channel 1 and channel 2, approximately half of the angular shift seen in both channels during the 1.0% ethanol injection (Figure 33).



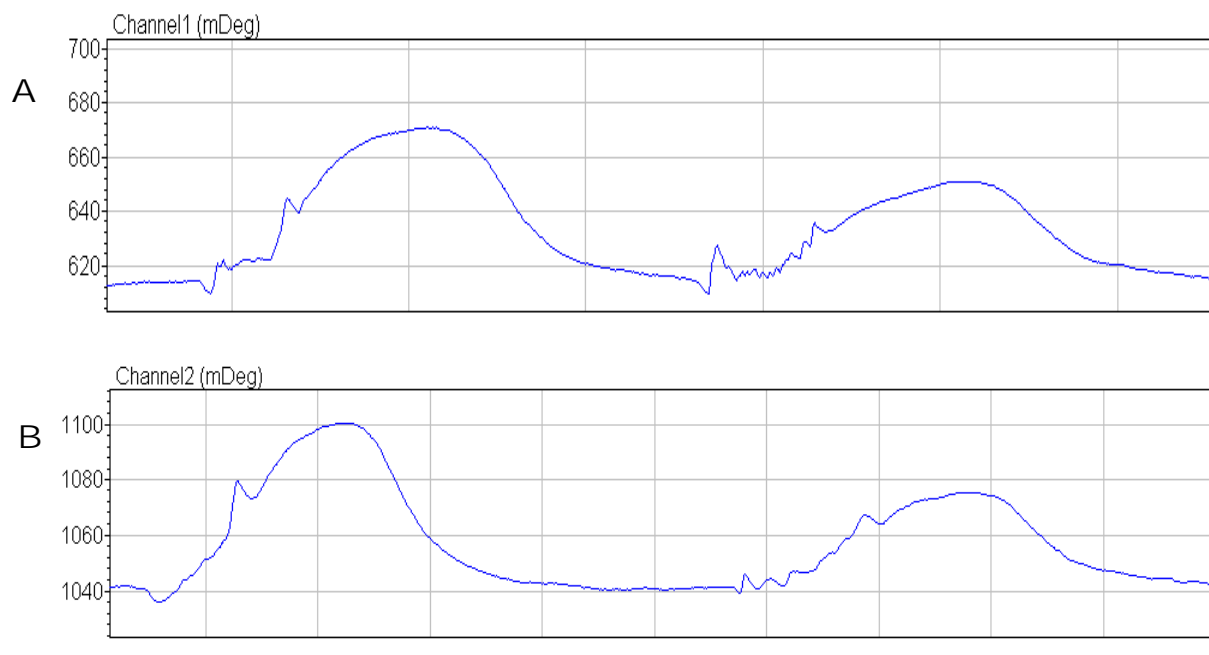


**Figure 33 -In-House Fluidics SPR Output: Channel 1, Channel 2, Ethanol Experiment**  
 In-house fluidic experiment using 1.00% and 0.50% ethanol injections to compare angular shift between channels and to factory fluidics. A) Results from channel 1 ethanol injections  
 B) Results from channel 2 ethanol injections.

Common in all the ethanol experiments performed using the experimental fluidic system was a more rounded shift profile contrary to plateau observed in the ethanol experiments using the factory fluidics of the BI-2000. These differences are a result of the 50  $\mu$ L channels used in the in-house fluidics compared to the 1  $\mu$ L channel factory flow gasket. This volume difference has no effect on maximum shift detected; however, because of the difference in channel volumes the evacuation time for the in-house fluidics is longer, producing a more rounded shift profile.

Initial observation of the data produced from the ethanol experiment shows the desired linear relationship between the dilution of ethanol and the resulting angular shift exists, and the expected 60 mDeg shift caused by the 1.00% ethanol was observed in both channel 1 and

channel 2 of the in-house fluidics. To assure that the data is valid, an ethanol experiment was performed on the factory fluidics immediately following the in-house ethanol experiments.

### **3.4 Follow-Up Ethanol Experiment**

The follow-up ethanol experiment revealed that the 1.00% ethanol readings in the experimental fluidics were the same as the current factory fluidics. The direct linear relationship existed between the dilution of ethanol and angular shift in the follow-up ethanol experiment performed on the factory fluidics, and the angular shift caused by the 1.00% injection of ethanol was the same at 60 mDeg in both channels. (Figure 34) Similar to the in-house fluidics, the 0.50% ethanol injection resulted in a 30 mDeg angular shift in both channels. (Figure 34) These results indicate validation of the results of the in-house ethanol experiment.

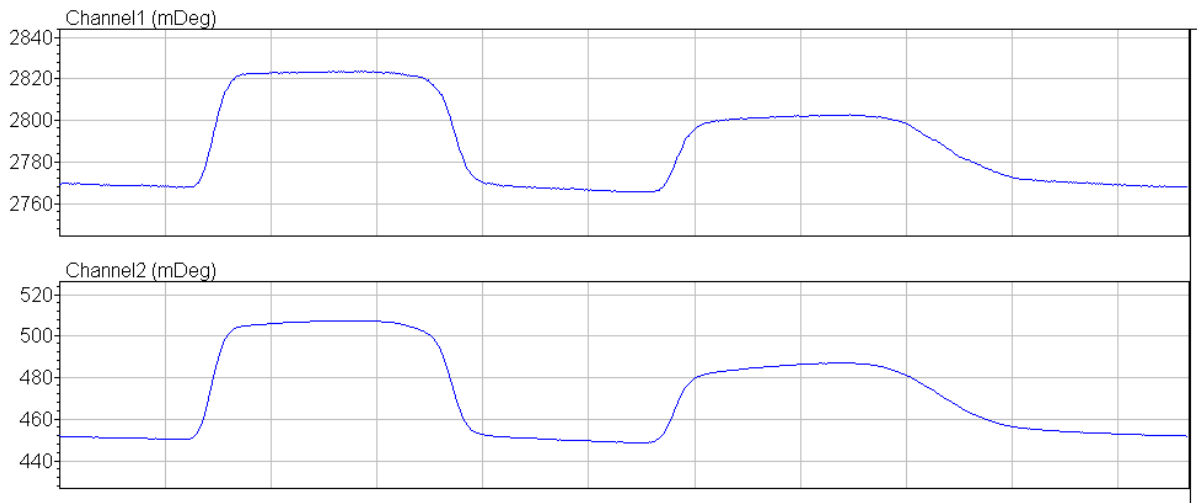


**Figure 34 - Factory Fluidics SPR Output: Channel 1, Follow-Up Calibration**

A quick calibration check to compare results of ethanol experiments on experimental fluidics, to the factory fluidics. Similar profiles are seen as well as similar quantities for angular shift.

### **3.5 Fibroblast Experiment**

To further validate that the Cal Poly in-house fluidics for the SPR instrument work properly, experiments were performed cleaving fibroblast cells with trypsin. The experiment was conducted on both factory fluidics and in-house fluidics for comparison. After culturing, initial images of the SPR sensor chips seeded with 3T3 fibroblasts and cultured in a CO<sub>2</sub> incubator for two days reveals 100% confluency with strong binding to the sensor surface (Figure 37). Transparency through the chip makes it difficult to assure that all the fibroblasts have adhered to the gold surface and not the glass bottom. The fibroblasts small size and suspended presence in the media used to culture the cells allows them to be both above and below the sensor chip when it is placed in the Petri dish. It is certain that many cells do exist on the gold surface of the chip through comparison to a bare gold chip as well as through slight mechanical removal of cells from the gold surface. Pictured below is the surface of a chip with the cells adhered to the surface (Figure 35-A). To the naked eye, the fibroblasts appear as a thin white film on the surface of the chip.

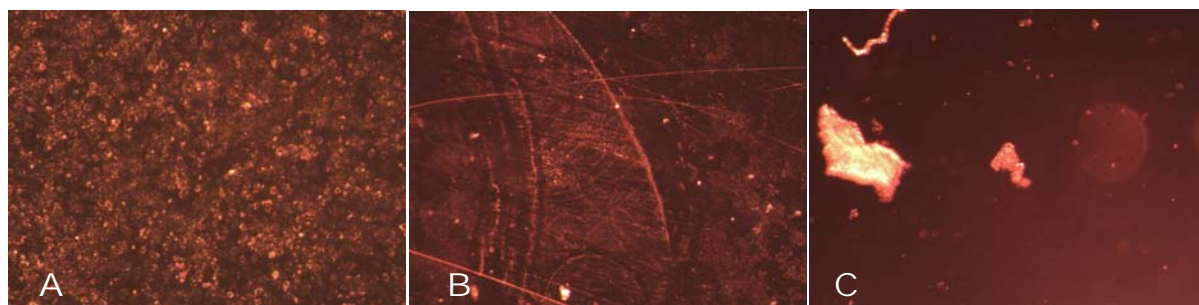


**Figure 35 – Microscope Image of SPR Sensor Chips Used in Fibroblast Experiments**

A) SPR sensor chip before experimentation loaded with 3T3 fibroblasts which are seen as small white specs on the surface. B) SPR sensor chip used with factory fluidics with very few remaining cells. C) SPR sensor chip used with experimental fluidics containing a large collection of cells clumped together.

Fibroblasts are easily removed using mechanical force such as brushing the cells off with a tissue. Removal of the cells from the surface can occur through slight application of force; as a

consequence, manipulation of the SPR sensor chip had to be carefully planned and executed. Cell adherence to the SPR sensor was assured by running PBS over the top of the cell laden chips. As the PBS washed the pink media from the SPR sensor chip, a thin white film of fibroblasts remained, proving that the cells were in fact bound to the surface of the chip.

Results generated by the optical sensor and interpreted by the BI software were highly unusual and unexpected for the in-house fluidics. The results expected were to be similar to the Lei et al. experiment discussed in Section 2.7.6.3 and seen in Figure 30. After establishing a baseline with the PBS introduction of trypsin should result in a downward exponential shift as the cells cleave from the surface of the SPR sensor chip. Finally, as PBS was reintroduced to the system a new baseline lower than the initial baseline due to the lack of cells on the surface of the chip was expected.

#### 3.5.1 Factory Fluidics Fibroblast Experiment Results

Using the factory fluidics, the SPR sensor chip was loaded over the prism and the flow cell was locked on top allowing PBS to flow over the cell. A baseline was established by flowing PBS over the fibroblast loaded SPR cell at 480 mDeg (Figure 36). Once trypsin was injected a downward exponential shift was observed. While the shift matches the trend seen in the Lei et al. experiment, the magnitude of the shift is much less at 60 mDeg (Figure 36) compared to 120 mDeg seen in the Lei et al. experiment (Figure 30). Finally, the PBS flow was resumed and the shift began to level out at a baseline much lower than the original baseline. The seemingly small shift in signal suggests the results may be invalid or that the SPR may need recalibration because the expected shift due to cell removal should be comparable to the Lei et al. experiment. The

sensor chip was placed back into the petri dish full of media without wiping for investigation under the microscope (Figure 35-B).

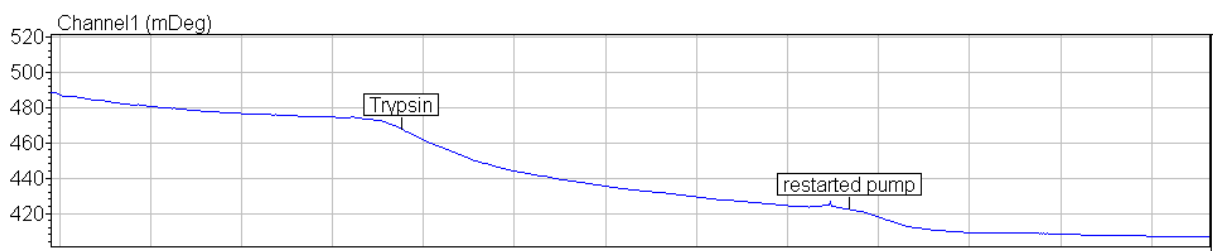


**Figure 36 – Factory Fluidics SPR Output: Channel 1, Fibroblast Experiment**  
Trail 1 of the fibroblast experiment conducted on the factory fluidics produced results similar to the Lei et al. experiment. (Figure 30) After injection of trypsin the signal exponentially drops as the cells cleave from the gold surface. Resumption of PBS flow establishes a new baseline.

The results from the second run of the fibroblast experiment using the factory fluidics, where the SPR sensor cell was wiped produced seemingly no apparent findings likely due to experimental error. Shown below (Figure 37) is the reading from the second experiment where what mostly occurs is strange spikes in angular shift, possibly caused by experimental anomalies introduced during system reconnection. When the trypsin was added and flow is stopped no significant shift was noted, simply random spikes upward and downward of the SPR signal. Baseline was never fully established, and wiping the SPR sensor surface clean seemed to have no effect.

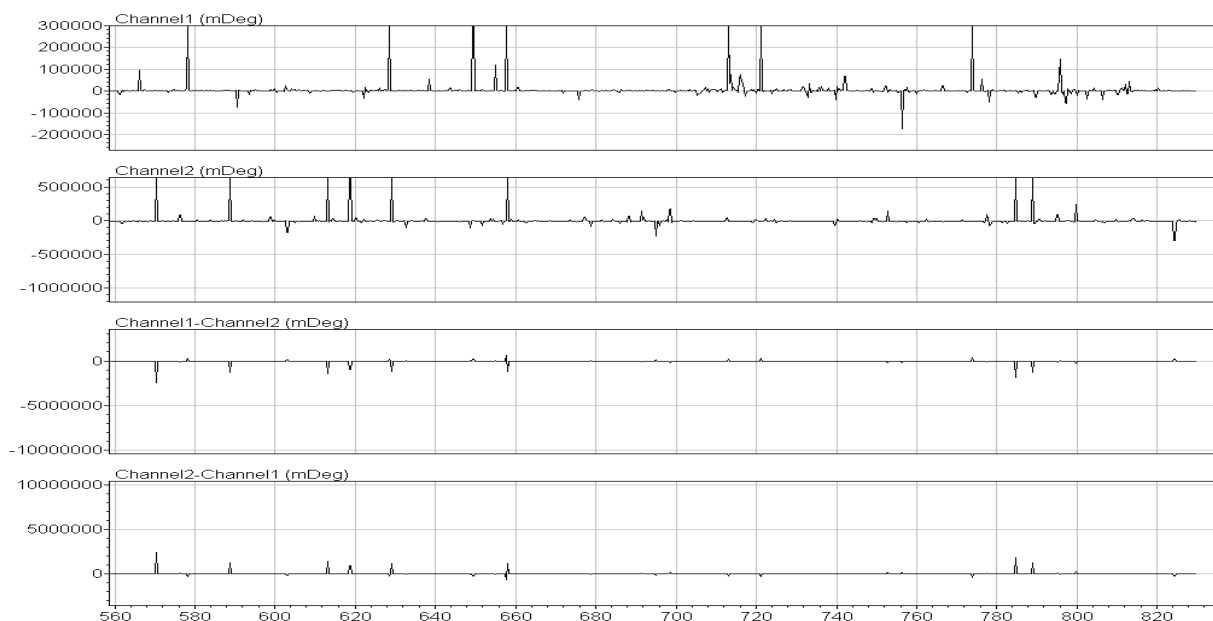


**Figure 37 – Factory Fluidics SPR Output: Channel 1, Channel 2, 1-2, 2-1, Fibroblast Experiment**

Trail 2 of the fibroblast experiment conducted on the factory fluidics produced no significant angular shift in SPR signal observed after the injection of trypsin. Spikes throughout the trial are a result of experimental anomalies.

### 3.5.2 In-House Fluidic Fibroblast Experiment Results

During the first run of the in-house fluidics, a leak formed during the injection of trypsin due to the uneven pressure caused by the lever arm on the flow cell. Because of the leak and subsequent cleanup, the initial test of the factory fluidics could not be conducted. Uneven pressure from the lever arm (Figure 38) that resulted in the leak was quickly remedied by carving a rubber stopper to more evenly distribute pressure from the lever arm to the surface of the flow cell.

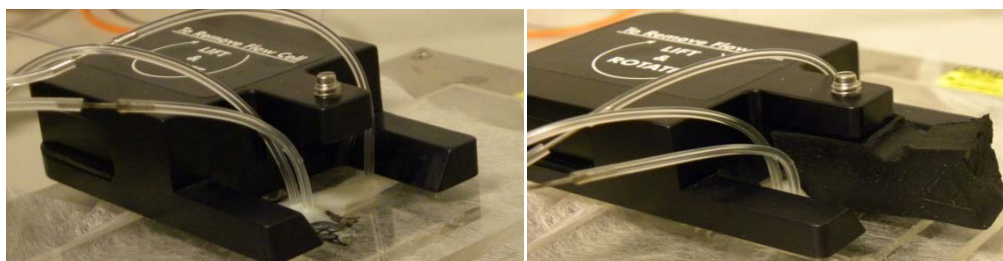


**Figure 38 – In-House Fluidics: Rubber Stopper Used to Distribute Pressure**

Left: Initial trial of in-house fluidics failed due to leaking caused by uneven pressure applied by the two arms of the swivel lever arm. Right: Using a carved rubber stopper, the pressure was more evenly distributed directly over the flow channels and the in-house fluidics worked as intended.

The goal of supplying even pressure distribution seemed to be successful and maintained a watertight flow above the SPR sensor chip inside the flow cell and gasket. After establishing a baseline SPR signal, the Labsmith valve was switched to the injection line. During the switch to the injection line an air bubble was introduced into the system causing extreme jumps in signal. After the air bubble passed, trypsin was injected into the experimental fluidics and forced through to the flow cell by the syringe pump. Through visual confirmation of the pink trypsin arriving to the clear flow cell, flow was stopped for one minute to allow time for the trypsin to cleave the cells from the surface of the chip. During the one minute interval, a slowly declining plateau was observed due to the fibroblast cleaving from the SPR sensor surface. After one minute, the syringe pump was reactivated allowing PBS to push the trypsin out and resume flow over the SPR sensor chip, causing a sharp drop in SPR angular shift. A new much lower baseline, in line with some aspects of the experimental expectations was observed upon resumed PBS flow (Figure 39). While the profile of the angular shift was not as expected, due to the introduction of an air bubble right before injection of trypsin, the shift noticed is approximately 130 mDeg which is consistent with the Lei et al. experiment.

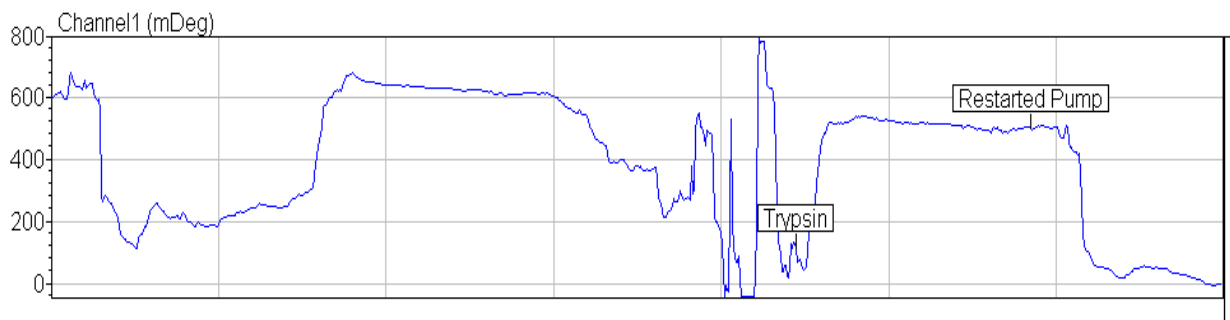


**Figure 39 – In-House Fluidics SPR Output: Channel 1, Fibroblast Experiment**

Trail 4 of the fibroblast experiment conducted on the In-House fluidics produced a significant angular shift in SPR signal observed after the injection of trypsin. Before injection the jumps in signal are a result of the pressure drops and spikes experienced when opening the injection valve and manually loaded the trypsin.



## **4 Conclusions/Discussion**

### **4.1 Restatement of Goals**

The objective of this thesis was to answer the question: *can laminate microfluidics be integrated with standard analytical SPR instrumentation?* The general hypothesis was that laminate microfluidics could be integrated with standard SPR analytic instrumentation. Using the BI-2000 SPR instrument as the standard analytics, in-house fluidics were developed to bypass the factory fluidics and allow direct connections to upstream in-house microfluidic devices. To explore this hypothesis the following goals were established:

- v. Design and fabricate low-cost fluidics for the BI-2000 SPR instrument to enable integration of in-house designed microfluidic devices;
- vi. Demonstrate fluidics that are leak and bubble free;
- vii. Comparable results of in-house fluidics with factory fluidics using ethanol solutions and assess success of in-house fluidics based on direct comparison;
- viii. Perform proof of concept experiments on BI-2000 SPR instrument to compare low-cost in-house fluidics with factory fluidics using 3T3 fibroblast cells, and to use the BI software to calculate SPR signal shift due to unbinding of fibroblasts from the sensor surface.

Experiments used in this thesis were designed to test each of the success criteria with the goal of answering the governing question.

## **4.2 Conclusions**

To answer the governing question of this thesis, success criteria were developed to assess the validity of the hypothesis that laminate microfluidic devices could be integrated with standard analytics. The following experiments were designed to specifically test each success criterion.

**i. Design and fabricate low-cost fluidics for the BI-2000 SPR instrument to enable integration of in-house designed microfluidic devices;**

The factory fluidics have several shortcomings, creating the desire for low-cost instrument fluidics. These shortcomings include: high cost (\$2500), inability to integrate with external microfluidic devices i.e. LOC PCR, and its inability to establish independent flow in each channel. Using PMMA, Tygon tubing, epoxy, PDMS, 3-way stopcocks, and syringe tips a low-cost in-house fluidic system was developed for approximately \$20, see Table 4.

**Table 3 – Cost of In-House Fluidics**

|                | Cost \$   |
|----------------|-----------|
| Syringe        | 1         |
| Syringe Tip    | 5         |
| Tygon Tubing   | 2         |
| PMMA Plate     | 3         |
| Epoxy          | 2         |
| 3-way Stopcock | 2         |
| PDMS           | 5         |
| <b>Total</b>   | <b>20</b> |

The flow cell and flow gasket were successfully developed through the use of a novel form of investment casting. Using the Cal Poly laser cutter to create a master mold for a wax cast that would ultimately be used to create channels in a PDMS flow gasket, proved to be an

inexpensive, quick way to manufacture a key component for the SPR fluidics. The flow gasket has well defined channels with appropriate dimensions to have two properly functioning channels in the BI-2000 system. Key differences exist between the factory flow gasket and the in-house flow gasket including: a much larger volume in the in-house channels at 50  $\mu\text{L}$  compared to the 1  $\mu\text{L}$  of the factory flow gasket, and shortened channels in the in-house fluidics due to size constraints. These differences in volumes led to differences in the SPR angular shift profiles using the same experimental parameters due to the volume differences between gaskets. These differences are a result of the evacuation time needed to clear the sample from the flow gasket. The larger volume channels of the in-house fluidics take longer to fill clear the channels causing a more rounded shift profile.

To properly integrate the in-house fluidics the sample injection port also needed to be fabricated. Using the factory fluidics on the BI-2000 to introduce sample required that a microsyringe loaded with sample be inserted into the handle of the injection valve. This system does not allow for the option of a direct connection of upstream microfluidic devices. To bypass the injection valve, a 3-way stopcock or Labsmith 3-port valve was used in conjunction with Tygon tubing and sheared syringe tips to form a connection with any upstream microfluidic device. The new junction serves as a more universal method of sample introduction to the BI-2000.

Overall, the goal outlined in this success criterion was achieved. The shortcomings of the factory fluidics, namely the high-cost stand alone nature of the factory system, were overcome using low-cost materials and manufacturing processes. The in-house fluidic system developed for this thesis is low-cost relative to the factory fluidics, enable integration of upstream

microfluidic devices, and the in-house fluidic system is also able to establish independent flow in each channel of the flow gasket over the SPR target.

**ii. Demonstrate fluidics that are leak and bubble free;**

Key to the success of future experiments using the in-house fluidics is that the system can remain leak and bubble free. Leakage and bubbles lead to false signal readings and sample contamination and render the experiment invalid. To test for leaks and bubbles in the in-house fluidics, a dilution of green dye #5 in deionized water was run through the fluidic system at a rate equal to the highest flow rate experienced during experimentation (0.150 mL/min). Manual injections of green dye #5 were also conducted through the injection line of the in-house fluidics to assure that all aspects of the fluidic system were leak and bubble free. (Figure 31) These tests were conducted on white paper to highlight the location any leaks that occurred and ease visualization of any bubbles that formed. After 5 minutes of continuous flow without leaks or bubble formation, it was determined that this success criterion was achieved and experimentation could begin using the in-house fluidics.

**iii. Comparable results of in-house fluidics with factory fluidics using ethanol solutions and assess success of in-house fluidics based on direct comparison;**

Using ethanol as the sample injection, against a carrier solution of deionized water, is a well documented experiment that elicits specific SPR angular shifts based on the dilution of ethanol. The manufacturer of the BI-2000 lists the expected the angular shift response for 1.00% and 0.50% ethanol solutions at 60 mDeg and 30 mDeg, respectively (Figure 28). Actual experimentation using the Cal Poly BI-2000 elicited the expected shift after calibration. (Figure

32) With an average SPR angular shift of 60 mDeg and 30 mDeg for the 1.00% and the 0.50% ethanol solutions respectively, the measured angular shift on the BI-2000 matched the literature provided by the manufacture. A linear relationship between the dilution of ethanol and the SPR angular shift that is elicited also existed in the BI-2000 as described in the literature.

Validation of the in-house fluidics was confirmed through direct comparison to the factory fluidics, which was validated against the manufacture's literature. Because the angular shift caused by injection ethanol solutions into deionized water is so well known, comparable results using the in-house fluidics provides definitive evidence to support the hypothesis of this thesis that laminate microfluidics can be integrated with standard analytic instrumentation. The SPR angular shift generated by injecting 1.00% and 0.50% ethanol into the in-house fluidics was 60 mDeg and 30 mDeg, respectively. (Figure 33) These results constitute a success of the experiment on the basis of the linear relationship that exists between the dilution of ethanol and SPR angular shift generated. The magnitude of shift caused by the ethanol matches the expected described in the literature [12] and matches the factory fluidics.

A final ethanol experiment was conducted on the factory fluidics for comparison with the results generated using ethanol solution in the in-house fluidics. Injections of 1.00% and 0.50% ethanol into the factory fluidics resulted in 60 mDeg and 30 mDeg angular shifts, respectively. Compared to the expected shift outlined in the literature of 60 mDeg and 30 mDeg, the factory fluidics matched. The signal shifts observed in the post in-house ethanol experiments conducted on the factory fluidics validates the success of the in-house fluidics.

Overall, the ethanol experiments successfully fulfilled the desired success criterion and provided clear evidence to support the hypothesis of this thesis. Results generated from injection of 1.00% and 0.50% ethanol into the in-house fluidics matched the factory fluidics not only in

numerical value, but also in the linear correlation that exists between ethanol dilution and SPR angular shift. The angular shifts seen in both the factory fluidics and the in-house fluidics also matched the manufacture's published results. The angular shift profiles observed in the in-house fluidics (Figure 33) varied from the square profile seen from the factory fluidics (Figure 34) as a result of manual injection of the ethanol solution and the large volume of the in-house fluidics. The increased, uneven pace of the manual injections resulted in small signal shifts before the main shift caused by the ethanol injection and the large volume chambers resulted in a rounded angular shift profile. This round profile is a result of the evacuation time, however, quantitatively, the angular shift observed matched directly with the expected results.

- iv. Perform proof of concept experiments on BI-2000 SPR instrument to compare low-cost in-house fluidics with factory fluidics using 3T3 fibroblast cells, and to use the BI software to calculate SPR signal shift due to unbinding of fibroblasts from the sensor surface.**

While success criterion iii was used to validate the success of the in-house fluidics, success criterion iv provides a more complex, real experiment to further assess the success of the in-house fluidics. Because no manufacture data exists on the fibroblast experiment, other experimental data sets [16] were used to determine the expected shift and experiments were conducted on both the factory fluidics and the in-house fluidics. The factory fluidics elicited a very similar response to the prior work done in the Lei et al. experiment. (Figure 30) This direct comparison represents a successful observation of the change in SPR signal due to the trypsin cleaving the fibroblast cells from the SPR sensor chip's surface.

Results from the in-house fluidic fibroblast experiment were also a quantitative success. During the injection of trypsin large spikes in SPR signal are observed (Figure 39) indicating the presence of bubbles within the system. These air bubbles were likely introduced during injection or by the Labsmith 3-port valve. While the trypsin is cleaving the fibroblasts a downward trend is noticed in the SPR angular shift suggesting that the cleaving event was being detected, however, the sporadic results show no qualitative correlation to the factory fluidics or the Lei et al. experiment. Comparison of the initial baseline to the baseline resulting from the removal of cells reveals a 130 mDeg shift, which matches the expected results in the Lei et al. experiment. Imaging after the experiment showed that the chip was void of cells proving the trypsin had effectively cleaved the cells.

Overall, the experiments successfully validated the final success criterion for the experiment. Inconsistency between the in-house fluidic fibroblast experiment results and the factory fluidic results suggest that more work needs to be performed to perfect fluid handling and injection of sample. In both experiments, the expected downward shift resulting from the cells cleaving from the surface was observed and quantitative success was also achieved in both the factory fluidics and the in-house fluidics. These successes provide clear evidence for hypothesis. Further testing should reveal that the in-house fluidics can provide an effective means for monitoring the cleaving event of fibroblasts due to trypsin and provide a qualitative comparison between the factory fluidics and the in-house fluidics.

### **4.3 Summary**

The underlying question of this thesis, *can laminate microfluidics be integrated with standard analytical instrumentation*, was successfully answered through the experimental evidence. Based on the success criteria used to evaluate the hypothesis laminate microfluidics can be integrated with standard analytical instrumentation. Low-cost in-house fluidics were developed to bypass the factory fluidics and allow connection between upstream microfluidic devices and the BI-2000 SPR.

This low-cost, in-house fluidic system was tested to assure that it could successfully function without forming leaks or bubbles. After successfully demonstrating that the fluidic system could successfully serve as a conduit for sample and carrier solution over the SPR sensor chip, it successfully measured angular shift resulting from ethanol solution. The results of the ethanol experiment closely matched the factory fluidics proving that the fluidic system was a success. The more complex fibroblast experiment resulted in a quantitative success in terms of generating comparable results between the in-house fluidics and the factory fluidics, and future work with the in-house fluidics should prove the in-house fluidics to be an acceptable apparatus to conduct fibroblast experiments with.



## **4.4 Future Work**

### **4.4.1 Future Fibroblast Experiments**

Finding substance in the fibroblast experiment would first require a few experiments to control some of the variables seen in the initial fibroblast experiment. The biggest unknown factor in the whole experiment is the response trypsin is supposed to elicit in the SPR instrument. High concentrations of sample can sometimes cause the SPR instrument to produce unpredictable results or no results, as seen when injecting high concentrations of ethanol, suggesting that 1X trypsin may be too potent to run through the SPR instrument.

An experiment should be done using the factory fluidics to gauge the angular shift caused by different dilutions of trypsin. The experiment would follow almost exactly the same protocol as calibration, exchanging deionized water for PBS and ethanol for trypsin. Should the high concentration trypsin indeed have been the culprit in the unusual results obtained during the first fibroblast experiment, a new experiment would need to be performed to assess the strength of trypsin needed to cleave cells from the surface. Fibroblasts would need to sit in a bath of the highest dilution of trypsin able to be detected by the SPR to assess the amount of time needed for all the cells to cleave from the surface.

Knowing these two factors the original fibroblast experiment could be rerun with a dilution of trypsin known to elicit a signal response to monitor the cleaving event. All future experiments involving SPR sensor chips and fibroblasts should be conducted in a way that allows the chips to be reused, requiring sterile procedure during as well as ample sterilization after the experiment to assure total removal of all experimental cells from all surfaces. In an attempt to correct the errors of the second run of the factory fluidics that resulted in no data, a tissue or cotton swab should be run along the bottom of the SPR sensor chip to remove any cells

that may have adhered during culture. Removal of cells on the bottom of the chip will assure even seating of the chip over the prism and that the laser has proper penetration to the gold layer to form the SPW.

Experiments using the experimental fluidics during the fibroblast experiment used the Labsmith 3-port valves which proved to be problematic with maintaining constant line pressure and resulted in sporadic readings from the SPR instrument. Redoing the experiment with the new three way stopcocks might eliminate the jumps in signal seen in the successful run of the experimental fluidics. Future experiments involving fibroblasts would be an excellent way for Cal Poly Biofluidics to take advantage of department resources and develop quantifiable data on the use of fibroblasts.

#### 4.4.2 Future Experimental Fluidics

In-between experiments, a better valve alternative (3-way stopcock) created a dramatic difference in the cost and performance of the experimental fluidics. Over time, as new technologies are developed and new manufacturing techniques become available at Cal Poly, the experimental fluidic system will become even less expensive and correct for certain complications during use. One main complication of using the experimental fluidics is placement of the flow cell and gasket as well as maintaining firm pressure during experimentation.

During the fibroblast experimentation a quick fix for the built in lever arm using a carved stopper to evenly apply force and maintain a watertight seal was developed but the stopper should probably be expanded on to assure consistent force is applied to the experimental fluidics for all future experiments. A system that does not impede the factory fluidics but during use of the experimental fluidics can be used to evenly and consistently secure the flow cell and flow

gasket to the SPR sensor chip is necessary for successful reproduction of experiments. The uneven nature of the hand carved cork means that a different distribution of pressure will be applied each time the lever arm is lowered potentially causing difference in the results.

On the side of low cost diagnostics both for world health and to conserve department resources, development of new low cost SPR sensor chips would be paramount for future experiments. Currently at \$15 a chip, the SPR sensor chips proved to be too cost prohibitive to continue work with the fibroblasts as the chips were disposed of because of their biohazardous nature. Recent studies have shown that thin layers of gold can easily be sputtered onto PMMA meaning that if the correct index matching fluid is found, the once expensive optical glass sensor chips can be manufactured at Cal Poly for low cost instead of purchased from an outside vendor. Exploration of the use of PMMA SPR sensor chips would be a worthwhile endeavor for all students looking to perform experimentation on the SPR.

Development of a PMMA SPR sensor could also eventually result in the development of an all inclusive SPR sensor, flow gasket, and flow cell. Using techniques developed in the Cal Poly microfabrication lab as well as the Cal Poly Machine shop, development of an all inclusive flow cell and sensor would be a giant step towards low-cost modular diagnostics.

# **Appendix A**

## Surface Plasmon Resonance User Guide (BI 2000)

### I. Pre-Use Setup

### II. Calibration

### III. Post-Use Clean-up

#### **Note on using this guide:**

The guide is written in outline format. Major tasks are next to whole numbers (i.e. 9.) If a major task is broken down into several small steps, these will appear as a subset of the whole number (i.e. 9.1, 9.2, 9.3 etc). Warnings or other useful information for a step appear in italics beneath the step. Always read a whole step before starting it. If the guide is unclear, please refer to the full user manual (**BI-2000 Manual v5.4**) located on the lab computer in the “SPR” folder on the desktop. In areas of this guide where reference to the manual may be useful, there is a page number given to aid in finding the applicable section.

***Warning:*** *If turning on the laser before placing a sensor chip on the prism surface, take care not to stare directly at the laser. Failure to heed the warning could result in damage to your eyes.*

## **I. Pre-Use setup**

**Time:** ~30minutes

**Equipment:** Syringe Pump, BI-2000, Computer with BI-2000 software installed, Uninterrupted Power Supply or surge protector

### **Materials:**

- a. sensor chip (gold or other appropriate metallic chip)
- b. 30ml DI water (or appropriate Carrier Solution)
- c. 2 cotton swabs
- d. kim wipes
- e. Cleaning ethonal
- f. index matching fluid
- g. glass rod
- h. tweezers

### **Pre-Use setup Procedure:**

1. Start degassing the carrier solution. (10-15 min)
2. Power on the BI-2000. Wait to turn on the laser until a sensor chip has been placed on the prism.
3. Clean the prism surface and flow cell surface

- 3.1. Use a kim wipe dampened with Ethanol to wipe the flow cell surface
- 3.2. Use a cotton applicator dampened with ethanol to gently clean the prism surface by moving it in an outward spiral starting at the center of the prism.
4. Place a sensor chip on the prism surface by:
  - 4.1. Using a glass rod, place a small drop of index matching fluid (3.0-5  $\mu$ L) on the center of the prism.
  - 4.2. Identify the metallic surface of the sensor chip

*The metallic side should be shinier than the other side. If unable to determine which side is plated, gently scratch the edge of the chip with the tweezers. The side that scratches is the metallic side.*

- 4.3. Using tweezers, place the sensor chip on the prism metallic side up.

*Pick up the sensor chip by the edges with a pair of tweezers. Place one edge of the sensor chip on the edge of the prism. Slowly lower the chip completely onto the prism. P. 21*

- 4.4. Turn on the laser.
- 4.5. Check for correct mounting by looking for a uniform intensity red blob in the viewing window.
- 4.6. If there dark spots or lines, shift the sensor chip using a cotton applicator along the edge until the trapped air bubble is removed.

- 4.7. The flow cell can also be placed on the sensor chip and gently pressed to attempt to squeeze the air bubble out.
- 4.8. If the air bubble cannot be removed, the sensor chip will have to be removed, cleaned and remounted.
5. Place the flow cell on the sensor chip surface by rotating the flow cell holder into the correct position.
6. Start the fluid system
  - 6.1. Check that all fluid lines are connected. Ensure that the waste bottle is connected and has room.
  - 6.2. Load two syringes with the degassed carrier solution.

*Remove all air bubbles from the syringes. This will help keep bubbles from clogging the lines.*
  - 6.3. Connect the syringes to the BI-2000.
  - 6.4. Check that the Mode Select Valve is in Serial.
  - 6.5. Check that the Injection Valve is in Load.
  - 6.6. Check that the Channel Select Valve is in CH1.
  - 6.7. Start the syringe pump at a high flow rate ( $\sim 150 \mu\text{L}/\text{min}$ ).
7. Flush the system of bubbles

- 7.1. After a few minutes (3-5min) place the Injection Valve in Inject.
- 7.2. After a minute place the Mode Select Valve to Single.
- 7.3. After a minute, place the Channel Select Valve in CH2.
- 7.4. reduce the flow rate to the desired experimental flow rate (~50  $\mu\text{L}/\text{min}$  is typical)
- 7.5. Return the Mode Select Valve to Serial.
- 7.6. Return the Injection Valve to Load.
- 7.7. Check the viewing window. Ensure that two dark squares are visible.

*The dark squares will not be visible in the viewing window until the fluid has reached the sensor.*

*If the squares are broken or distorted, gently press on the flow cell to dislodge the bubbles.*

8. Check all lines and valves to ensure that there is no leakage.
9. Allow 20-30 minutes of steady state operation for back ground to stabilize.

- 9.1. Turn on the Computer and start the BI software.
- 9.2. Start monitoring both channels.
- 9.3. Place all recording channels in auto by clicking *setup* -> *plot* -> check *auto* in all the boxes.
- 9.4. Wait for the baseline to stabilize.



## II. Calibration

**Time:**

**Equipment:** Syringe Pump, BI-2000, Computer with BI-2000 software installed, Uninterrupted Power Supply or surge protector

**Materials:**

- a. sensor chip (gold or other appropriate metallic chip)
- b. 30ml DI water (or appropriate Carrier Solution)
- c. Dilute Ethanol Solution.
  - 1. 1200 $\mu$ L 1% (v/v) ethanol Solution.
  - 2. 1200 $\mu$ L .5% (v/v) ethanol Solution.
  - 3. 1200 $\mu$ L .25% (v/v) ethanol Solution.
  - 4. 1200 $\mu$ L .125% (v/v) ethanol Solution.
  - 5. 1200 $\mu$ L .0625% (v/v) ethanol Solution.

## Calibration procedure

1. Perform the Pre-Use setup procedure using a bare gold sensor chip
2. Check that the waste container is at least half empty.
3. Place the Injection Valve in Load.
4. Place the Mode Selector Valve in Channel 1.
5. Check that the BI Software is monitoring both channels.
6. Check that two dark lines are visible in the viewing window.
7. Set the syringe pump to a 50 $\mu$ L/min flow rate.
8. Activate the SPR control program.

8.1. Set input gain to 1X and sample rate to 10 points/second. *Setup -> Acquisition ->*

8.2. Leave the System Calibration Value for Channel 1 and 2 at the current values

8.3. Display Channel 1, Channel 2, Channel 1 - Channel 2 and Channel 2- Channel 1.

*Setup -> Plot -> Input 1-4*

8.4. Set the Y-axis for Channel-1, Channel-2, Channel1-Channel2 and Channel2-Channel1 to Auto.

*Do this by double left clicking on the appropriate Y-axis and checking the Auto box.*

8.5. Set the injection timer. *Setup -> Injection Timer*

8.5.1. Enter 50  $\mu$ L/min for flow rate

8.5.2. Enter 100  $\mu$ L/min for Sample Loop Volume

8.5.3. Press Calculated then OK.

8.6. Click the blue arrow button to begin data acquisition.

8.7. Make sure a stable baseline has developed before proceeding. This may take 5-15 minutes depending upon several experimental factors. (Please see Chapter 6 )

9. Check the Injection Valve in Load

*The baseline signal should not change. If the baseline signal does change, residue from previous use is leaching into the system and should be flushed out (Please see Section 5.6) or there may be a clog in the system that should be alleviated (Please see Section 5.6).*

10. Load the provided 100  $\mu$ L glass injection syringes with 1% ethanol solution.

10.1. Firmly insert the syringe needle into the Injection Valve (front left valve), and inject the 1% ethanol solution by slowly pressing on the syringe plunger.

10.2. At this moment, the baseline of the SPR signal-time curve should be quite stable.

10.3. Place the Injection Valve to Inject.

10.4. Pull the syringe out of the valve.

*After a short while, the injected sample plug will have entered the flow cell. This will cause a large change of the Channel 1 and Channel 2 signal in the plot. The response will rise to a plateau and then drop off.*

10.5. Once the timer reaches zero, turn the injection valve back to Load position.

11. Repeat the injection 3 times and record the average change in response measured for the 1% ethanol injection.

12. Place the Mode Selector Valve in Channel 2.
13. Repeat step 11 for Channel 2.
14. Place the Mode Selector Valve in Channel 1.
15. Repeat Steps 11-15 for the .5% solution
16. Repeat Steps 11-15 for the .25% solution
17. Repeat Steps 11-15 for the .125% solution
18. Repeat Steps 11-15 for the .0625% solution
19. Check that the signal scales properly with concentration.
  - 19.1. Plot the average values for each injection on a graph.
  - 19.2. Ensure that a line through all data points is linear.
  - 19.3. If it is not linear, the solutions should be remade and the data collection portion of the calibration performed again.
  - 19.4. If it is linear, proceed to step 21.
20. Calculate the new calibration value.
  - 20.1. Divide 60 by the number of mDeg recorded as the average value of for the 1% ethanol solution.
  - 20.2. Multiply the value of step 20.1 by the old calibration value.

*Setup -> Calibration -> Channel 1/2 sensitivity.*
21. Enter the new calibration value.

New Calibration Value = Old Calibration value X 60/(average value of 1% ethanol)

### III. Post-Use Clean-up

**Time:** ~30minutes

**Equipment:** Syringe Pump, BI-2000, Computer with BI-2000 software installed, Uninterrupted

Power Supply or surge protector

#### **Materials:**

30ml DI water

2 cotton swabs

kim wipes

Cleaning ethonal

tweezers

## **Post-Use Clean-up Procedure**

1. Stop the Syringe pump.
2. Turn off the laser.
3. Replace the Carrier Solution syringes with DI water Syringes
4. Thoroughly flush the system with DI Water.
  - 4.1. Place the Injection Valve in Injection
  - 4.2. Place the Mode Valve in Single
  - 4.3. Start the Syringe Pump at 150  $\mu\text{L}/\text{min}$  for 10-20 minutes.
  - 4.4. Toggle each valve several times. Ensure that each valve remains in position for at least a minute.
5. Clean out the injection port
  - 5.1. Load DI water into an injection syringe.
  - 5.2. Insert the injection syringe half way into the injection port.
  - 5.3. Inject DI water into the injection port. This will force water out the front of the injection port.
  - 5.4. Wipe clean with a kim wipe.
  - 5.5. Repeat steps 5.1 - 5.4 at least three times.
6. After the system is flushed with water. Flush the system with air.

- 6.1. Stop the Syringe pump.
- 6.2. Load both Syringes with air.
- 6.3. Check the Injection valve in Inject.
- 6.4. Check the Mode Valve in Single.
- 6.5. Manually push air through the system until waste stops entering the Waste Collection Bottle.
- 6.6. Load air in an injection syringe and inject air in into the injection port.
- 6.7. Place the Injection valve in Loading.
- 6.8. Load air in an injection syringe and inject air in into the injection port until waste stops entering the Waste Collection Bottle.

7. Clean the Flow Cell.

- 7.1. Lift and rotate the Flow Cell so it is off the chip.
- 7.2. Remove the Flow Cell.
- 7.3. Wipe the Flow Cell surface clean with a Kim wipe and ethanol.

8. Remove the SPR Sensor Chip from the prism surface.

*Caution: Take care not to scratch the prism surface.*

- 8.1. Use a cotton applicator to nudge the sensor chip off the edge of the prism.
- 8.2. Gently pick up the sensor chip with a pair of tweezers. The index matching fluid will impose adhesive force.
- 8.3. The sensor chip must be cleaned prior to reuse or should be discarded.
9. Wipe the prism clean with lens paper moistened with ethanol.
10. Turn off the Syringe Pump.
11. Turn off the SPR.
12. If done with data analysis.
  - 12.1. Save data.
  - 12.2. Turn off computer.



## **Appendix B**

### **Colorectal Cancer**

Colorectal cancer is defined as any cancer that forms in the colon or rectum. Colorectal cancer often begins as a polyp, which is a benign tumor on the inner lining of colon or rectum. Polyps can later form into cancerous tumors known as adenomatous polyps. [37] On average it will take a polyp 10 to 15 years to form into a cancerous tumor. [37] 95 percent of colorectal cancers are adenocarcinoms, meaning they are formed in the glands that produce mucous and other fluids inside the colon and rectum. [38]



**Figure 40 – Colon Polyp**

Image taken from a sigmoidoscopy of a colorectal polyp which will be biopsied and tested to determine if it is cancerous.

Colorectal cancer is the third leading cause of death worldwide with an approximate toll of 640000 lives yearly. [39] Nearly 70% of the yearly death toll resulting from cancer is held by low to middle income countries as a result of lack of early detection and treatment. [37] Initial problems associated with colorectal cancer include gastrointestinal bleeding, bowel obstruction leading to constipation, pain, and vomiting, and irregular bowel movements. [38]

Early detection of colorectal cancer or adenomatous polyps has been shown to reduce the risk of death resulting from colorectal cancer 90%, however, only 40% of cancers are detected before they metastasize and spread to the body. [39] Once colorectal cancer has metastasized

patients survival rate is reduced to 11%. [39] Screening is the most effective defense against colorectal cancer broken up into two main groups, screening for polyps that will potentially form into cancer and screening for colorectal cancer itself. The most common methods of screening are flexible sigmoidoscopy, colonoscopy, and fecal occult blood test.

Sigmoidoscopy utilizes a camera attached flexible lighted tube known as a sigmoidoscope to visualize the inside of the colon and rectum looking for polyps and cancerous growths. The sigmoidoscope is approximately two feet long making it unable to examine the entire colon. Sigmoidoscopy can result in moderate discomfort for the patient and requires relatively expensive equipment for limited results. If a polyp is found using a sigmoidoscope it must be biopsied and tested using immunohistochemistry to evaluate if the polyp is cancerous. If cancerous a colonoscopy must be performed.

Colonoscopy is similar to sigmoidoscopy but instead uses a larger diameter tube that can extend the entire distance of the colon. Before a colonoscopy can be done the bowels and colon must be cleared of fecal matter requiring use of laxatives and enemas the night before the procedure. A sedative must be used on the patients to perform the colonoscopy to relax the patient for the procedure. Similar to the sigmoidoscopy, colonoscopy is moderately invasive, uncomfortable, and requires moderately expensive equipment in a clinical setting to be performed.

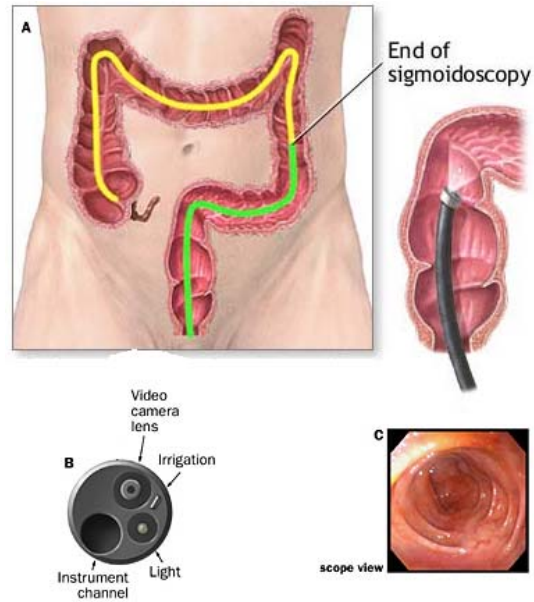


**Figure 41 – Sigmoidoscopy and Colonoscopy**

A) A diagram of the length at which a sigmoidoscopy (green) and colonoscopy (yellow) travel through the colon and rectum. While the sigmoidoscopy is less intrusive and requires less preprocedure preparation it is unable to extend the full length of the colon. B) Top view of the scope used on sigmoidoscopes used to locate and biopsy and polyps or unusually growths. C) Image produced by the camera lens which the physician uses to navigate the colon and biopsy any polyps.

Fecal occult blood tests (FOBT) are used to test the presence of blood in stool. The test is based on the premise that the blood vessels on extruded polyps or cancerous tumors are more susceptible to mechanical shear during a bowel movement resulting in ruptured vessels. The ruptured vessels will leave trace amounts of blood on the stool, often too little to visualize, indicating an unusual growth in the colon or rectum. FOBT are performed by the patients in their home and require a restricted diet to help prevent false positives. Fecal Immunochemical Tests are performed in a laboratory on the FOBT testing for the presence of globin, an indicator of the presence of blood from the lower bowels. [40] The FIT takes approximately two weeks to process the results; if positive a colonoscopy must be done to examine the source of the blood in the stool. [40]

Each screening method for colorectal cancer has severe disadvantages regarding cost of experiment, length of time needed for results, and convenience to patient. Sigmoidoscopy and

colonoscopy procedures require relatively expensive equipment, a clinical setting, and a moderately to severely uncomfortable procedure. If an irregularity is found during a colonoscopy or sigmoidoscopy further immunohistochemistry must be done to evaluate if the biopsied tissue is cancerous or cause for concern. The FOBT provides a less invasive screening option, however laboratory testing usually requires two weeks to complete and if irregularities are found physicians must resort to colonoscopy to explore the source of the irregularity. A similar and potentially more effective method of screening may exist in biomarker detection.

# **Appendix C**

## **Fabrication Using Cal Poly Facilities**

### Cost Effective Biofluidics

Methods of designing low cost microfluidics are being explored both locally and nationally as available resources begin to shrink. Cal Poly Biofluidics group will be utilizing these methods to develop novel approaches at modular diagnostics. Taking advantage of physicochemical properties through micro scale manipulation of molecules, Cal Poly's Biofluidics is developing novel mixers, filters, and detection systems using microfluidic devices. Developing these microfluidic devices from a simple PMMA mold and creating multiple PDMS castings from the mold offers the potential for quick low cost manufacturing of micro scale diagnostic systems. This paper will outline the design and fabrication of PMMA molds used to create PDMS casts which is fairly simple and straight forward.

### AutoCAD Modeling

Using the laser cutter to design the PMMA mold requires the use of AutoCAD to develop the model and a programmed set of laser speeds and intensities to manipulate cutting depth, cutting style, and cutting speed. Using AutoCAD four properties of the laser are able to be controlled:

Power: The percentage of the lasers 100 W capacity that is used to make a cut.

Pulses Per Inch (PPI): The number of beam pulses used to make the cut in the material.

Speed: The speed at which the laser moves, adjusting speed can be useful in cutting different thicknesses

Vector/Raster: Assign different layers to be raster cut or vector cut depending on desired feature.

- Raster refers to an array pattern of printing that will cut the desired pattern in a line by line fashion.
- Vector printing uses a coordinate system of cutting that will trace the pattern of the object to make the cut.

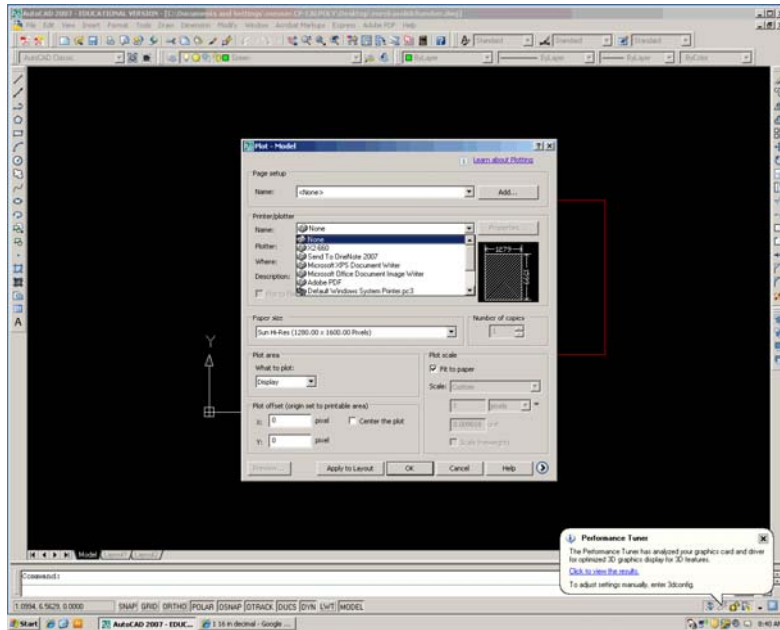
Designing the mold in AutoCAD follows the basic principles of designing in AutoCAD with the exception that line weight must be defined for each layer, most commonly at 0.00mm. The use of layers is essential in setting multiple cutting depths and/or creating an etch pattern. An etch pattern is used to make a negative mold of the intended casting causing the grooves, channels, and features to be raised from the surface and transversely embedded into the PDMS surface when casting occurs. To create an etch pattern a solid hatch should be used on all the surface areas and the speed should be set to 100 to create the smoothest surface possible.

Reference: At speed 100, power 100, PPI 1000 the laser cutter will raster etch approximately .01 inches deep. To make deeper features multiple passes may be used.

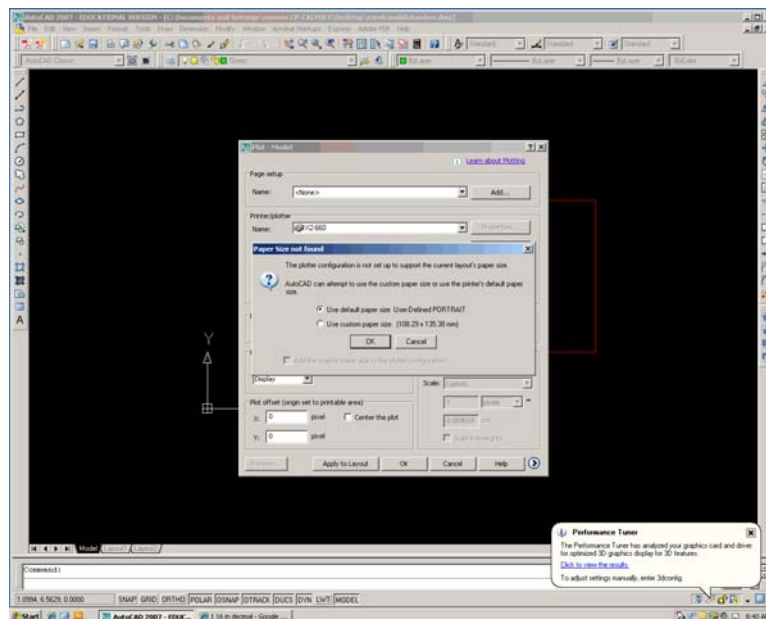
### Plotting

The laser cutter options of Speed, Power, PPI, and Raster/Vector are chosen in the plotting menu. Using the following instructions all features of the plot can be defined and sent to the laser cutter's cache to be plotted onto the PMMA mold.

1. Assign the plotter, for the Mustang '60 lab the plotter will be the X2-660

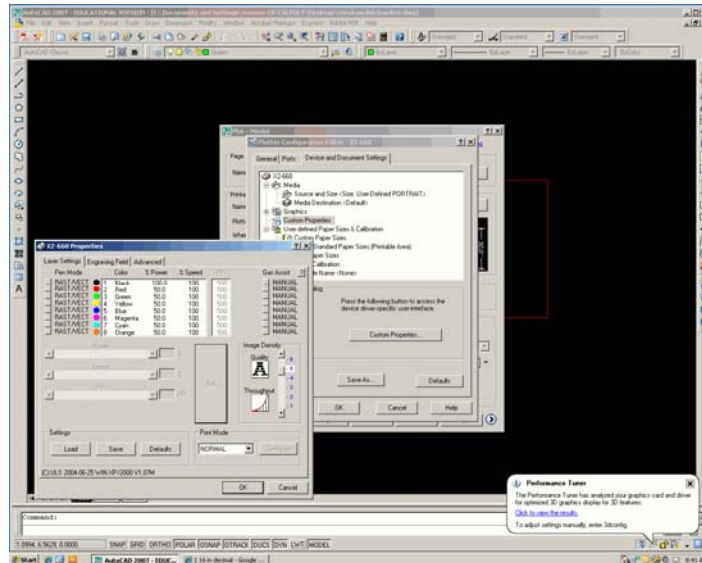


2. Use default landscape as plot size when prompted immediately after selecting the plotter.

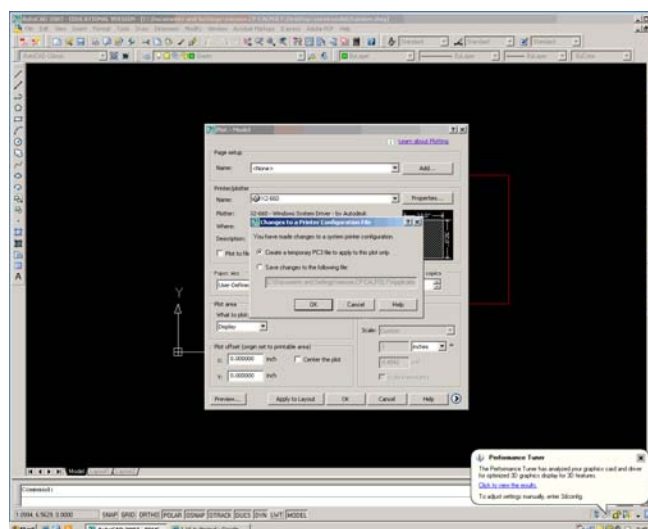


3. Click on Define Properties

4. Select Custom properties



5. Assign each layer that will be used to make cuts in the mold a power, speed and PPI
  - a. Using a vector cut power 100, speed 4, PPI 1000 will make a smooth cut through  $\frac{1}{4}$  " PMMA
  - b. Using a vector cut power 2, speed 4, PPI 975 will make an approximately 100 micron etch into PMMA
  - c. Raster should be used at speed 100 to make the smoothest possible etch
6. When prompted create a temporary PP3 for plotting purposes.



7. Change the plot settings to Extents in the drop down menu



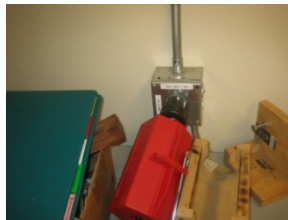
8. The location in the laser cutter where the cutting is done by clicking center plot or assigning a base point for the laser to begin.
9. Unclick fit to page scaling, instead choose 1:1 scale
10. Click Print

### Using the Laser Cutter

Before plotting the design on PMMA using the laser cutter, the laser cutter must first be turned on and set up for cutting. Access must be gained to the Mustang '60 lab where the laser cutter is housed by either enrolling in ME 240 or obtaining a “gold card” access and passing the red tag safety tests. Lab hours and protocols are posted on their website

<http://me.calpoly.edu/machineshop/>. Once access is to the Mustang '60 shop is gained the laser cutter may be used as follows:

1. Unlock the power cord and plug in the laser cutter.



2. Turn on the laser cutter using the orange switch on the right side of the laser cutter

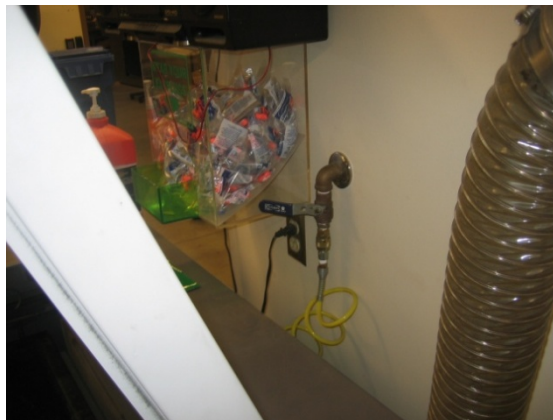


3. Flip the light switch up on the wall around the left corner of the laser cutter to turn on the ventilation system

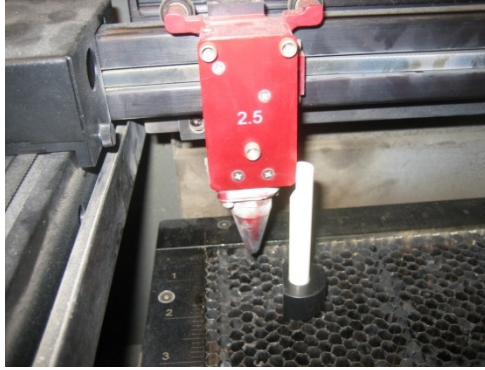
- a. Very important to turn on the ventilation system as fumes from melted PMMA are toxic.



4. Turn on the air valve behind the laser cutter



5. Once warmed up place the part to be cut in the laser cutter and set the Z access accordingly.
  - a. Placing the small plastic tool, located on the inside left rail, upright on your PMMA piece and adjust the platform height by pressing “Z” and using the up and down arrows until the plastic piece just tips.



6. Using the controls on the front of the laser cutter select the file to be printed
  - a. First keep the hood of the laser cutter up and press select to watch a “dry run” of the cut where a visible red laser will show the path of the laser cutter.
  - b. If the path is acceptable close the hood and press select
    - i. If the piece being cut is relatively small compared to working area of the laser cutter, paper should be placed over the free space and weighted down with washers which are found on the inside left rail to increase airflow near the part.



Once finished in the laser cutter the part should be cleaned and safely stored until used to make the PDMS cast.

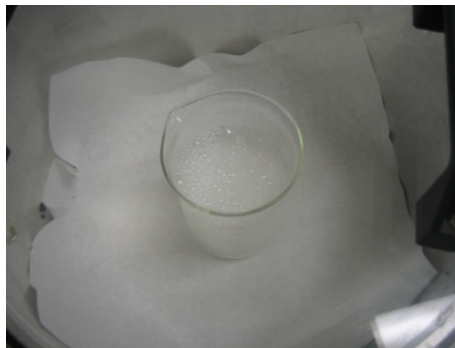
## Making the PDMS cast

A PDMS cast can now be made from the negative mold using the following technique.

1. Preheat the lab oven to 150° C, using the Cal Poly Materials Engineering clean room the oven should be set between 5 and 6.



2. Mix the PDMS with the hardening agent in a 10:1 ratio in a clean container such as a beaker.
3. Remove all bubble from the PDMS using a vacuum chamber
  - a. Carefully meter the vacuum as to not allow the PDMS bubbles overflow the container



4. Clean the mold assuring that it is completely free from all oils and debris
5. Create a simple boat from aluminum foil for the mold to sit in while the PDMS cures in the oven

6. Evenly pour the degassed PDMS over the mold avoiding overflowing the aluminum foil boat.
7. Place boat in oven for 15 minutes to cure
8. Carefully remove boat after 15 minutes using

WARNING: Mold will be extremely hot

9. Using a utility knife carefully cut the sides of the molds allowing the mold to release from the cast.

Tips:

- If ports will be used to allow flow into and out of the channels, the appropriate tubing can be placed in the mold before curing to create a smooth formed outlet or inlet
- When creating through holes in the mold first cut a pilot hole using the laser cutter then use appropriate drill bit to create the desired hole
- When degassing use an oversized container to degas more rapidly
- Do not degas using a container with seams as bubbles will form along the seams
- Keep protective covering on the PMMA as long as possible to avoid any surface scratches

## **Appendix D**

### **D.1 Instrument Warm-Up**

Before experimentation on the BI-2000 was able to begin, the manufacture suggested that the laser be allowed to warm-up for approximately 20 minutes. When the laser was properly warmed up, the BI-2000 provides a steady baseline on both channels. Baseline refers to the constant angular shift caused by consistent flow of carrier solution. Experimentation suggested for our system that the 20 minutes the manufacturer suggests for warm-up is a slight underestimate of the appropriate warm-up time. During multiple trials to evaluate this warm-up time, the SPR signal drift was observed for approximately 60 to 90 minutes while running the carrier solution through the factory fluidics. Shown below (Figure 32) is an example of signal drift observed during the initial calibration of the BI-2000. Before the calibration procedure can be performed, the SPR output must exhibit a steady signal. After the signal stabilized to within  $\pm 5$  mDeg, the calibration was initiated.

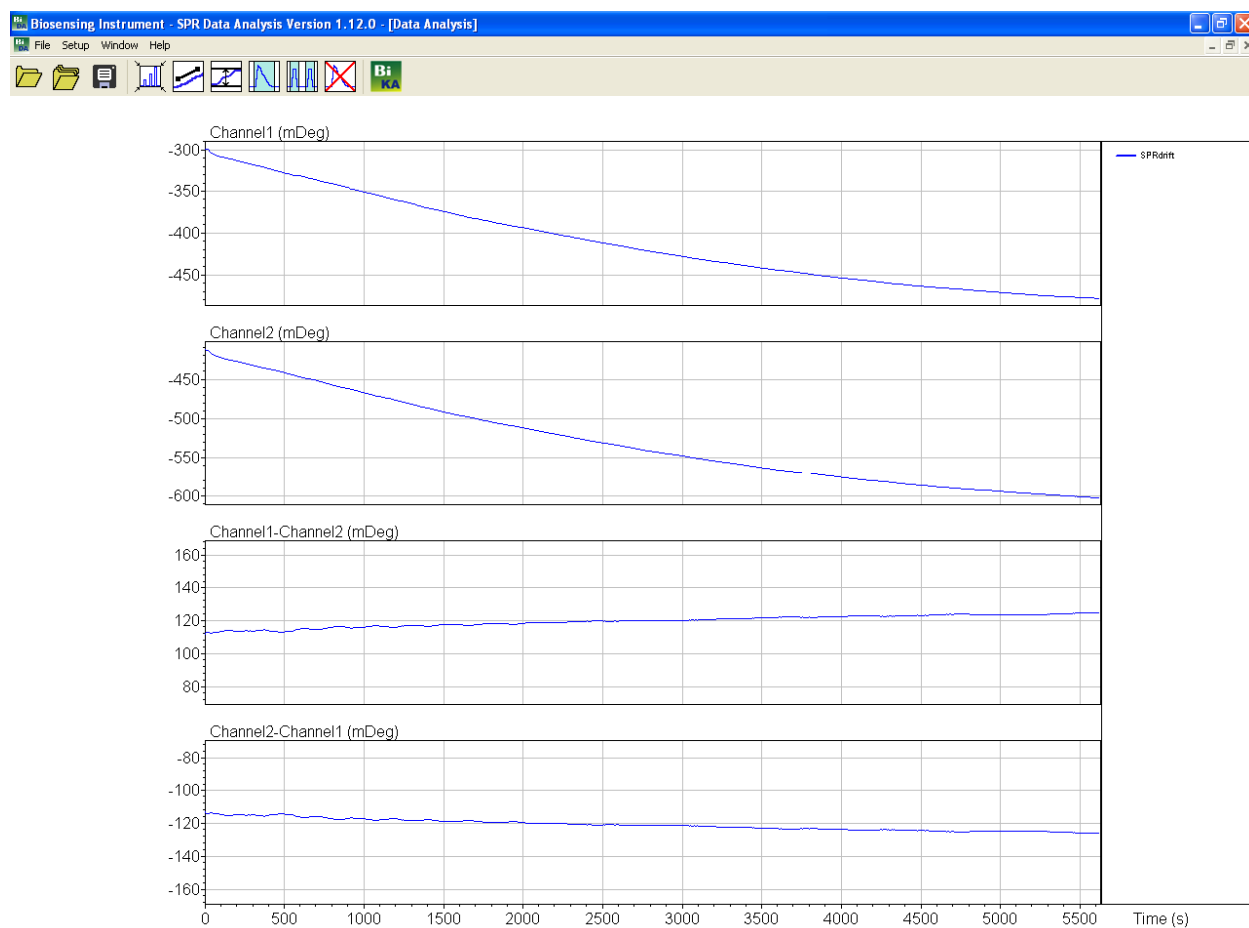


**Figure 42 – SPR Output: Channel 1, Channel 2, 1-2 and 2-1, Drift**

The angular shift plotted as a function of time shows the drift experience during warm up. Before experimentation can begin on the SPR machine, the laser used to generate the SPW must be warmed up. During the warm-up phase the baseline caused by running deionized water over the surface of the chip will significantly drift in both channels. For measurement accuracy the laser warms up for approximately 60 to 90 minutes after which experimentation can begin once the baseline levels.

Occasionally, after a relatively steady signal would develop on the SPR, the signal still had frequent and sporadic jumps of  $\pm 5$  mDeg (Figure 33). These vibrations are most likely attributed to noise on each channel, which using the channel-difference algorithm in the BI software should be subtracted. The noise is likely a result of: the temperature fluctuations in the laboratory where the BI-2000 is housed, the fluorescent lighting, the running computer located approximately 12" from the machine, and the general vibrations of the building.[36] The signal

noise observed in each channel were expected to be inconsequential due to the software's channel difference algorithm, which can subtract out noise that is found equally on both channels leaving only the difference between the channels to display; however, in practice, this algorithm sometimes amplified the signal noise.

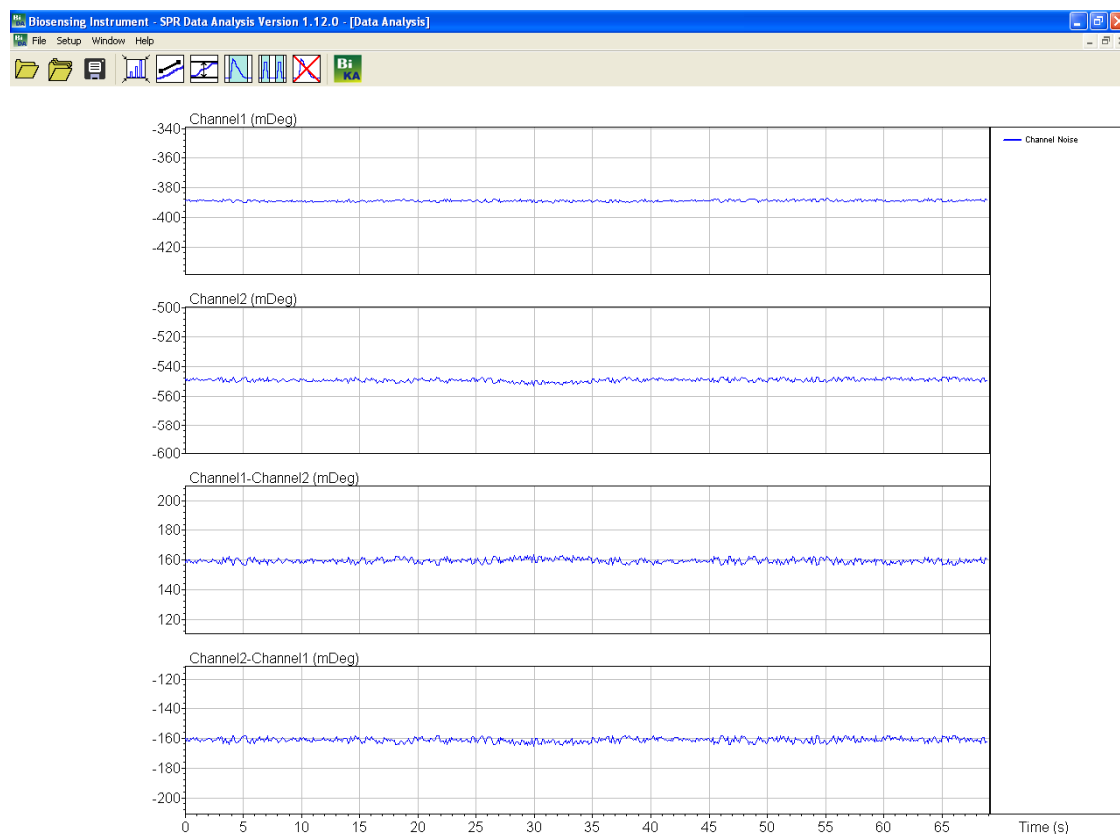


**Figure 43 – SPR Output: Channel 1, Channel 2, 1-2 and 2-1, Noise**

SPR signal after 60 minutes of warm up showing noise variance in signal. Once the baseline has leveled out small tremors appear in both channels. The noise canceling feature of the channel difference algorithm seems to fail and smoothing out the baseline, actually amplifying the tremors on the display.

## **D.2 Instrument Calibration**

Calibration was accomplished successfully and showed acceptable results in both channels. A half step series of ethanol dilutions, starting from 1.00% to .0625%, were injected into the injection valve of the factory fluidics. As the ethanol solution reached the SPR sensor



chip, a sharp upward angular shift was observed. The shift caused by the 1.00% ethanol started as a sharp upward shift which quickly plateaued as the SPR gasket filled with the 1.00% ethanol solution and as the deionized water flowing behind pushed the ethanol out, the shift sharply returned to the expected baseline caused by the flowing deionized water. After three injections of 1.00% ethanol on channel 1, an average shift of 105 mDeg was measured and recorded. Expected angular shift caused by 1.00% ethanol, using a calibration value of 3000 mDeg/V, is 60 mDeg. A new calibration value must be assigned to channel 1 to cause it to have a 60 mDeg shift when 1.00% ethanol is added. The value is derived from the new-calibration-value equation listed above (Figure 14). The new calibration value determined for channel 1 is 1716 mDeg/V. Calibration on channel 2 was performed similarly to channel 1 by injecting three separate boluses, 100  $\mu$ L, of 1.00% ethanol using a calibration value of 3000 mDeg/V. The average angular shift measured was 105 mDeg, indicating that a new calibration value needed to be assigned for channel 2. The new calibration value for channel 2, based on the new-calibration-value equation, was 1711 mDeg/V. Listed below, (Table 3) are the measured angular shifts caused by the different dilutions of ethanol.

**Table 4 – Calibration Data**

**Channel 1**

|                 |          |          |          |          |         |
|-----------------|----------|----------|----------|----------|---------|
| Percent Ethanol | 1.0000%  | 0.5000%  | 0.2500%  | 0.1250%  | 0.0625% |
| Trial 1         | 108.132  | 53.36    | 26.307   | 13.391   | 8.147   |
| Trial 2         | 98.365   | 50.978   | 28.049   | 14.576   | 8.119   |
| Trial 3         | 108.132  | 51.454   | 25.634   | 13.56    | 8.799   |
| Average         | 104.8763 | 51.93067 | 26.66333 | 13.84233 | 8.355   |
| Std Dev         | 5.63898  | 1.260512 | 1.246309 | 0.640968 | 0.38477 |

**Channel 2**

|                 |          |          |          |          |          |
|-----------------|----------|----------|----------|----------|----------|
| Percent Ethanol | 1.0000%  | 0.5000%  | 0.2500%  | 0.1250%  | 0.0625%  |
| Trial 1         | 109.974  | 54.106   | 30.271   | 14.911   | 8.994    |
| Trial 2         | 100.406  | 52.73    | 27.6     | 15.449   | 9.126    |
| Trial 3         | 105.162  | 54.996   | 29.529   | 15.167   | 8.827    |
| Average         | 105.1807 | 53.944   | 29.13333 | 15.17567 | 8.982333 |
| Std Dev         | 4.784027 | 1.141653 | 1.378758 | 0.269105 | 0.149841 |

The purpose of the different dilutions was to assure that as the ethanol content steps down 50% the angular shift that results steps down by half as well. Seen in figure 34, a strong visual correlation exists between the half strength step dilutions of ethanol and the half step angular shift in the SPR detection system. Comparing the results in Table 3, the half step correlation is quantifiably verified for both channel 1 and channel 2

The table above shows the angular shift caused by each ethanol injection. Five different dilutions were injected three times each for statistical significance. After each set of injections of one dilution of ethanol were done, an average was taken for quantitative comparison and in the case of the 1.00% solution, for a new calibration value assignment. Comparing channel 1 and 2 the shift caused by the different dilutions is very comparable. Across each channel, the half step dilutions also caused a close to half reduction in resulting signal shift as expected.

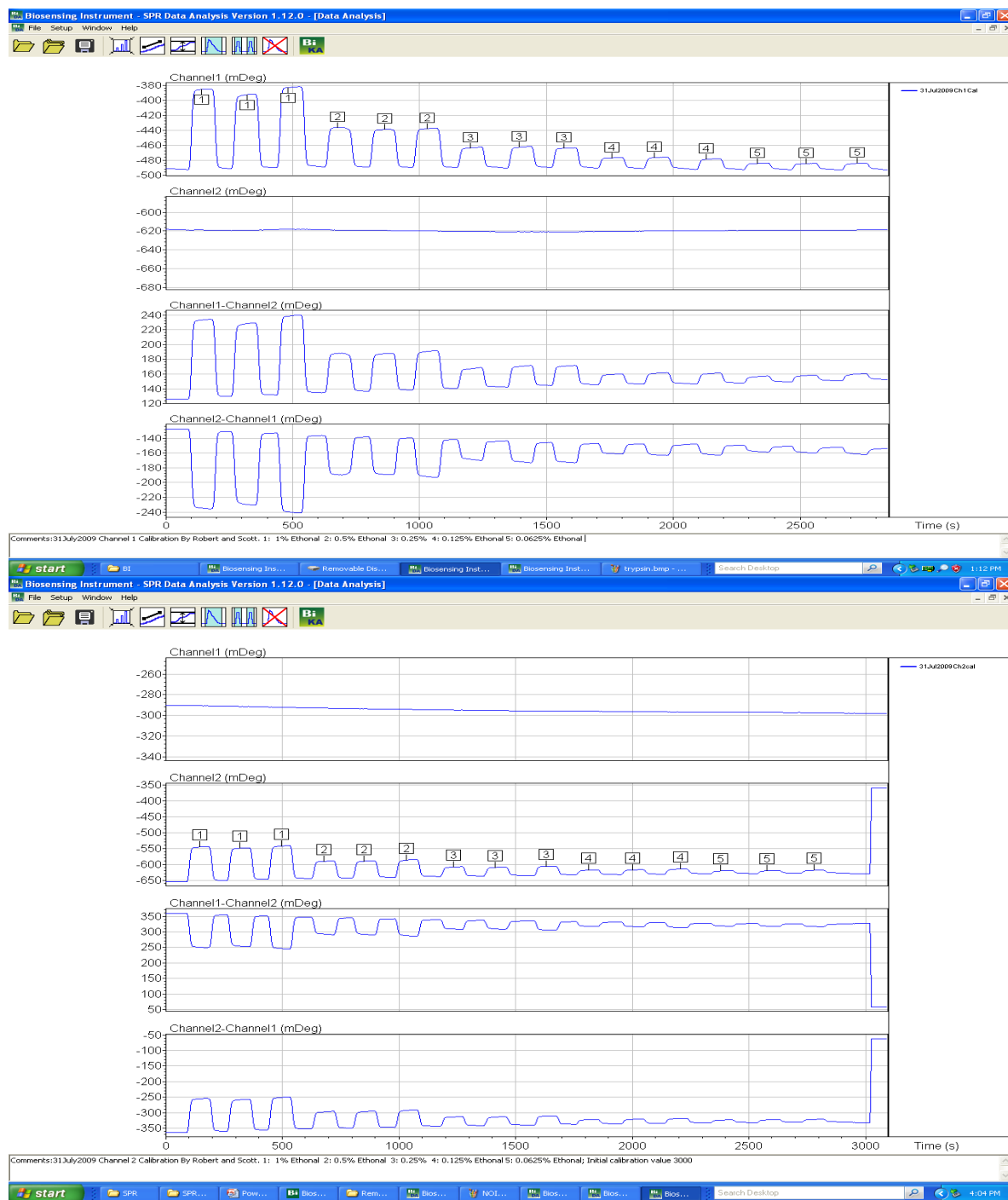


**Figure 44 – SPR Output: Channel 1, Channel 2, 1-2 and 2-1, Calibration**  
 Results of the calibration on both channels, showing the half step pattern that directly correlates to the half step dilution injection. Each dilution was injected three times and labeled as follows: 1-1.0000%, 2-0.5000%, 3-0.2500%, 4-0.1250%, 5-0.0625%. The half step pattern is the expected profile for calibration.

1. Chin CD, Linder V, Sia SK. Lab-on-a-chip devices for global health: past studies and future opportunities. *Lab Chip*. 2007;7(1):41-57.
2. The Bill & Melinda Gates Foundation. Available at: <http://www.gatesfoundation.org/Pages/home.aspx> [Accessed May 8, 2010].
3. Ko JS, Yoon HC, Yang H, et al. A polymer-based microfluidic device for immunosensing biochips. *Lab Chip*. 2003;3(2):106-113.
4. WHO | The WHO agenda. Available at: <http://www.who.int/about/agenda/en/index.html> [Accessed May 8, 2010].
5. MTO - Microsystems Technology Office. Available at: <http://www.darpa.mil/mto/> [Accessed May 9, 2010].
6. Wagner R. Sampling and sample preparation. *Fresenius' Journal of Analytical Chemistry*. 1976;282(4):315-321.
7. Lichtenberg J, de Rooij NF, Verpoorte E. Sample pretreatment on microfabricated devices. *Talanta*. 2002;56(2):233-266.
8. Kuefer R, Varambally S, Zhou M, et al. {alpha}-Methylacyl-CoA Racemase: Expression Levels of this Novel Cancer Biomarker Depend on Tumor Differentiation. *Am J Pathol*. 2002;161(3):841-848.
9. Moreira D. Efficient removal of PCR inhibitors using agarose-embedded DNA preparations. *Nucleic Acids Res*. 1998;26(13):3309-3310.
10. Bogardt AH, Hemmingsen BB. Enumeration of phenanthrene-degrading bacteria by an overlay technique and its use in evaluation of petroleum-contaminated sites. *Appl Environ Microbiol*. 1992;58(8):2579-2582.
11. Introduction: Sample Preparation. Available at: <http://www.forumsci.co.il/HPLC/SPE/introduction.html> [Accessed May 19, 2010].
12. Biosensing Instrument Inc., BI-2000 SPR System *User's Manual*. V5.4, 2008
13. Leng SX, McElhaney JE, Walston JD, et al. ELISA and multiplex technologies for cytokine measurement in inflammation and aging research. *J. Gerontol. A Biol. Sci. Med. Sci*. 2008;63(8):879-884.
14. Ramos-Vara JA. Technical Aspects of Immunohistochemistry. *Veterinary Pathology Online*. 2005;42(4):405-426.
15. Wang ZH, Jin G. A Label-Free Multisensing Immunosensor Based on Imaging Ellipsometry. *Analytical Chemistry*. 2003;75(22):6119-6123.
16. Lei KF, Law WC, Suen Y, et al. A vortex pump-based optically-transparent microfluidic platform for biotech and medical applications. *Proceedings of the Institution of Mechanical Engineers, Part H: Journal of Engineering in Medicine*. 2007;221(2):129-141.
17. Zhang Y, Xu M, Du M, Zhou F. Comparative studies of the interaction between ferulic acid and bovine serum albumin by ACE and surface plasmon resonance. *ELECTROPHORESIS*. 2007;28(11):1839-1845.
18. Schasfoort RBM, Tudos AJ. *Handbook of surface plasmon resonance*. Royal Society of Chemistry; 2008.
19. 1. Palm-sized biosensor for point-of-care and field applications. Available at: <http://www.nanowerk.com/spotlight/spotid=6609.php> [Accessed June 3, 2010].
20. Wood RW. On a Remarkable Case of Uneven Distribution of Light in a Diffraction Grating Spectrum. *Proc. Phys. Soc. London*. 1902;18(1):269-275.

21. Raether H, Kretschmann. Radiative decay of non-radiative surface plasmons excited by light. *Zeitschrift Für Naturforschung Section A A Journal Of Physical Sciences*. 23:2135.
22. Otto A. Excitation of nonradiative surface plasma waves in silver by the method of frustrated total reflection. *Zeitschrift für Physik A Hadrons and Nuclei*. 1968;216(4):398-410.
23. Nuster R, Paltauf G, Burgholzer P. 3H-1 Sensitivity of Surface Plasmon Resonance Sensors for the Measurement of Acoustic Transients in Liquids. In: *2006 IEEE Ultrasonics Symposium*. Vancouver, BC, Canada; 2006:768-771.
24. Liedberg B, Nylander C, Lunström I. Surface plasmon resonance for gas detection and biosensing. *Sensors and Actuators*. 1983;4:299-304.
25. Homola J, Yee SS, Gauglitz G. Surface plasmon resonance sensors: review. *Sensors and Actuators B: Chemical*. 1999;54(1-2):3-15.
26. Ferrel, T. L., T. A. Callcott, and R. J. Warmack, Plasmons and Surfaces, *American Scientist*, 73, 344-353, 1985.
27. Yu PY, Cardona M. *Fundamentals of semiconductors: physics and materials properties*. Springer; 2005.
28. Solé JG, Bausá LE, Jaque D. *An introduction to the optical spectroscopy of inorganic solids*. John Wiley and Sons; 2005.
29. Hecht E, Zajac A. *Optics*. 3rd ed. Addison Wesley Publishing Company; 1997.
30. SPR 4-Phase Reflectivity Calculation. Available at: <http://unicorn.ps.uci.edu/calculations/fresnel/fcform.html> [Accessed July 9, 2010].
31. Sinicrope FA, Gill S. Role of cyclooxygenase-2 in colorectal cancer. *Cancer Metastasis Rev*. 2004;23(1-2):63-75.
32. Wang Y, Coffey RJ, Osheroff N, Neufeld KL. Topoisomerase II $\alpha$  Binding Domains of Adenomatous Polyposis Coli Influence Cell Cycle Progression and Aneuploidy. *PLoS ONE*. 2010;5(4):e9994.
33. Udvardi MK, Czechowski T, Scheible W. Eleven Golden Rules of Quantitative RT-PCR. *Plant Cell*. 2008;20(7):1736-1737.
34. Surface Plasmon Resonance. Available at: <http://www.biosensingusa.com/BI-SPRTechnology.html> [Accessed July 9, 2010].
35. Surface Plasmon Resonance. Available at: <http://www.biosensingusa.com/Application101.html> [Accessed July 9, 2010].
36. Homola J. Surface Plasmon Resonance Sensors for Detection of Chemical and Biological Species. *Chemical Reviews*. 2008;108(2):462-493.
37. WHO | Cancer. Available at: <http://www.who.int/mediacentre/factsheets/fs297/en/> [Accessed June 30, 2010].
38. Colon and Rectal Cancer Home Page - National Cancer Institute. Available at: <http://www.cancer.gov/cancertopics/types/colon-and-rectal> [Accessed July 30, 2010].
39. Colon and Rectum Cancer Early Detection. Available at: <http://www.cancer.org/Cancer/ColonandRectumCancer/MoreInformation/ColonandRectumCancerEarlyDetection/index?from=colontesting> [Accessed June 30, 2010].
40. 1. Fast Stats. Available at: <http://seer.cancer.gov/faststats/selections.php?#Output> [Accessed June 30, 2010].